CFT CORRELATORS AND ANALYTICS

A Dissertation

by

SUNNY GUHA

Submitted to the Office of Graduate and Professional Studies of
Texas A&M University
in partial fulfillment of the requirements for the degree of

DOCTOR OF PHILOSOPHY

Chair of Committee,	Katrin Becker
Committee Members,	Christopher Pope
	Teruki Kamon
	Stephen Fulling
Head of Department,	Grigory Rogachev

August 2020

Major Subject: Physics

ABSTRACT

Analytic methods to solve conformal field theories (CFT) have yielded a lot of mileage in recent years. This dissertation builds up on these analytical techniques (lightcone methods and inversion formulas) and extends them to new avenues including defect CFTs and double-twist analytics. First, we use embedding formalism to construct correlators for d-dimensional CFT in the presence of q co-dimensional defect. All possible invariants appearing in correlators of arbitrary representation of operators are constructed for the first time in a defect setting. This allows constraining the defect CFT by studying crossing relations of operators in arbitrary representations. Second, inversion formula is utilized to compute anomalous dimensions and three-point coefficient corrections for double-twist operators in arbitrary dimensions. We develop a new technique in Mellin space to compute closed form expression of these corrections which are valid at any finite value of conformal spin. Finally, a new connection is established between conformal correlator expansion and perturbative diagrammatic expansion in Wilson-Fisher theory in $4-\epsilon$ dimensions. To derive this connection we develop novel techniques for representing scalar and twist contributions to correlators using Mellin space. Our techniques generalize to other theories with ϵ-expansion as well.

DEDICATION

To my parents.

ACKNOWLEDGMENTS

It is impossible for me to quantify my gratitude on a page so as a CFT dissertation I advise the reader to scale my gratitude by a large factor.

First and foremost I would like to thank my Ph.D. advisor Dr. Katrin Becker for all the invaluable mentorship and help she has provided me. I am also very grateful to Dr. William Linch for mentoring me throughout my Ph.D., his continuous support and countless inspiring discussions. I would like to offer special thanks to Dr. Melanie Becker, who, although no longer with us, continues to inspire by her research and dedication to the students she guided.

I would like to thank Dr. Christopher Pope, Dr. Falk Hassler, Dr. Daniel Butter for interesting physics and non-physics discussion during "String-lunch". I also thank Dr. Christopher Pope, Dr. Teruki Kamon and Dr. Stephen A. Fulling for agreeing to be on my committee.

I would like to thank the current and past graduate students and postdocs in TAMU high energy theory group including Arash Azizi, Yaniel Cabrera, Balakrishnan Nagaraj, Yaodong Zhu, Zhijin Li, Aritra Saha, Surya Kiran Kanumilli, Lakshya Agrawal, Daniel Robbins, Daniel Butter, Falk Hassler and Andrew Royston. They have all been great colleagues and mentors. A very special thanks goes to Taylor Whitehead for being a great and helpful friend during the past five years.

A very special gratitude goes to my girlfriend Archana Tale for listening to my physics rants patiently. You kept me sane during the last two years. Finally I would like to thank my parents for their love and support for all my endeavours.

CONTRIBUTORS AND FUNDING SOURCES

Contributors

This work was reviewed by a dissertation committee consisting of Professor Katrin Becker, Professor Christopher Pope and Professor Teruki Kamon of the Department of Physics and Astronomy and Professor Stephen Fulling of the Department of Mathematics.

Funding Sources

My graduate study was supported by a teaching fellowship from Texas A&M University and a research fellowship from Dr. Katrin Becker.

NOMENCLATURE

CFT	Conformal Field Theory
QFT	Quantum Field Theory
DCFT	Defect Conformal Field Theory
SCT	Superconformal Transformation
D	Dilatation Generator
K_μ	Special Conformal Generator
Δ	Scaling Dimension
OPE	Operator Product Expansion
CPW	Conformal Partial Wave
SYM	Super Yang-Mills
SCFT	Superconformal Field Theory

TABLE OF CONTENTS

LIST OF FIGURES

FIGURE Page

LIST OF TABLES

1. INTRODUCTION

In this chapter we review the basics and the current status of conformal field theories leading up to the research projects described in this dissertation.

1.1 Basics

Conformal field theory (CFT) play a central role in many areas of theoretical physics from condensed matter to quantum gravity. CFTs are quantum field theories (QFTs) that (in d dimensions) are invariant under the global conformal group $SO(d{+}1,1)$ instead of Poincaré group $SO(d{-}1,1)$. A study of CFT is essential for a better understanding of various phenomena that involve phase transitions, critical points, AdS/CFT duality etc. CFTs are also important from the point of view of renormalization flow. This flow is the evolution of coupling constants (beta function) from Ultraviolet (UV) to Infrared (IR) region. At certain points in this trajectory (“fixed points") the beta function vanishes and the theory becomes scale invariant and conformal. A remarkable fact about this process is that very different UV theories can flow to the same IR fixed point making CFT a universal IR behaviour of these UV theories. This “universality" unifies application of CFTs to multiple areas of physics and makes study of CFT important.

The Poincaré group consists of Lorentz (rotation) and translational symmetries. Conformal group is the extension of this to $SO(d+1,1)$. This added symmetry reduces the number of free parameters and makes CFT relatively easy to solve[1]. A nice analogy for the QFT/CFT relation is the relation between ideal gas (simplistic, CFT) and Van der Waals gas (real world, complicated, QFT).

The added symmetries in a CFT are 1) scale invariance and 2) special conformal invariance. Poincaré transformations are transformations of the form,

$$x^\mu \to \Lambda^\mu_\nu x^\nu + a^\mu \,, \tag{1.1}$$

[1]“solve" refers to computation of observables.

where Λ^{μ}_{ν} is the Lorentz tensor. Scaling symmetry is a scaling transformation on both the position and time coordinates. In relativistic quantum field theories, it scales (by λ) all the coordinates with the same amount.

$$x^{\mu} \to \lambda x^{\mu} \,. \tag{1.2}$$

Special conformal transformation is a complicated non-linear transformation whose effect is the following,

$$x'^{\mu} = \frac{x^{\mu} - (x \cdot x) b^{\mu}}{1 - 2(b \cdot x) + (b \cdot b)(x \cdot x)} \,. \tag{1.3}$$

These additional symmetries give rise to interesting CFT properties which we will review in the upcoming sections.

1.1.1 Conformal Algebra

The underlying group of a d-dimensional CFT is $SO(d+1,1)^2$, which has $(d+1)(d+2)/2$ generators. The details of the algebra have been worked out in many excellent reviews and articles [1, 2, 3]. In this section we will briefly go over the conformal algebra. We list down the algebra of the generators below,

$$\begin{aligned}
&[D, P_{\mu}] = i P_{\mu} \,, \\
&[D, K_{\mu}] = -i K_{\mu} \,, \\
&[K_{\mu}, P_{\nu}] = 2i \left(\eta_{\mu\nu} D - L_{\mu\nu} \right) \,, \\
&[K_{\rho}, L_{\mu\nu}] = i \left(\eta_{\rho\mu} K_{\nu} - \eta_{\rho\nu} K_{\mu} \right) \,, \\
&[P_{\rho}, L_{\mu\nu}] = i \left(\eta_{\rho\mu} P_{\nu} - \eta_{\rho\nu} P_{\mu} \right) \,, \\
&[L_{\mu\nu}, L_{\rho\sigma}] = i \left(\eta_{\nu\rho} L_{\mu\sigma} + \eta_{\mu\sigma} L_{\nu\rho} - \eta_{\mu\rho} L_{\nu\sigma} - \eta_{\nu\sigma} L_{\mu\rho} \right) \,.
\end{aligned} \tag{1.4}$$

D and K_{μ} are the scaling and special conformal generator respectively. All other commutators vanish. The Lorentz algebra remains intact. In coordinate representation the generators have the

[2] We have considered euclidean conformal group here. The unitary representations of Lorentzian conformal group can be analytically continued to euclidean signature.

following form in terms of x (position) and its derivatives,

$$
\begin{aligned}
&P_\mu = -i\partial_\mu \,, \\
&L_{\mu\nu} = -i\left(x_\mu\partial_\nu - x_\nu\partial_\mu\right)\,, \\
&D = -ix^\mu\partial_\mu \,, \\
&K_\mu = 2x_\mu\left(x^\rho\partial_\rho\right) - x^2\partial_\mu \,.
\end{aligned}
\tag{1.5}
$$

General conformal transformations act on the metric in the following manner,

$$
\eta_{\rho\sigma}\frac{\partial x'^\rho}{\partial x^\mu}\frac{\partial x'^\sigma}{\partial x^\nu} = \Lambda(x)\eta_{\mu\nu} \,.
\tag{1.6}
$$

As is evident from the equation above, conformal transformation leave the metric invariant up-to an overall scale, $\lambda(x)$. If $\lambda = 1$, we recover Poincaré transformations. Physically the action of conformal transformations is to leave angle between rays invariant (instead of leaving distance invariant). The infinitesimal action of the generators on the coordinates is given by,

$$
\begin{aligned}
&x'^\mu = x^\mu + c^\mu, \text{ Translations} \\
&x'^\mu = x^\mu + \lambda x^\mu, \text{ Dilatations} \\
&x'^\mu = x^\mu + w^\mu_\nu x^\nu, \text{ Lorentz} \\
&x'^\mu = x^\mu + 2\left(b_\sigma x^\sigma\right)x^\mu - x^2 b^\mu, \text{ SCT (parameter } b)
\end{aligned}
\tag{1.7}
$$

The key objects of interest in a CFT are local operators $\mathcal{O}(x)$. We will discuss local operators in detail in later sections. The action of conformal generators on the local operators are given as,

$$
\begin{aligned}
&[P_\mu, \mathcal{O}(x)] = i\partial_\mu\mathcal{O}(x), \quad [D, \mathcal{O}(x)] = i\left(\Delta + x^\mu\partial_\mu\right)\mathcal{O}(x)\,, \\
&[K_\mu, \mathcal{O}(x)] = i\left(x^2\partial_\mu - 2x_\mu x^\nu\partial_\nu - x_\mu\Delta\right)\mathcal{O}(x)\,, \\
&[L_{\mu\nu}, \mathcal{O}(x)] = i\left(x_\mu\partial_\nu - x_\nu\partial_\mu + \mathcal{S}_{\mu\nu}\right)\mathcal{O}(x)\,.
\end{aligned}
\tag{1.8}
$$

$\mathcal{S}_{\mu\nu}$ is the representation of spin operator corresponding to $\mathcal{O}(x)$. Δ is called the *scaling dimension* and is the eigenvalue of the state/operator under dilatation operator. In a CFT the dilatation generator is used for space-slice evolution instead of Hamiltonian. This is the essence of radial quantization which we discuss below.

1.1.2 Radial Quantization

In a QFT, correlators and scattering amplitudes are the primary observables. However in a CFT due to scale invariance the particle description makes no sense[3]. This absence makes the S-matrix and scattering amplitude description unfeasible. Thus the only observables in CFTs are correlators. In this section we will inspect correlators from the point of view of Hilbert space and Quantum mechanical evolution. Hilbert spaces are defined on space-like slices (foliation of space-time in surfaces of equal time: Figure 1.1). Space-time is composed of union of infinite equal time slices.

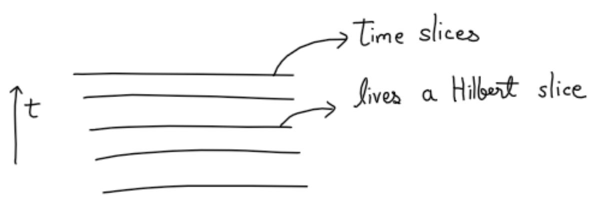

Figure 1.1: Foliation of space-time.

In each time slice (t=constant), we can create an “in" state by inserting[4] operators in the past of the surface (Figure 1.2). Similarly we can create “out state" by inserting operators in the future (Figure 1.3). Correlators are basically overlaps between “in" and “out" states = $\langle\psi_{out}|\psi_{in}\rangle$. If the “in" and “out" state are at different times, then a time evolution needs to be performed. We perform this evolution using $U = e^{iH\Delta t}$ where H is the Hamiltonian (the generator of time trans-

[3]Particles manifest themselves as delta functions in the spectral decomposition of two point function. The spectral decomposition of CFT two-point function is a continuous function which implies that there are no localized distributions and hence no particles.

[4]Operators are inserted in the path integral. The path-integral is over field configuration from past infinity to current time slice (for “in" state). The current time slice boundary condition is left unfixed to create the in-state.

Figure 1.2: Construction of in-state.

Figure 1.3: Construction of out-state.

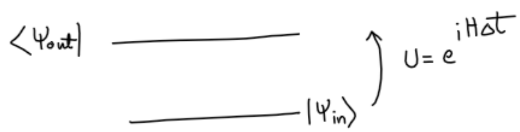

Figure 1.4: Evolution of states.

lation). Now the overlap looks like $\langle\psi_{out}|U|\psi_{in}\rangle$ (Figure 1.4). In a CFT due to added symmetry we can foliate the space-time in spheres of increasing radius. A similar representation for "in" and "out" states exists for radial quantization states (Figure 1.5). The evolution between the spheres is

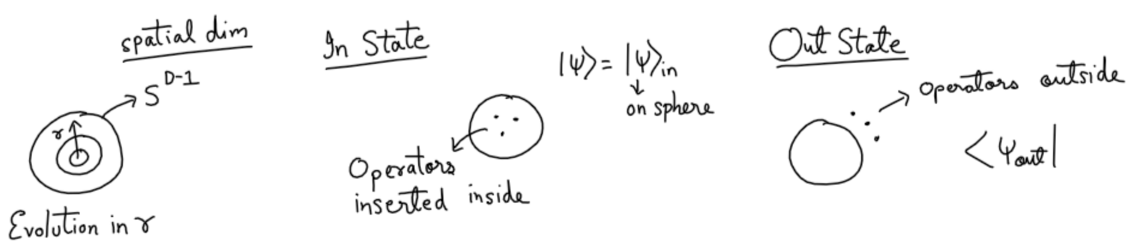

Figure 1.5: Radial quantization.

controlled by the Dilatation operator $U = e^{iD\Delta\tau}$ where $\tau = \log(r)$. Because evolution is generated by dilatation, we will label the states by scaling dimensions (eigenvalues of dilatation operator) Δ.

1.1.3 State Operator Correspondence

State Operator Correspondence refers to the one-to-one relation between states and operators. In CFT this relation is reversible (unlike QFT). Using dilatation operation the states on sphere can be shrunk to a point (local operator) and vice-versa (Figure 1.6). As an example we will look at

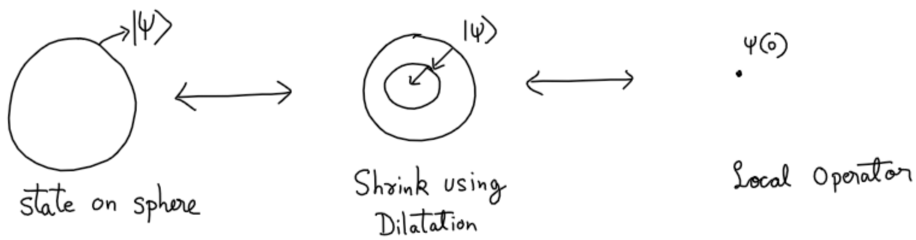

Figure 1.6: State operator correspondence.

vacuum state which is a state with no insertion,

$$|0\rangle \to \text{No Insertion}, \quad \Delta = 0, \qquad D|0\rangle = 0\,. \tag{1.9}$$

The eigenvalue of vacuum under dilatation is 0. The vacuum is also annihilated by all other generators of conformal group. Now imagine if we insert an operator of weight Δ at origin,

$$\Phi_\Delta|0\rangle \equiv |\Delta\rangle\,. \tag{1.10}$$

Then simple operation of (1.8) gives us the following,

$$D|\Delta\rangle = \Delta|\Delta\rangle, \qquad K_\mu|\Delta\rangle = 0\,. \tag{1.11}$$

We define the operators (states) that are annihilated by K_μ as **primary operators**. Acting on these primary operators with P_μ one generates a tower of **descendant operators**,

$$P_\mu P_\nu \cdots P_\sigma |\Delta\rangle \equiv P_\mu P_\nu \cdots P_\sigma O_\Delta(x) = \partial_\mu \partial_\nu \cdots \partial_\sigma O_\Delta(x)\,. \tag{1.12}$$

With the correspondence in hand the objects of interest in CFT are local operators. We will study properties of local operators and correlators of local operators.

1.1.4 OPE

Operator Product Expansion (OPE) is a special property of field theory where two operators (close by) can be replaced by linear combination of operators. Formally it is represented as,

$$\mathcal{O}_i(x)\mathcal{O}_j(0)|0\rangle = \sum_k C_{ijk}(x,P)\mathcal{O}_k(0)|0\rangle\,. \tag{1.13}$$

The sum k runs over all primary operators and $C_{ijk}(x,P)$ is a differential operator packaged together with the three point coefficient C_{ijk}. The three-point coefficients are theory specific data[5]. The differential operator serves to generate the family of descendants for a primary,

$$C_{ijk}(x,\partial) = C_{ijk}x^{\Delta-2\Delta_{\mathcal{O}}}\left(1+\frac{1}{2}x\cdot\partial+\alpha x^\mu x^\nu \partial_\mu\partial_\nu+\beta x^2\partial^2+\dots\right)\,, \tag{1.14}$$

where,

$$\alpha = \frac{\Delta+2}{8(\Delta+1)}, \quad \text{and} \quad \beta = -\frac{\Delta}{16\left(\Delta-\frac{d-2}{2}\right)(\Delta+1)} \tag{1.15}$$

The coefficients and the terms in the expansion (1.14) are completely fixed by conformal algebra. Mathematically OPE can be thought of as having two operators surrounded by a sphere (radial quantization setting)[6]. Using path integral the state on the sphere is obtained and using scaling symmetry the state on sphere can be shrunk to a point thus obtaining a series of local operators.

Typically in a QFT OPE is used only in the asymptotically short limit. In a CFT the OPE

[5] The analogous quantity in a QFT is the three-point coupling.
[6] It is essential that this ball should not contain any other operators.

structure becomes much richer. An OPE in CFT gives a convergent series expansion at finite point separation. OPE satisfy associativity and this gives rise to crossing symmetry of a CFT.

1.1.5 CFT Data

Operators are the building blocks of CFT. Primary operators are the only essential ingredients since descendants can be generated from primaries. Primary operators are specified by their spin (J) and their scaling dimensions (Δ). This is all the data needed in a free CFT, however for interacting CFT the information of interactions is also required. This is contained in three-point coefficients (C_{ijk}). Specifying the list of primary operators, their scaling dimensions and the three point coefficient specifies a CFT completely.

The fact that CFTs can be specified by these quantities only is not very surprising as the extended symmetry of the conformal group compared to Poincaré group leads to fewer "degrees of freedom". It turns out that the CFT data is not completely arbitrary but is tightly constraint. We will discuss this further.

1.2 Correlators

Correlators are the principle observables in a CFT. We will look at all correlators upto 4-point functions. One point functions are trivially zero (except for identity operator) since no Lorentz or conformal invariant structure can be constructed out of one-point position. In this section our focus is on scalar correlators as correlators for all other representations can be built from scalars [4].

1.2.1 Two-Point Correlators

Two-point correlators are simple as there is only one possible conformal structure that can be present. We will work this out in detail. The most general conformal transformation has the following effect on the two-point correlator,

$$\langle \phi_1 (x_1) \phi_2 (x_2) \rangle = \left| \frac{\partial x'}{\partial x} \right|_{x=x_1}^{\Delta_1/d} \left| \frac{\partial x'}{\partial x} \right|_{x=x_2}^{\Delta_2/d} \langle \phi_1 (x'_1) \phi_2 (x'_2) \rangle \tag{1.16}$$

The restriction imposed by each generator is,

$$\begin{aligned}
&\text{Poincare} : \langle \phi_1(x_1)\,\phi_2(x_2)\rangle = f(|x_1 - x_2|) \ , \\
&\text{Dilation} : \langle \phi_1(x_1)\,\phi_2(x_2)\rangle = \lambda^{\Delta_1+\Delta_2}\langle \phi_1(\lambda x_1)\,\phi_2(\lambda x_2)\rangle \ , \\
&\text{Special Conformal} : \Delta_1 = \Delta_2\, .
\end{aligned} \tag{1.17}$$

Compiling all of theses together we obtain the following expression for a two point function.

$$\langle \phi_1(x_1)\,\phi_2(x_2)\rangle = \begin{cases} \frac{1}{|x_1-x_2|^{2\Delta_1}} & \text{if } \Delta_1 = \Delta_2 \\ 0 & \text{if } \Delta_1 \neq \Delta_2 \end{cases} \tag{1.18}$$

We have used the scaling freedom to scale operators to fix the coefficient of the two point correlator to unity. Two-point correlator is only non-vanishing for identical operators. It is sufficient for the representations and scaling dimension to be equal. CFTs in general do not have two operators having identical scaling dimension.

1.2.2 Three-Point Correlators

Just as before, once we use all the generators to fix the form we obtain the following three point function,

$$\langle \phi_1(x_1)\,\phi_2(x_2)\,\phi_3(x_3)\rangle = \frac{C_{123}}{x_{12}^{\Delta_1+\Delta_2-\Delta_3}\,x_{23}^{\Delta_2+\Delta_3-\Delta_1}\,x_{13}^{\Delta_1+\Delta_3-\Delta_2}} \qquad \text{where } x_{ij} = |x_1 - x_j| \tag{1.19}$$

The form of three-point correlator is fixed upto a constant. We cannot scale away the constant as in the two-point function. This coefficient is the additional data once needs to specify a CFT and is the same one that appeared in OPE expansion (3.3). These constants refer to interactions as they are absent in a free theory.

1.2.3 Four-Point Correlators

With four points one can define two conformal invariant combinations,

$$u = \frac{x_{12}^2 x_{34}^2}{x_{13}^2 x_{24}^2}, \quad v = \frac{x_{23}^2 x_{14}^2}{x_{13}^2 x_{24}^2}\,. \tag{1.20}$$

Applying the symmetries of conformal group we obtain the following form,

$$\langle \phi\,(x_1)\,\phi\,(x_2)\,\phi\,(x_3)\,\phi\,(x_4)\rangle = \frac{g(u,v)}{x_{12}^{2\Delta_\phi} x_{34}^{2\Delta_\phi}} \tag{1.21}$$

To simplify things further we will use conformal symmetry to fix the points in a similar manner (Figure 1.7).

1. Use SCT to move x_4 to ∞
2. Use translation to move x_1 to origin.
3. Using rotations and dilatation, we can move x_3 to (1,0,..,0)
4. Using rotation that fix x_3, we can move x_2 to (z, $\bar{z}$,0,..,0)

We have moved all points on a plane with points x_1,x_3 and x_4 on a line and point x_2 is free to move on the plane with coordinates $z, \bar{z}$ (1.22) where $z = x + iy$.

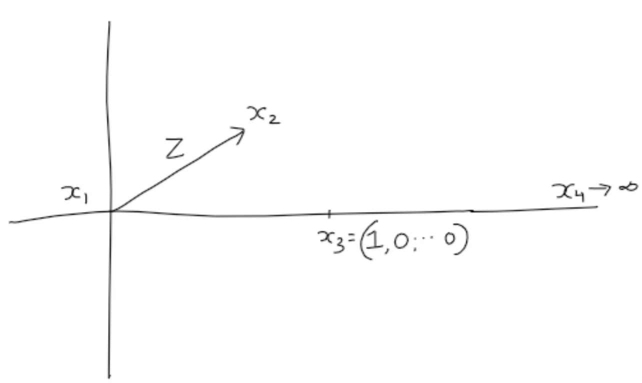

Figure 1.7: Four points on a plane.

In terms of $z, \bar{z}$ the conformal invariants can be written as,

$$u = z\bar{z}, \quad v = (1-z)(1-\bar{z})\,. \tag{1.22}$$

For a four-point scalar correlator we obtain the following final result,

$$\langle \phi\,(x_1)\,\phi\,(x_2)\,\phi\,(x_3)\,\phi\,(x_4)\rangle = \frac{g(z,\bar{z})}{x_{12}^{2\Delta_\phi} x_{34}^{2\Delta_\phi}} \tag{1.23}$$

The function $g(z, \bar{z})$ is known as conformal partial wave and its functional form is completely fixed (using conformal invariance) up-to theory specific data. The kinematic factors appearing in the four-point function (1.23) correspond to s-channel.

1.2.4 Spinning Correlators

Till now the analysis has been limited to scalar correlators. Spinning correlators follow the same basic principle, however the kinematic factors for spinning correlator are more complicated due to multiple Lorentz indices. Embedding formalism [5, 4] is an efficient formalism to calculate correlators in CFT. Dirac in [6], first pointed that conformal group of CFT in d dimension is isomorphic to Lorentz algebra of $d+2$ dimensions ($SO(d+1,1)$). Embedding formalism utilizes this fact and defines the d-dimensional theory on a section of null cone in $d+2$-dimensions theory ($X^2 = 0$). The utility of going to two higher dimensions is that we can replace non-linear conformal transformations with linear Lorentz transformation of $d+2$-dimensions. This results in simplification of calculations.

In embedding-formalism we uplift operators from d-dimension to $d+2$ dimensions,

$$\phi_{mu\nu\cdots}(x) \Longleftrightarrow \Phi_{MN\cdots}(X)\,. \tag{1.24}$$

The advantage of this uplift is that one only needs to consider Lorentz invariants to construct correlators (instead of conformal invariants). However to get the actual physical degrees of freedom out we need to impose certain constraints. We impose transversality constraint (this constrains the operator to remain on the null cone),

$$X^M \Phi_{MN\cdots}(X) = 0\,. \tag{1.25}$$

We also need to impose homogeneity under scaling for the operators,

$$\Phi_{\cdots}(\lambda X) = \lambda^{-\Delta}\Phi_{\cdots}(X)\,. \tag{1.26}$$

To return back to physical space we utilize the following “gauge" $X^M = (1, x^2, x^\mu)$. The projection is done via the following equation,

$$\phi_{\mu\nu\cdots}(x) = \Phi_{MN\cdots}(X)\frac{\partial X^M}{\partial x^\mu}\frac{\partial X^N}{\partial x^\nu}\cdots \tag{1.27}$$

To see the advantage of embedding formalism, we will look at two point correlator of spin-1 operators. With spin-1 operators one can construct following Lorentz invariants,

$$\langle \phi_M(X)\phi_N(Y)\rangle = \frac{\eta_{MN}}{(XY)^\Delta} + \alpha\frac{\frac{Y_N X_N}{XY}}{(XY)^\Delta}\,. \tag{1.28}$$

We only obtain two Lorentz invariants for the two point correlator (of spin-1). This gives rise to an unfixed coefficient α. Using the constrains (1.25) we obtain α = -1. Projecting the result down to physical space gives,

$$\langle \phi_\mu(x)\phi_\nu(y)\rangle = \frac{\delta_{\mu\nu} - \frac{2(x-y)_\mu(x-y)_\nu}{(x-y)^2}}{(x-y)^{2\Delta}}\,. \tag{1.29}$$

1.3 Consistency

The associative nature of CFT gives rise to crossing relation. This self cosistency relation of CFT can be used to constrain the CFT-date.

1.3.1 Confromal Blocks

In (1.23) the form of 4-point correlator was fixed up-to a function $g(z, \bar{z})$, the conformal partial wave (CPW). CPW can be decomposed further into contributions from operators appearing in the channel,

$$g(z, \bar{z}) = 1 + \sum_{O} C_O^2 g_O(z, \bar{z}) \, . \tag{1.30}$$

In the above equation C_O^2 is the three-point coefficient and $g_O(z, \bar{z})$ is the conformal block. The conformal block $g_O(z, \bar{z})$ contains contribution of operator-O and its descendants. A closed form expression for conformal block was first computed by Dolan and Osborne [7, 8]. The form of $g_O(z, \bar{z})$ is completely fixed by conformal symmetry, representation of O (intermediate operator) and representation of ϕ (external operator). Let L_{ab} be the generator of conformal algebra $SO(d+1, 1)$ with Casimir of the representation $C = -\frac{1}{2} L_{ab} L^{ab}$. We first define $\mathcal{L}_i^{ab}$ as the action of differential operator L_{ab} acting on $\phi(x_i)$. The Casimir acting on the first two operators is,

$$\mathcal{D}_{1,2} \equiv -\frac{1}{2} \left(\mathcal{L}_1^{ab} + \mathcal{L}_2^{ab} \right) \left(\mathcal{L}_{ab,1} + \mathcal{L}_{ab,2} \right) \, . \tag{1.31}$$

The action on the block is give as [7, 8],

$$\mathcal{D} g_{\Delta,\ell}(u, v) = \lambda_{\Delta,\ell} g_{\Delta,\ell}(u, v) \, . \tag{1.32}$$

The eigenvalues of the Casimir are $\lambda_{\Delta,\ell} = \Delta(\Delta - d) + \ell(\ell + d - 2)$ and the differential operator in $z, \bar{z}$ coordinate is given as,

$$\mathcal{D} = 2 \left(z^2(1-z)\partial_z^2 - z^2 \partial_z \right) + 2 \left(\bar{z}^2(1-\bar{z})\partial_{\bar{z}}^2 - \bar{z}^2 \partial_{\bar{z}} \right) + 2(d-2) \frac{z\bar{z}}{z - \bar{z}} \left((1-z)\partial_z - (1-\bar{z})\partial_{\bar{z}} \right) . \tag{1.33}$$

To solve the differential equation, asymptotic condition $x_{12} \to 0$ in (1.14) is also required. Putting everything together we obtain the following solution for conformal blocks in 4 dimensions,

$$g_{\Delta,\ell}^{(4d)}(u, v) = \frac{z\bar{z}}{z - \bar{z}} \left(k_{\Delta+\ell}(z) k_{\Delta-\ell-2}(\bar{z}) - k_{\Delta-\ell-2}(z) k_{\Delta+\ell}(\bar{z}) \right) \, , \tag{1.34}$$

where,

$$k_\beta(x) \equiv x_2^{\beta/2} F_1\left(\frac{\beta}{2}, \frac{\beta}{2}, \beta, x\right) \qquad \beta = \Delta + \ell\,. \tag{1.35}$$

A closed form expression for conformal block only exist in even dimensions. For odd dimensions one has to resort to series expansions.

1.3.2 Crossing Symmetry

OPE of local operators follow the associativity law. In the equation below the brackets refer to OPE performed,

$$((\phi_1\phi_2)\phi_3) = (\phi_1(\phi_2\phi_3)) \tag{1.36}$$

This associativity gives rise to two different ways of computing the four-point correlator. In s-channel OPE of $\phi(x_1), \phi(x_2)$ and $\phi(x_3), \phi(x_4)$ is computed separately and in t-channel OPE of $\phi(x_1), \phi(x_4)$ and $\phi(x_2), \phi(x_3)$ is computed separately. Since it is the same four-point correlator that is computed, both the channels must be equal (Figure 1.8). This is known as crossing symmetry.

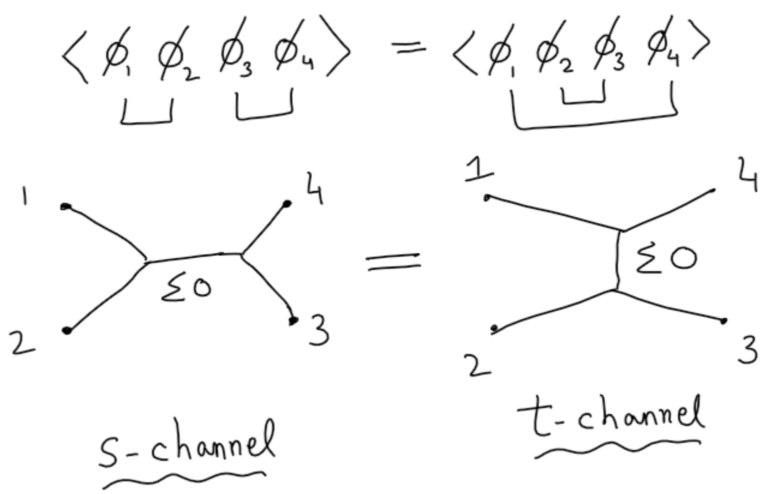

Figure 1.8: Crossing symmetry.

Under crossing symmetry the configuration of operators changes in the following manner,

$$u \longleftrightarrow v\,. \tag{1.37}$$

The four point correlator (of identical scalars) under the crossing symmetry is,

$$\frac{g(z,\bar{z})}{x_{12}^{2\Delta_\phi}x_{34}^{2\Delta_\phi}} = \frac{g(1-z,1-\bar{z})}{x_{14}^{2\Delta_\phi}x_{23}^{2\Delta_\phi}}\,. \tag{1.38}$$

Henceforth we will stick to $z, \bar{z}$ notation. The above equation simplifies to,

$$g(z,\bar{z}) = \frac{(z\bar{z})^{\Delta_\phi}}{((1-z)(1-\bar{z}))^{\Delta_\phi}}g(1-z,1-\bar{z}) \tag{1.39}$$

This is the **bootstrap equation**. Since we are working with identical external scalars the intermediate operators appearing in the expansion of CPW on both channels are the same. Both sides of (1.39) contain infinitely many terms in $d \geq 3$ dimensions[7]. The bootstrap equation is highly non-trivial to solve. Progress was made using numerical linear programming methods in the seminal work of Rattazzi, Rychkov, Tonni and Vichi in [9] to bound scaling dimensions of scalars. Over the last decade significant numerical work has been done in 3D Ising CFT, O(N) models and other CFTs in various dimensions [10, 11, 12, 13, 14]. These numerical methods yield the most precise calculation of critical exponents in 3d Ising Models [14]. In this work we aim to solve (1.39) using analytic methods. The next few sections are dedicated to progress using analytic methods.

1.3.3 Unitarity Bounds

Bootstrap equation constrains the CFT-data and with that, the space of CFTs. It turns out that unitarity imposes strict lower bounds on the scaling dimensions of operators. The bounds are,

$$\Delta \geq \begin{cases} \frac{d-2}{2} & (\ell = 0) \\ \ell + d - 2 & (\ell > 0) \end{cases} \tag{1.40}$$

[7]This will be explained in the next section.

The unit operator is the only operator that has scaling dimension 0. The unitarity bounds are computed by calculating inner product of operators. Unitarity also imposes reality condition on the three-point coefficients $C_{\phi\phi O}$. This turns out to be very important and it is the main reason why the whole machinery of bootstrap works.

1.4 Lightcone Bootstrap

To make progress towards solving (1.39) analytically it seems reasonable to takes certain limits (arrangements of operators) to simplify the crossing equation. One such limit is lightcone (or double lightcone) limit, which is $u \to 0$ limit of the crossing equation. Physically this implies that one operator approaches the lightcone of the other. We expand the crossing equation in terms of conformal blocks and three-point coefficients,

$$(z\bar{z})^{-\Delta_\phi} \sum_{\mathcal{O}} C^2_{\phi\phi\mathcal{O}} g_{\Delta,\ell}(z,\bar{z}) = ((1-z)(1-\bar{z}))^{-\Delta_\phi} \sum_{\mathcal{O}} C^2_{\phi\phi\mathcal{O}} g_{\Delta,\ell}(1-z, 1-\bar{z})\,. \tag{1.41}$$

In the above equation ϕ is the external scalar in the 4-point correlator $\langle\phi\phi\phi\phi\rangle$ and $\mathcal{O}$ is the intermediate channel operator. We take the following limit $z \ll 1-\bar{z} \ll 1$[8]. In this limit the operator approaches two lightcones instead of one. Hence this should be called "double lightcone limit", unfortunately in literature this is still referred to as lightcone limit. Following [15], we utilize the following relabelling $\bar{z} \to 1-\bar{z}$ to transform the lightcone limit as, $z \ll \bar{z} \ll 1$. The right hand side of (1.41) can now be expanded in small $\bar{z}$,

$$g_{\Delta,\ell}(\bar{z}, 1-z) = \bar{z}^h k_{2\bar{h}}(1-z) + O\left(\bar{z}^{h+1}\right)\,, \tag{1.42}$$

where,

$$k_{2h}(x) = x^h_2 F_1(h,h,2h,x)\,, \tag{1.43}$$

[8]This is the lightcone limit in $z, \bar{z}$ coordinates.

where h is notation for half twist and $\bar{h}$ is conformal spin (we later denote this as β),

$$h \equiv \frac{\Delta - \ell}{2} = \frac{\tau}{2}, \qquad \bar{h} \equiv \frac{\Delta + \ell}{2} = \frac{\tau}{2} + \ell\,. \tag{1.44}$$

The left side of (1.41) simplifies to $z^{-\Delta_\phi}(1 + O(\bar{z}))$. The overall crossing equation becomes,

$$z^{-\Delta_\phi} + \ldots = \sum_{\mathcal{O}} C^2_{\phi\phi\mathcal{O}} \bar{z}^{h-\Delta_\phi} k_{2\bar{h}}(1-z) + \ldots \tag{1.45}$$

We still have to take the small z limit in the right hand side. In this limit the right side generates a logarithmic singularity,

$$\lim\nolimits_{z\to 0} k_{2\bar{h}}(1-z) \sim -\log(z) + O(z\log(z)) \tag{1.46}$$

We have encountered a puzzle, the RHS of (1.45) has a logarithmic singularity (in $z \to 0$ limit) and LHS has polynomial singularity. The way to resolve this puzzle is to have an infinite sum on the right hand side (infinite operators). Summing over infinitely many terms enhances the logarithmic singularity to polynomial. We explain this process using a toy example first.[9]

1.4.1 Toy Example

We consider the following series expansion,

$$\lim_{z\to 0} \sum_{n=0}^{\infty} z e^{-nz}\,. \tag{1.47}$$

Summing up the series and then taking the limit results in the following,

$$\lim_{z\to 0} \frac{e^z z}{e^z - 1} = 1\,. \tag{1.48}$$

However, if the limit was taken first then each term in the series would vanish and the final result would be 0. This discrepancy is due to the fact that the sum over infinitely many terms and the

[9]This example was demonstrated by David Simmons-Duffin during TASI school.

limit do not commute. The exponent part of the above sum has the following behaviour,

$$\sum_{n=0}^{\infty} e^{-nz} = \frac{e^z}{e^z - 1} \,. \tag{1.49}$$

Each term on the left side is regular at $z = 0$, however the sum of all the terms gives rise to divergence at $z = 0$. Summing over infinite terms “enhances" divergence.

1.4.2 Back to Blocks

Just as the toy example above, the discrepancy in (1.45) can be resolved by summing the right hand side over infinitely many operators. The power law behaviour can only come to fruition if the right hand side has operators having twist $2\Delta_\phi$ and having all infinite spins. These type of operators are called double twist operators and they have the following schematic form,

$$[\phi, \phi]_{n,l} = \phi \partial^{\mu_1} \cdots \partial^{\mu_t} \partial^{2n} \phi \tag{1.50}$$

These can be thought of as being bound state of two operators ϕ. The behaviour of OPE coefficients of the double twist operators was computed in [16] using AdS/CFT to be (in the large $\bar{h}$ limit),

$$C^2_{\phi\phi[\phi\phi]}(\bar{h}) \sim \frac{2^{3-2\bar{h}}\sqrt{\pi}}{\Gamma(\Delta_\phi)^2} \bar{h}^{-2\Delta_\phi - \frac{3}{2}} \,. \tag{1.51}$$

In small z and large $\bar{h}$ (1.45) has the following form,

$$k_{2\bar{h}}(1-z) \approx 2^{2\bar{h}} \sqrt{\frac{\bar{h}}{\pi}} K_0(2\bar{h}\sqrt{z}) \quad (\bar{h} \gg 1, 2\bar{h}\sqrt{z} \text{ fixed }) \,. \tag{1.52}$$

We combine (1.51), (1.52) and perform the integral over $\bar{h}$

$$\sum_{\mathcal{O} \in [\phi\phi]_0} C^2_{\phi\phi O} k_{2\bar{h}}(1-z) \approx \frac{1}{2} \int d\bar{h} \frac{8}{\Gamma\left(\Delta_\phi\right)^2} \bar{h}^{2\Delta_\varphi - 1} K_0(2\bar{h}\sqrt{z}) = z^{-\Delta_\diamond} \,. \tag{1.53}$$

The polynomial behaviour of (1.45) is reproduced by the double-twist operators. The scaling dimension of the double twist operator is $[\phi, \phi]_{n,\ell} = 2\Delta_\phi + 2n + \ell$. In a generalized free theory (GFT is free theory, where correlators are simply wick contractions) the left side of 1.45 is exact and there are no correction terms. In GFT the result derived above holds exactly [17, 18]. Arbitrary interacting CFT in $d \geq 3$ contains an infinite number of double twist operator of a similar form discussed above but with a slight addition. The scaling dimensions are,

$$[\phi, \phi]_{n,\ell} = 2\Delta_\phi + 2n + \ell + \gamma(n, \ell)\,. \tag{1.54}$$

The addition, $\gamma(n, \ell)$ is called the anomalous dimensions. It is present only in interacting theories and it asymptotically goes to zero in the large spin limit. This is a universal behaviour in CFT.

1.5 Inversion Formula

In [19] a formula that inverts the partial-wave expansion of a four-point function was developed. This formula provides access to anomalous dimension and OPE coefficients. In this section we review the inversion formula. We start with the conformal partial wave and perform a spectral decomposition following [20],

$$\mathcal{G}(z, \bar{z}) = 1 + \sum_{J=0}^{\infty} \int_{d/2-i\infty}^{d/2+i\infty} \frac{d\Delta}{2\pi i} c(J, \Delta) F_{J,\Delta}(z, \bar{z}) \tag{1.55}$$

The OPE functional $c(J, \Delta)$ contains poles at the location of physical operators. We close the contour to pick up these physical poles. The function $F_{J,\Delta}(z, \bar{z})$ can be decomposed in terms of physical (Δ) and shadow ($d - \Delta$) conformal blocks,

$$F_{J,\Delta}(z, \bar{z}) = \frac{1}{2} \left(G_{\Delta,J}(z, \bar{z}) + \frac{K_{J,d-\Delta}}{K_{J,\Delta}} G_{d-\Delta,J}(z, \bar{z}) \right)\,, \tag{1.56}$$

where the coefficients are,

$$K_{J,\Delta} = \frac{\Gamma(\Delta - 1)}{\Gamma\left(\Delta - \frac{d}{2}\right)} \kappa_{J+\Delta}, \quad \kappa_\beta = \frac{\Gamma\left(\frac{\beta}{2} - a\right) \Gamma\left(\frac{\beta}{2} + a\right) \Gamma\left(\frac{\beta}{2} - b\right) \Gamma\left(\frac{\beta}{2} + b\right)}{2\pi^2 \Gamma(\beta - 1) \Gamma(\beta)}\,. \tag{1.57}$$

$F_{J,\Delta}(z,\bar{z})$ in (1.56) are orthogonal and can be used to invert the equation to get the OPE functional,

$$c(J,\Delta)=\mathcal{N}(J,\Delta)\int d^2z\mu(z,\bar{z})F_{\Delta,J}(z,\bar{z})\mathcal{G}(z,\bar{z})\,, \tag{1.58}$$

where the normalization and measure are given as,

$$\mathcal{N}(J,\Delta)=\frac{\Gamma\left(J+\frac{d-2}{2}\right)\Gamma\left(J+\frac{d}{2}\right)K_{J,\Delta}}{2\pi\Gamma(J+1)\Gamma(J+d-2)K_{J,d-\Delta}}\qquad \mu(z,\bar{z})=\left|\frac{z-\bar{z}}{z\bar{z}}\right|^{d-2}\frac{((1-z)(1-\bar{z}))^{a+b}}{(z\bar{z})^2}\,. \tag{1.59}$$

Simon Caron-Huot in [19] noted that when going from Euclidean to Lorentzian in (1.58) the correlator develops branch cuts. By deforming the contour the discontinuities of the branch cuts can be captured. To extract OPE data associated to the s-channel of four-point function the final Lorentzian inversion formula is,

$$C^t(\Delta,J)=\frac{\kappa_{J+\Delta}}{4}\int_0^1 dzd\bar{z}\mu(z,\bar{z})G_{J+d-1,\Delta+1-d}(z,\bar{z})\,\mathrm{dDisc}[\mathcal{G}(z,\bar{z})]\,, \tag{1.60}$$

where μ is the measure,

$$\mu(z,\bar{z})=\left|\frac{z-\bar{z}}{z\bar{z}}\right|^{d-2}\frac{((1-z)(1-\bar{z}))^{a+b}}{(z\bar{z})^2}\,. \tag{1.61}$$

dDisc is the double discontinuity around branch cuts and $G_{J+d-1,\Delta+1-d}(z,\bar{z})$ is the inverting kernel conformal block. The poles of $C(\Delta,J)$ encode the squared OPE coefficients $C_{\mathcal{O}}=-\operatorname*{Res}_{\Delta=\Delta_O}C\left(\Delta,J_{\mathcal{O}}\right)$. The higher order poles of function $C(\Delta,J)$ encode powers of anomalous dimensions.

$$c(\Delta,J)\sim\sum_{O_j}\frac{-C_{\mathcal{O}_j}}{\Delta-J-2\Delta_\varphi-\gamma_J}+\cdots=\sum_{p=0}^{\infty}\sum_{O_j}\frac{-C_{\mathcal{O}_j}\gamma_J^p}{(\Delta-J-2\Delta_\varphi)^{p+1}}+\dots \tag{1.62}$$

We will use the inversion formula to compute anomalous dimensions in a later chapter.

1.6 Contribution

In this section we will briefly list down our contributions in the field of CFT structure and analytic. These three projects are described in their respective chapters.

1.6.1 Defect CFT Correlators

Till now our analysis has been almost solely focused on "pure" CFTs. However real world systems are messy and have impurities associated to them. CFT theories with impurities are know as defect CFTs. Conformal theories with defects have a range of applications from condensed-matter physics to particle physics. Experimental systems inherently contain a boundary (a type of defect) making the study of defects essential. The simplest example of a defect is a co-dimension one defect, a boundary. Boundary defects (within the context of CFT) in 2 dimensions have been thoroughly studied by Cardy. Boundary defects in general dimensions were first studied beginning in [21] and an embedding formalism was set up for co-dimension one defects in [22]. The extension to general co-dimension defects was studied in [23]. Defects in conformal setting can only be hyperplane or spherical because of scale invariance.

A CFT with defects has both bulk operators and defect local operators (which reside on the defect). The defect local operators transform under the broken conformal group $SO(p+1,1)\times SO(q)$ where $p+q=d$ (q is the co-dimension of the defect). In addition to the CFT data of the bulk sector, there is also the CFT data of the defect sector and the couplings between the two sectors. In this work we will refer to the entire theory with both the sectors as a *defect CFT*. The presence of a defect induces a rich structure in the bulk sector. For example, a bulk local operator (O) near a defect can be expanded in terms of defect local operators ($\hat{O}$),

$$O(x^\mu)\sim\sum_k b_{O\hat{O}_k}\frac{\hat{O}_k(x^a)}{|x^i|^{\Delta-\hat{\Delta}}}+\dots, \tag{1.63}$$

where x^a and x^i are coordinates parallel and perpendicular to the defect respectively. The decomposition (1.63) leads to bulk local operators having non-zero vacuum expectation values. We can also expand two defect operators in terms of other defect operators (regular OPE),

$$\hat{O}_1(x^a)\hat{O}_2(y^a) \sim \sum_k \hat{f}_{12k} \frac{\hat{O}_k(y^a)}{|x^a - y^a|^{\Delta_1+\Delta_2-\hat{\Delta}_k}} + \dots . \tag{1.64}$$

The defect sector behaves like an ordinary p-dimensional CFT with $SO(p+1,1)$ as its conformal group and an additional $SO(q)$ global symmetry. Since the defect sector is exchanging energy with the bulk there is no conserved stress-energy tensor for the theory living on the defect.

Correlators in a defect CFT have been studied to a much lesser extend compared to regular CFT. In our work described in the next chapter, we fill this gap and compute correlators for arbitrary representation in defect CFT.

1.6.2 Analytics of Double Twist

As mentioned before, any CFT can be specified by giving its scaling dimensions and three-point coefficient. Crossing symmetry imposes constraints on the CFT data and has been conjectured to fix it completely. A general property of CFT is that in $d > 2$ they contain an infinite number of primaries in the form of double twist operators which we discussed before. In interacting theories the scaling dimension of double twist operators gets and additional contribution, $\gamma^{\Delta,J}$, the anomalous dimension. $\gamma^{\Delta,J}$ vanishes in the case of a free theory and is non-zero only in interacting theories. Anomalous dimension of double twist operators has a universal behaviour in arbitrary conformal field theories and we calculate $\gamma^{\Delta,J}$ for any d-dimensional CFT. On a technical note we have used integral representation of conformal blocks (Mellin space) to obtain a closed form expression for conformal blocks in (1.60) for identical scalar operators. We compute anomalous dimension due to arbitrary spin-J exchange in a closed form expression. In addition to this we also compute corrections to OPE coefficients for double twist operators for a general d dimension CFT. To our knowledge the general result has never been computed before.

1.6.3 Relation to Diagrammatic Expansion

The traditional approach of solving Quantum field theories is using perturbative diagrammatic expansion (Feynman diagrams). These techniques have been employed to CFTs like Wilson-

Fischer theory as well. Since CFT can be solved via crossing symmetry (bootstrap) as well, we set out to find relation between diagrammatic expansion and conformal correlator expansion for Wilson-Fischer theory in [24].

Our goal is to show parity between diagrammatic expansion and conformal correlator expansion. We evaluate the perturbative diagrams in position space (as conformal correlators are computed in position space). To make calculations simple we have chosen the $z \to 0$ limit of calculations. Wilson-Fisher [25, 26] theory consists of a single scalar and resides in $d = 4 - \epsilon$ dimensions. We first calculate tree and one loop diagram in this theory,

$$\begin{aligned}
\text{tree} : &\int \frac{d^4x_6}{x_{16}^2\, x_{46}^2\, x_{36}^2\, x_{26}^2} = \log(1-\bar{z})\frac{\log(z)-\log(\bar{z})}{\bar{z}} \equiv \log(1-\bar{z})B_0 \\
\text{1-loop} : &\int \frac{d^4x_5\, d^4x_6}{x_{15}^2\, x_{45}^2\, x_{56}^4\, x_{26}^2\, x_{36}^2} \\
&= \log(1-\bar{z})\Big(\frac{\log(z)-\log(\bar{z})}{4\bar{z}}\Big) + \log^2(1-\bar{z})\Big(\frac{\zeta_2 - \mathrm{Li}_2(1-\bar{z}) + 2\log(z) - 2\log(\bar{z})}{2\bar{z}}\Big) \\
&\equiv \log(1-\bar{z})\Big(\frac{B_0}{4}\Big) + \log^2(1-\bar{z})\Big(\frac{B_1}{4} + B_0\Big)
\end{aligned} \tag{1.65}$$

B_0, B_1 are functions that repeat at each discontinuity $\log(1-\bar{z})$. On expanding the conformal correlator in small coupling we obtain exactly the same functions at double discontinuities. We start with the conformal correlator $\langle\phi\phi\phi\phi\rangle$ and expand it in small coupling-g. $O(g)$ term is absent but we get the following results for higher orders,

$$O\left(g^2\right) : -\log(1-\bar{z})^2\frac{B_0}{4}, \quad O\left(g^3\right) : \log(1-\bar{z})^2\frac{B_1}{4} - \log(1-\bar{z})^3\frac{B_0}{24} \tag{1.66}$$

We find similar functions appearing in conformal correlator expansion. We have repeated this experment to higher order in both the perturbative and correlator expansion and again find similar functions appearing in both the expansions. In addition to this we developed a novel method to expand conformal correlators using the Mellin space representation. This allows one to expand correlators in arbitrary space-time dimensions. This was not possible with previous methods of computation.

2. CORRELATORS OF MIXED SYMMETRY OPERATORS IN DEFECT CFT*

Crossing symmetry relations constrain the data of a CFT. These equations can be solved numerically (e.g. [9, 27]) or analytically (e.g. [17]). An ordinary CFT gives rise to a crossing relation at the four-point correlator level. However a defect CFT gives rise to crossing relations starting at the two-point correlator level. The knowledge of correlation functions (tensor structures) is essential in the study of crossing relations. In [23] tensor structures for symmetric traceless operators were computed for two-point correlators. In this chapter we build upon those results and extend it to n-point correlators of operators in arbitrary mixed symmetry representations. In particular, we compute all possible invariants and tensor structures that could arise in a one-point, two-point and three-point correlator of various bulk and defect operators. We also indicate the invariants that could arise in an n-point correlator. One and two-point correlators for defects in arbitrary representations of $SO(q)$ are also computed. The knowledge of correlators is essential in initiating the bootstrap program for defect CFTs. This chapter is based on [28] by the author and his collaborator.The knowledge of correlators is essential in initiating the bootstrap program for defect CFTs. This chapter is based on [28] by the author and his collaborator.

2.1 Formalism

2.1.1 Encoding Tensors as Polynomials

We present a very quick review of the process of encoding tensors as polynomials in this section. For a detailed analysis the reader may refer to [29]. The encoding of tensors as polynomials makes computation much easier to handle. Consider a generic mixed symmetry representation of the $SO(d+1,1)$ group given by a Young diagram:

*Reprinted with permission from "Correlators of Mixed Symmetry Operators in Defect CFTs" by S. Guha and B. Nagaraj, 2018, *JHEP* 2018 : 10, Copyright [2018] by the authors.

$\lambda =$ 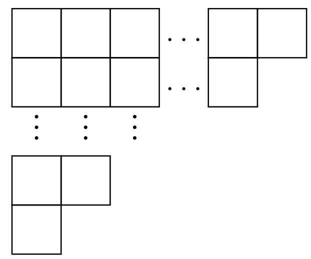 .

The Young diagram can be parametrized in two ways. The first way is to provide the heights of columns $h \equiv (h^{(1)}, h^{(2)}, \ldots, h^{(n^C)})$, where $h^{(i)}$ is the height of the i^{th} column and n^C is the total number of columns. The second way is to provide the lengths of rows $l \equiv (l^{(1)}, l^{(2)}, \ldots, l^{(n^R)})$, where $l^{(i)}$ is the length of the i^{th} row and n^R is the total number of rows. Given these parametrizations, the total number of boxes is given by,

$$|\lambda| = \sum_{i=1}^{n_C} h^{(i)} = \sum_{i=1}^{n_R} l^{(i)}. \tag{2.1}$$

A mixed symmetric tensor can be encoded as a polynomial by contracting its indices using one of the two sets of auxiliary vectors $\boldsymbol{\theta} = (\theta^{(1)}, \theta^{(2)}, \ldots, \theta^{(n^C)})$ and $\boldsymbol{z} = (z^{(1)}, z^{(2)}, \ldots, z^{(n^R)})$. The vectors $\boldsymbol{\theta}$ are anti-commuting and encode the polynomial in an anti-symmetric basis, while the vectors $\boldsymbol{z}$ are commuting and encode the polynomial in a symmetric basis. Across a row $\boldsymbol{z}$ vector remains the same and down a column $\boldsymbol{\theta}$ remains the same. As an example for both bases,

$$\begin{array}{|c|c|c|}\hline z_1 & z_1 & z_1 \\ \hline z_2 & z_2 & z_2 \\ \hline \end{array} \qquad \begin{array}{|c|c|c|}\hline \theta_1 & \theta_2 & \theta_3 \\ \hline \theta_1 & \theta_2 & \theta_3 \\ \hline \end{array}\,.$$

A given Young representation is symmetric along the rows and anti-symmetric along the columns. Separate columns (rows) are symmetric (anti-symmetric) among themselves. The grassmanian nature of $\boldsymbol{\theta}$-vectors is the following,

$$\theta^{(i)}_m \theta^{(j)}_n = (-1)^{\delta_{ij}} \theta^{(j)}_n \theta^{(i)}_m, \tag{2.2}$$

where indices m and n label the components of the auxiliary vectors. This relation encodes the anti-symmetry of $\boldsymbol{\theta}$-vectors only within the same column. We choose to do anti-symmetrization first using $\boldsymbol{\theta}$-vectors and then impose symmetrization by the action of $(z{\cdot}\partial_\theta)$ derivatives. Therefore, a mixed symmetry tensor can be encoded as:

$$\tilde{f}(\boldsymbol{z}) = \prod_{i=1}^{n_R} \prod_{j=1}^{\min(l^{(i)},n^C)} \left(z^{(i)} \cdot \partial_{\theta^{(j)}}\right) f(\boldsymbol{\theta}), \tag{2.3}$$

where,

$$f(\boldsymbol{\theta}) = \theta^{(1)}_{m_1} \dots \theta^{(1)}_{m_{h_1}} \theta^{(2)}_{m_{h_1+1}} \dots \theta^{(2)}_{m_{h_1+h_2}} \dots \theta^{(n_C)}_{m_{h_1+\dots+h_{n_C-1}+1}} \dots \theta^{(n_C)}_{m_{|\lambda|}} f^{m_1 \dots m_{|\lambda|}}. \tag{2.4}$$

The tracelessness condition can be imposed by demanding that certain dot products vanish:

$$\begin{aligned} f^{m_1 \dots m_{|\lambda|}} \text{ traceless} &\Longleftrightarrow f(\boldsymbol{\theta})|_{\theta^{(i)} \cdot \theta^{(j)}=0} \\ &\Longleftrightarrow \tilde{f}(\boldsymbol{z})|_{z^{(i)} \cdot z^{(j)}=0}. \end{aligned} \tag{2.5}$$

To explicitly see the procedure of encoding tensors as polynomials, we consider two examples involving a symmetric two-tensor $S^{(mn)}$ and an anti-symmetric two-form $B^{[mn]}$. The two representations are,

$$A^{(mn)} = \begin{array}{|c|c|} \hline \theta^{(1)} & \theta^{(2)} \\ \hline \end{array} \qquad B^{[mn]} = \begin{array}{|c|} \hline \theta^{(1)} \\ \hline \theta^{(1)} \\ \hline \end{array}.$$

We first convert the tensors into polynomial by contracting them with appropriate $\boldsymbol{\theta}$-vectors,

$$A^{mn} \to A(\boldsymbol{\theta}) = A^{mn} \theta^{(1)}_m \theta^{(2)}_n, \qquad B^{mn} \to B(\boldsymbol{\theta}) = B^{mn} \theta^{(1)}_m \theta^{(1)}_n. \tag{2.6}$$

Once the polynomials have been constructed in $\boldsymbol{\theta}$-basis, symmetrization can be applied (2.3),

$$\left(z^{(1)} \cdot \partial_{\theta^{(1)}}\right) \left(z^{(1)} \cdot \partial_{\theta^{(2)}}\right) A(\boldsymbol{\theta}), \qquad \left(z^{(1)} \cdot \partial_{\theta^{(1)}}\right) \left(z^{(2)} \cdot \partial_{\theta^{(1)}}\right) B(\boldsymbol{\theta}). \tag{2.7}$$

Evaluating them we obtain the following result,

$$A^{mn} z^{(1)}_m z^{(1)}_n, \qquad B^{mn}(z^{(1)}_m z^{(2)}_n - z^{(1)}_n z^{(2)}_m). \tag{2.8}$$

Both the symmetric and anti-symmetric properties of the tensors have been captured.

So far, we have encoded a mixed symmetric tensor in the d-dimensional physical space where the CFT lives. In the next section, we will encode the tensor in a higher dimensional space-time where the action of the conformal group becomes linear.

2.1.2 Embedding Formalism

We will briefly review the embedding space formalism and the procedure to encode mixed symmetric operators as polynomials in this space. For a detailed description of embedding space formalism, we refer the reader to [4, 29]. The conformal group of a d-dimensional Euclidean CFT is $SO(d+1,1)$. This is also the Lorentz group in a $(d+2)$-dimensional Minkowski space. The $(d+2)$-dimensional space-time which we refer to as embedding space is the natural space associated with conformal transformations [6]. The non-linear action of a conformal transformation in d-dimensional space becomes a linear Lorentz transformation in the embedding space. Let P denote the coordinates of the embedding space. Points in the physical space are identified with null rays in the embedding space,

$$P^2 = 0, \qquad P \sim \alpha P \quad \text{where } \alpha \in \mathbb{R}^+. \tag{2.9}$$

The first relation implies that everything in the theory lives on the light cone. We adopt lightcone coordinates to represent points on the cone. The second relation implies a gauge freedom in the identification of P up to re-scaling. We can fix this gauge by setting $P^+ = 1$. This slice of the null cone is known as the Poincaré section. Physical points in $x \in \mathbb{R}^d$ are mapped to null points in this Poincaré section:

$$x \to P^M|_x = (P^+, P^-, P^m) = (1, x^2, x^m). \tag{2.10}$$

The metric of the embedding space is the Lorentzian metric of $(d+1,1)$ space-time,

$$P \cdot P = \eta_{MN} P^M P^N = -P^+ P^- + \delta_{mn} P^m P^n. \tag{2.11}$$

Operators in the physical space can be lifted to the embedding space. Consider a mixed symmetry tensor $f_{m_1 \ldots m_{|\lambda|}}(x)$ of dimension Δ in the physical space. This tensor can be uplifted to $F_{M_1 \ldots M_{|\lambda|}}(P)$ in the embedding space and satisfies the following conditions:

- Homogeneity: $F_{M_1 \ldots M_{|\lambda|}}(\alpha P) = \alpha^{-\Delta} F_{M_1 \ldots M_{|\lambda|}}(P)$,
- Transversality: $P^{M_i} F_{M_1 \ldots M_i \ldots M_{|\lambda|}} = 0$.

Operators in embedding space can once again be encoded as polynomials. We will use the auxiliary vectors $\boldsymbol{\Theta} = (\Theta^{(1)}, \Theta^{(2)}, \ldots, \Theta^{(n^C)})$ to encode anti-symmetry and
$\boldsymbol{Z} = (Z^{(1)}, Z^{(2)}, \ldots, Z^{(n^R)})$ to encode symmetry of the indices. We choose to write polynomials in the anti-symmetric basis (or $\boldsymbol{\Theta}$-basis) first and impose symmetrization via derivatives,

$$\tilde{F}(P, \boldsymbol{Z}) = \prod_{i=1}^{n_R} \prod_{j=1}^{\min(l^{(i)}, n^C)} \left(Z^{(i)}.\partial_{\Theta^{(j)}}\right) F(P, \boldsymbol{\Theta}), \tag{2.12}$$

where,

$$F(P, \boldsymbol{\Theta}) = \Theta^{(1)}_{M_1} \ldots \Theta^{(1)}_{M_{h_1}} \Theta^{(2)}_{M_{h_1+1}} \ldots \Theta^{(2)}_{M_{h_1+h_2}} \ldots \Theta^{(n^C)}_{M_{h_1+\ldots+h_{n^C-1}}+1} \ldots \Theta^{(n^C)}_{M_{|\lambda|}} F^{M_1 \ldots M_{|\lambda|}}(P). \tag{2.13}$$

Once again the tracelessness condition can be encoded by demanding that certain dot products vanish:

$$\begin{aligned} F^{M_1 \cdots M_{|\lambda|}}(P) \text{ traceless/ transverse} &\iff F(\boldsymbol{\Theta})|_{\Theta^{(p)} \cdot \Theta^{(q)}=0, P \cdot \Theta^{(p)}=0} \\ &\iff \tilde{F}(\boldsymbol{Z})|_{Z^{(p)} \cdot Z^{(q)}=0, P.Z^{(p)}=0}. \end{aligned} \tag{2.14}$$

The Θ and Z vectors satisfy the following properties,

$$\Theta^{(i)}_a \cdot \Theta^{(j)}_a = 0, \quad Z^{(i)}_a \cdot \Theta^{(j)}_a = 0, \quad Z^{(i)}_a \cdot Z^{(j)}_a = 0. \tag{2.15}$$

The subscript refers to the operator the auxiliary vectors are associated with while the superscript on the auxiliary vectors indicates the column(row) for the $\boldsymbol{\Theta}(\boldsymbol{Z})$-vectors. In a given Young representation, one $\boldsymbol{Z}$-vector is used for contractions across a row while one $\boldsymbol{\Theta}$-vector is used for contractions along a column. The transversality condition also means that any polynomial constructed out of $\boldsymbol{\Theta}$ and $\boldsymbol{Z}$-vectors should be invariant under the following shift,

$$\Theta_a^{(i)} \to \Theta_a^{(i)} + \alpha^{(i)} P_a, \quad Z_a^{(i)} \to Z_a^{(i)} + P_a. \tag{2.16}$$

Here $\alpha^{(i)}$ carries the same Grassmanian signature as $\Theta^{(i)}$. Any quantity constructed out of $\boldsymbol{\Theta}$ and $\boldsymbol{Z}$ must be invariant under this symmetry as well. In the rest of the paper we will construct invariant objects out of $\boldsymbol{\Theta}$ that satisfy the transversality and tracelessness condition. Transversality implies that the product of the auxiliary vectors with their respective P also vanish:

$$P_a \cdot \Theta_a^{(i)} = 0, \quad P_a \cdot Z_a^{(i)} = 0. \tag{2.17}$$

It is convenient to build all the invariant structures using C_{MN} (C-tensor) which is transverse by construction,

$$C_a^{(i)MN} = P_a^M \Theta^{(i)N} - P_a^N \Theta^{(i)M}. \tag{2.18}$$

$C^{(i)MN}$ is also the smallest unit of $\Theta^{(i)}$ that satisfies transversality. A similar C-tensor can be constructed out of $\boldsymbol{Z}$-vectors. All other invariant structures will be constructed by contractions of C-tensor with various position vectors (P_a) and C-tensors. Contractions of more than two $C^{(i)MN}$ can be written in terms of contractions of two $C^{(i)MN}$,

$$C_1^{MP} C_{2PR} C_3^{RN} = -\frac{1}{2}(C_1^{PR} C_{2PR}) C_1^{MN}. \tag{2.19}$$

Therefore, we do not need to go beyond two C-tensor terms. To recover the uncontracted notation of tensors from a polynomial, we act on them with the following Todorov differential operator,

$$D_M = \frac{d-2}{2} \frac{\partial}{\partial \Theta^M} + \Theta \cdot \frac{\partial}{\partial \Theta} \frac{\partial}{\partial \Theta^M}. \tag{2.20}$$

Todorov differential operator is constructed to recover traceless symmetric tensors from polynomials [30]. To recover free-indices for a spin-l operator we apply the derivative l times

$$O_{M_1 \cdots M_l}(P) = \frac{1}{l!(d/2-1)_l} D_{M_1} \cdots D_{M_l} O^l(P, \Theta^1 \cdots \Theta^l). \tag{2.21}$$

Here $(a)_l$ is the Polchhammer symbol. As discussed earlier, while constructing polynomials we first use an anti-symmetric basis and then apply derivatives to impose the symmetrizations. An equally valid approach would be to first write everything in a symmetric basis and then apply the anti-symmetrization via derivatives. We will commit to using the former approach for the rest of the paper. Owing to its inherent anti-symmetry, the $\boldsymbol{\Theta}$ basis usually has a lower number of tensor structures compared to $\boldsymbol{Z}$-basis. We reiterate that after taking the derivatives and projecting the results back to d-dimensions, the final result is basis-independent.

To encode conserved operators we need an additional constraint. Conserved operators in physical space satisfy,

$$\partial_m S^{mn\cdots} = 0. \tag{2.22}$$

To implement this in embedding space, first we need to free an index from the polynomial expression. This is implemented by acting with the Todorov derivative operator (2.20). Once an index has been freed, it can be contracted with a regular partial derivative to impose the conservation. Schematically it looks like:

$$\partial^M D_M S(\Theta) = 0. \tag{2.23}$$

A detailed discussion of conserved tensors with its subtleties is given in [4].

2.2 Embedding Formalism with a Defect

2.2.1 Defect

A defect is an extended object (operator) living in an ambient space. A q co-dimension defect breaks the full d-dimensional conformal group $SO(d+1,1)$ into $SO(p+1,1) \times SO(q)$ where $p + q = d$. Following [31, 23], such a defect is naturally identified in the embedding space as a q-dimensional time-like hyperplane intersecting the null cone. Projecting the intersection onto the Poincaré section results in defect in the physical space. Orientation of a hyperplane in the embedding space can be specified by providing a set of q vectors ($P_\alpha,\ \alpha = 1, \ldots, q$) that are orthogonal to it. The vectors P_α satisfy the following properties,

$$P_\alpha \cdot X = 0, \qquad X \cdot X = 0, \qquad P_\alpha \cdot P_\beta = \delta_{\alpha\beta}, \tag{2.24}$$

where X is a point on the null cone. The inner product between two vectors X and Y in the embedding space naturally splits into two separate inner products of the $SO(p+1,1)$ and $SO(q)$ group:

$$X \cdot Y = (\eta_{MN} - P_{\alpha M} P_{\alpha N})\, X^M Y^N + P_{\alpha M} P_{\alpha N} X^M Y^N. \tag{2.25}$$

It is convenient to split the coordinates into two sets: the first $p+2$ coordinates that are parallel to the defect and the last q coordinates that are transverse to the defect. We will use letters $A, B, ...$ to label the former and $I, J, ...$ to label the latter.

$$M = (A, I) \qquad A = 1, 2, \ldots, p+2 \qquad I = 1, 2, \ldots, q \tag{2.26}$$

The inner product (2.25) can be denoted as,

$$\begin{aligned} X \cdot Y &= (\eta_{MN} - P_{\alpha M} P_{\alpha N})\, X^M Y^N + P_{\alpha M} P_{\alpha N} X^M Y^N, \\ &= X \bullet Y + X \circ Y, \end{aligned} \tag{2.27}$$

where we have defined

$$\begin{aligned} &X \bullet Y \equiv (\eta_{MN} - P_{\alpha M} P_{\alpha N})\, X^M Y^N \\ &X \circ Y \equiv P_{\alpha M} P_{\alpha N} X^M Y^N. \end{aligned} \tag{2.28}$$

The above definitions allow us to make contact with the split representation used in [23] to study defects. In the physical space, $X \cdot Y \longrightarrow -(1/2)(x-y)^2$. Therefore equation (2.27) is merely stating that the square of the distance between two points is equal to sum of the squares of parallel and orthogonal distance to the flat defect. The perpendicular distance of a point (X) from a defect is given by,

$$P_{\alpha M} P_{\alpha N} X^M X^N = (P_\alpha \cdot X)(P_\alpha \cdot X) = X \circ X \,. \tag{2.29}$$

Formally we denote a q co-dimension defect as $D^q(P_\alpha)$. Projecting the intersection of the hyperplane and the null cone onto the Poincaré section yields either a flat or a spherical defect depending on the orientation of the hyperplane. We will briefly discuss the two types below.

2.2.1.1 Flat Defect

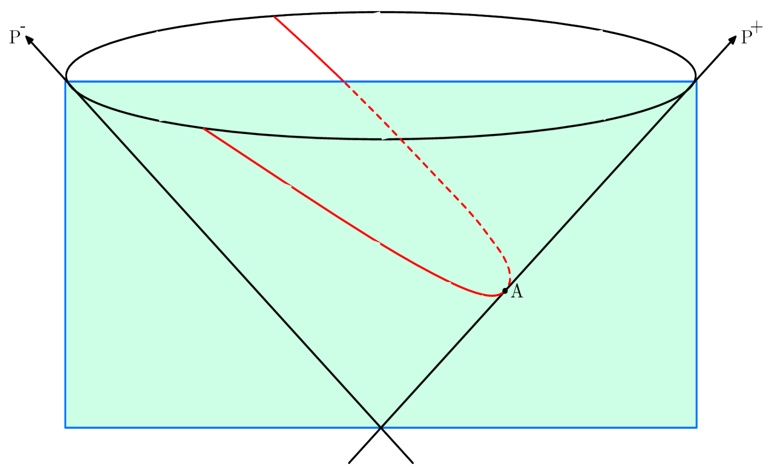

Figure 2.1: The intersection of a defect hyperplane with the Poincaré section.

A flat defect arises when the P^+-axis lies on the defect hyperplane. The intersection of the hyperplane with the Poincaré section results in only one point of intersection (Figure 2.1). Examples of flat defects include lines, planes and boundaries. Since P^+-axis lies on the hyperplane, we can conveniently choose the P_α vectors to be:

$$P_\alpha = (\overbrace{0,\ldots,0}^{p+2}, \underbrace{0,...,1,...,0}_{\text{1 at position } \alpha}) \qquad \alpha = 1,2,\ldots,q. \tag{2.30}$$

With the choice (2.30) for P_α vectors, we get

$$\begin{aligned} X \bullet Y &\equiv (\eta_{MN} - P_{\alpha M} P_{\alpha N})\, X^M Y^N = \eta_{AB} X^A Y^B \\ X \circ Y &\equiv P_{\alpha M} P_{\alpha N} X^M Y^N = \delta_{IJ} X^I Y^J. \end{aligned} \tag{2.31}$$

A bulk operator near a flat defect can be decomposed in terms of local operators living on the defect. This expansion is known as a bulk-to-defect expansion and in the embedding space looks like:

$$\Phi(P)|_D = \frac{b_{\Phi 1}}{(P \circ P)^{\Delta/2}} + \sum_{\hat{O}} \frac{b_{\Phi \hat{O}} \hat{O}(P)|_D}{(P \circ P)^{\frac{\Delta - \hat{\Delta}}{2}}} + \text{descendants.} \tag{2.32}$$

Each defect local operator ($\hat{O}$) in (2.32) appears with a coupling-strength $b_{\Phi\hat{O}}$. This expansion is brought about by constructing a quantizing sphere centered on the defect and enclosing the bulk operator. The state on the sphere can then be shrunk to the center using scaling transformation resulting in defect local operators. Evaluating non-vanishing $\langle \Phi \hat{O} \rangle$ is essential for enumerating the representations that occur in this expansion.

2.2.1.2 Spherical Defect

We obtain a spherical defect when the defect hyperplane does not contain the P^+-axis (Figure 2.2). Spherical defects are characterized by their radius and center [1] [31]. In addition to the bulk-to-defect expansion, there is an additional expansion channel known as the defect-to-bulk channel [31]. A spherical defect can be written in terms of bulk primaries placed at the center of the defect. This channel is defined by enclosing the defect, and any operators on it, by a quantizing sphere. The projected state on this sphere can be shrunk down to a point (at the center of the defect) using

[1] Since all lengths are relative in a conformal theory, the point at infinity (which is normalized as $\Omega = (0, 1, 0)$) acts as a reference point for the calculation of radius of the defect.

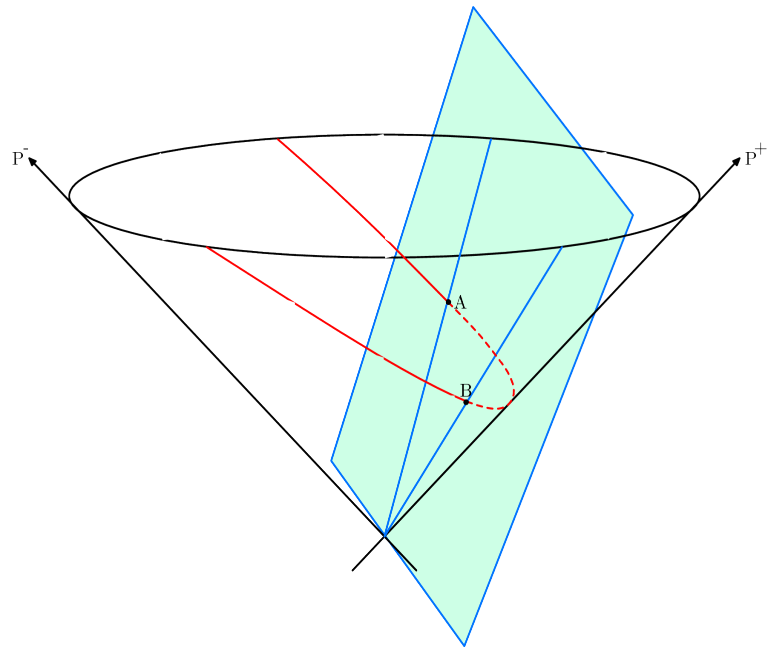

Figure 2.2: The intersection of a hyperplane (not containing $P^{+} - axis$) with the Poincaré section.

scaling transformation. Schematically this is represented by,

$$D^{q}(P_{\alpha}) = \sum_{\Phi} c_{\Phi 1}\Phi(C) + \text{descendants}. \tag{2.33}$$

In [32], it was shown that in the limit where radius of the defect is very small ($R \to 0$),

$$D^{q}(P_{\alpha}) = \sum_{\Phi} c_{\Phi 1} R^{\Delta}\Phi(C) + O(R^{2}). \tag{2.34}$$

Following a similar procedure, it can be shown that including a defect local operator $\hat{O}$, sitting on the defect, in the defect-to-bulk expansion gives a similar result with a different coefficient,

$$\hat{O}(Y)D^{q}(P_{\alpha}) = \sum_{\Phi} c_{\Phi\hat{O}} R^{\Delta}\Phi(C) + O(R^{2}). \tag{2.35}$$

If multiple defect local operators are present, then the OPE of defect local operators can be used multiple times to reduce all of them in terms of a single defect operator.

2.2.2 Formalism

Having seen how to incorporate a defect in embedding space, let us now concentrate on defining operators and fields in presence of a defect. Throughout this work, our main focus will be on the flat defect case. However the results we present in this section are equally applicable to the case with spherical defects. The difference between the two defects arises when projecting the embedding space result back to physical space. We now have to deal with two kinds of operators: bulk operators and defect operators. Bulk operators transform under the complete group $SO(d+1,1)$ while the defect operators transform under the broken group $SO(d-q+1,1) \times SO(q)$. The uplift of a bulk operator to the (broken) embedding space will once again have to satisfy homogeneity, transversality and tracelessness conditions defined in the previous section. All the inner products split into two invariants (2.27). This implies,

$$P_a \bullet \Theta_a^{(i)} = -P_a \circ \Theta_a^{(i)}, \qquad \Theta_a^{(i)} \bullet \Theta_a^{(j)} = -\Theta_a^{(i)} \circ \Theta_a^{(j)}. \tag{2.36}$$

Once again, we will use subscript in the embedding space vectors to identify different operators that might be under consideration. A similar relation holds for the $\boldsymbol{Z}$-vectors,

$$Z_a^{(i)} \bullet Z_a^{(i)} = -Z_a^{(i)} \circ Z_a^{(i)}. \tag{2.37}$$

Owing to the grassmanian nature of the $\boldsymbol{\Theta}$-vectors, in the split representation both of the products of Θ-vectors vanish individually for $(i=j)$:

$$\Theta_a^{(i)} \bullet \Theta_a^{(i)} = 0, \qquad \Theta_a^{(i)} \circ \Theta_a^{(i)} = 0. \tag{2.38}$$

Since all the operators are on the null cone,

$$P_a \bullet P_a = -P_a \circ P_a. \tag{2.39}$$

The C-tensor C^{MN} introduced in the previous section breaks into three units [23] - C^{AB}, C^{AI} and C^{IJ}. Fortunately not all of them are independent and these units follow the relation:

$$
\begin{aligned}
C^{(i)}_{AB} Q^A R^B &= \frac{P \bullet R}{P \circ G} C^{(i)}_{AI} Q^A G^I - \frac{P \bullet Q}{P \circ G} C^{(i)}_{AI} R^A G^I, \\
C^{(i)}_{IJ} Q^I R^J &= \frac{P \circ Q}{P \bullet G} C^{(i)}_{AI} G^A R^I - \frac{P \circ R}{P \bullet G} C^{(i)}_{AI} G^A Q^I.
\end{aligned} \tag{2.40}
$$

The above relations imply that all invariant-structures can be built out of just $C^{(i)}_{AI}$. To make a polynomial in embedding space, we contract its indices with $\boldsymbol{\Theta}$-vectors.

Defect local operators transform under the broken group $SO(p+1,1) \times SO(q)$. This implies that they carry separate quantum numbers corresponding to the parallel conformal group $SO(p+1,1)$ and the orthogonal group $SO(q)$. We will use auxiliary vectors $\{\Theta^{(i)}_{\hat{a}}, Z^{(i)}_{\hat{a}}\}$ and $\{\Phi^{(j)}_{\hat{a}}, W^{(i)}_{\hat{a}}\}$ corresponding to each broken group respectively. Position and auxiliary vectors associated with a defect operator are represented with a *hat* symbol(e.g. $P_{\hat{a}}$). Enumerating all possible bulk and defect position and auxiliary vectors:

$$
P_a, P_{\hat{a}}, \Theta^{(i)}_a, \Theta^{(i)}_{\hat{a}}, \Phi^{(i)}_{\hat{a}}, Z^{(i)}_{\hat{a}}, W^{(i)}_{\hat{a}}. \tag{2.41}
$$

Since a defect local operator lies on the defect hyperplane, the vectors associated to it have the following properties:

$$
P_{\hat{a}I} = 0, \quad \Theta^{(i)}_{\hat{a}I} = 0, \quad \Phi^{(i)}_{\hat{a}A} = 0, \quad Z^{(i)}_{\hat{a}I} = 0, \quad W^{(i)}_{\hat{a}A} = 0. \tag{2.42}
$$

The independent C-tensors for defect local operators are C^{AB} and C^{AI}.

$$
\begin{aligned}
C^{(i)AB}_{\hat{a}} &= P^A_{\hat{a}} \Theta^{(i)B}_{\hat{a}} - P^B_{\hat{a}} \Theta^{(i)A}_{\hat{a}} \\
C^{(i)AI}_{\hat{a}} &= P^A_{\hat{a}} \Phi^{(i)B}_{\hat{a}}
\end{aligned} \tag{2.43}
$$

There would be C-tensor for the $\boldsymbol{Z}$-basis as well, however they only amount to replacing the $\boldsymbol{\Theta}$-vectors with $\boldsymbol{Z}$-vectors. In this work, we call transverse objects constructed out of C-tensors as *invariants*. *Invariants* will serve as building blocks for *tensor structures*, which are the final structures appearing in correlators.

The number of independent invariants in **Θ**-basis can be obtained by considering all possible contractions between the position and auxiliary vectors that are under consideration (e.g. $P_a \bullet \Theta^{(i)}_{\hat{b}}$) minus the constraints imposed by demanding transversality of the auxiliary vector. Demanding transversality imposes a constraint for each Θ-vector (bulk or defect) however Φ-vectors impose no constraint as they are transverse by construction. If we ignore the fact that each auxiliary vector also has an i index (labelling the column number for Θ vector), then given n_1 bulk operators and n_2 defect operators, the number of independent invariants is:

$$3n_1^2 - 2n_1 + 2n_2^2 - 3n_2 + 5n_1 n_2. \tag{2.44}$$

We will provide another more rigorous derivation of the above relation in section (2.6) by listing down all possible independent invariants. It is essential to keep in mind that this relation only gives the number of independent invariants in the **Θ**-basis. The action of derivatives (to impose symmetrization) will reduce this number.

Unless otherwise stated we will work with parity-even invariants and tensor structures. Finally, we introduce a compact notation for position contractions involving bulk-bulk, bulk-defect and defect-defect operators.

$$P_{ab} = (P_a \circ P_b) \quad P_{a\hat{b}} = (-2P_a \bullet P_{\hat{b}}) \quad P_{\hat{a}\hat{b}} = (-2P_{\hat{a}} \bullet P_{\hat{b}}). \tag{2.45}$$

An additional benefit of using the **Θ**-basis is that the dependence on the co-dimension of the defect is made manifest due to anti-symmetry. The maximum number of a given $\Theta^{(i)}$ that can appear in a tensor structure is limited by the co-dimension of the defect (q). This limits the height of the Young representation.

2.3 One-Point Correlators

A distinguishing feature of a defect CFT is the non-vanishing nature of one-point correlators involving bulk local operators. Any bulk operator (near the defect) can be expanded in terms of defect operators (1.63,2.32). Since a one-point correlator of identity operator is non-zero in a CFT, (2.32) implies that a one-point correlator of a bulk operator is non-zero. Consider a bulk operator in an arbitrary representation λ.

$$\langle O_{\Delta,\lambda}(P_1, \mathbf{\Theta}_1)\rangle \tag{2.46}$$

Only one invariant can be constructed with a single bulk operator,

$$H_1^{(i,j)} = \frac{C_1^{(i)AI} C_{1AI}^{(j)}}{(P_1 \circ P_1)} \quad \text{where } i \neq j. \tag{2.47}$$

The parenthesis in (i,j) does not imply symmetrization. If the number of columns of the operator representation is l, then taking into account the i-index in the above equation we find that there are $l(l-1)/2$ possible invariants. The tensor structures appearing in the correlation function must be constructed out of $H_1^{(i,j)}$ and should satisfy the homogeneity and transversality constraints:

$$\langle O_{\Delta,\lambda}(P_1, \beta_1^{(i)}\Theta_1^{(i)})\rangle = (\beta_1^{(1)})^{h(1)} \cdots (\beta_1^{(l_1)})^{h(l_1)} \langle O_{\Delta,\lambda}(P_1, \mathbf{\Theta}_1)\rangle, \tag{2.48}$$

$$\langle O_{\Delta,\lambda}(\alpha P_1, \mathbf{\Theta}_1)\rangle = \alpha^{-\Delta_1} \langle O_{\Delta,\lambda}(P_1, \mathbf{\Theta}_1)\rangle. \tag{2.49}$$

The final form of a one-point correlator is obtained after taking appropriate derivatives (to impose symmetrization),

$$\langle O_{\Delta,\lambda}(P_1, \boldsymbol{Z}_1)\rangle = \left(Z_1^{\lambda_1} \cdot \partial_{\Theta_1}^{\lambda_1}\right) \frac{T_B(\mathbf{\Theta}_1)}{(P_1 \circ P_1)^{\Delta/2}}. \tag{2.50}$$

$T_B(\mathbf{\Theta}_1)$ is an appropriate tensor structure satisfying homogeneity and transversality. Let us consider some specific cases.

2.3.1 Symmetric Traceless

We begin by considering spin-l fields. The Young diagram for them is given as,

$$\begin{array}{|c|c|c|c|}\hline \Theta_1^{(1)} & \Theta_1^{(2)} & \cdots & \Theta_1^{(l)} \\ \hline \end{array}$$

One-point correlator has to be constructed out of (2.47). For a spin-l operator we obtain,

$$\langle O_{\Delta,l}(P_1, Z_1^{(1)})\rangle = \left(Z_1^{(1)} \cdot \partial_{\Theta_1^{(1)}}\right) \cdots \left(Z_1^{(1)} \cdot \partial_{\Theta_1^{(l)}}\right) \frac{T_B(\Theta_1, \Theta_2, \cdots, \Theta_l)}{(P \bullet P)^{\Delta/2}}. \tag{2.51}$$

T_B is a function of $H_1^{i,j}$. As an example, T_B for spin 2 field is,

$$T_B(\Theta_1, \Theta_2) = H_1^{(1,2)}. \tag{2.52}$$

For an odd-spin operator, it is not possible to write down any function that has the right homogeneity. Owing to this fact, a one-point correlator of an odd-spin operator is zero. Upon the application of the $Z\partial_\Theta$-derivatives on (2.52), we obtain the following result,

$$\langle O_{\Delta,l}(P_1, Z_1)\rangle = \frac{(H_{Z_1Z_1})^{l/2}}{(P \circ P)^{\Delta/2}}. \tag{2.53}$$

l is even in the above case and $H_{Z_1Z_1}$ is (2.47) with Θ_1 replaced by Z_1. When $q = 1$ (boundary defect) we observe that $H_{Z_1Z_1} = 0$ and only the scalar operator has a non-zero one point correlator. This has been pointed out in multiple references (e.g. [22]). The $\boldsymbol{Z}$-derivatives are particularly simple for the traceless symmetric case and they only amount to replacing all the $\boldsymbol{\Theta}$-vectors with a single $\boldsymbol{Z}$-vectors. We will utilize this trick in all the symmetric traceless cases that we encounter.

2.3.2 Forms

We find that the one-point correlator of any m-form vanishes when considering parity-even invariants. However, this is not true if we consider parity-odd invariants. We will discuss parity-odd cases later in section (2.7). With just one Θ, it is impossible to construct an invariant for a m-form.

2.3.3 Two Column Operator

Finally, we consider mixed symmetric operators in a two-column representation.

$$\begin{array}{|c|c|}\hline \Theta_1^{(1)} & \Theta_1^{(2)} \\ \hline \vdots & \vdots \\ \hline \Theta_1^{(1)} & \Theta_1^{(2)} \\ \hline \end{array}$$

Both the columns have to be of equal height to obtain a non-zero correlator. For a two-column operator of height $h_1^{(1)} = h_1^{(2)} = h$ we obtain the following tensor structure,

$$\frac{(H_1^{12})^h}{(P \circ P)^{\Delta/2}}. \tag{2.54}$$

The symmetrization will be imposed by the following derivative,

$$\left(Z_1^{(1)} \cdot \partial_{\Theta_1^{(1)}}\right)\left(Z_1^{(1)} \cdot \partial_{\Theta_1^{(2)}}\right) \cdots \left(Z_1^{(h)} \cdot \partial_{\Theta_1^{(1)}}\right)\left(Z_1^{(h)} \cdot \partial_{\Theta_1^{(2)}}\right). \tag{2.55}$$

An operator with $h = 2$ (window operator) gives the following result after the action of symmetrization,

$$H_{Z_1 Z_1} H_{Z_2 Z_2} - H_{Z_1 Z_2} H_{Z_1 Z_2}. \tag{2.56}$$

When $q = 2$, the above expression evaluates to zero. In general, for a q co-dimension defect we get non-zero vacuum expectation value to a mixed symmetry operator of maximum height min$(q-1, d-q+1)$ [2]. In [32], a duality between defects of different co-dimensions was pointed out:

$$q \quad \Longleftrightarrow \quad d+2-q. \tag{2.57}$$

We perform a check of this duality in terms of the height of an operator that can get a non-zero correlator and note the results in the table below (Table 2.1).

2.4 Two-Point Correlators

Two and three-point correlators capture all the data of a defect CFT. In a defect CFT cross-ratios start appearing at the two-point (bulk) correlator level. This is the reason why bootstrap methods can be applied at this level. In this section we will list down two-point correlators.

[2] We thank Marco Meineri [33] for pointing this out.

Dimension	Codimension	Height h
$d+2-q$	q	$\min(q-1, d-q+1)$
q	$d+2-q$	$\min(d-q+1, q-1)$

Table 2.1: Non vanishing criteria for two column operator.

2.4.1 Bulk-Defect

We will first consider two-point correlators involving a bulk operator and a defect operator. These correlators are important as they contain information about the bulk and defect couplings. The defect operators that can appear in the bulk-to-defect expansion of a bulk operator (1.63) can be identified by considering all non-zero bulk-defect two-point correlators. In fact, all possible operators appearing in the defect channel expansion can be found using the procedure given here. Consider the two point correlator,

$$\langle O_{\Delta_1,\lambda_1}(P_1, \mathbf{\Theta}_1)\hat{O}_{\hat{\Delta},\lambda_2,\hat{\lambda}_2}(P_2, \mathbf{\Theta}_2, \mathbf{\Phi}_2)\rangle. \tag{2.58}$$

The defect local operator has two representations corresponding to the two groups (parallel λ and transverse $\bar{\lambda}$). For the defect operator, its vectors obey the following constraints:

$$P_{\hat{2}}^{I} = 0 \quad \Theta_{\hat{2}}^{(i)I} = 0 \quad \Phi_{\hat{2}}^{(i)A} = 0.$$

We obtain the number of invariants to be 5 from (2.44). One of them was already present at one-point correlator level,

$$H_a^{(i,j)} \quad \text{i} \neq \text{j}. \tag{2.59}$$

We encounter 4 additional invariants,

$$
\begin{aligned}
H^{(i,j)}_{a\hat{a}} &= \frac{C^{(i)AB}_{a} C^{(j)}_{\hat{a}AB}}{P_a \bullet P_{\hat{a}}}, \qquad & G^{(i)}_{a\hat{a}} &= \frac{P_a \circ \Phi^{(i)}_{\hat{a}}}{(P_a \circ P_a)^{1/2}}, \\
\tilde{G}^{(i,j)}_{a\hat{a}} &= \frac{C^{(i)AI}_{a} P_{aA} \Phi^{(j)}_{\hat{a}I}}{(P_a \circ P_a)}, \qquad & K^{(i)}_{a\hat{a}} &= \frac{C^{(i)AI}_{a} P_{\hat{a}A} P_{aI}}{(P_a \circ P_a)^{1/2} (P_a \bullet P_{\hat{a}})}.
\end{aligned}
\tag{2.60}
$$

Putting everything together we get the following invariants:

$$
H^{(i,j)}_{1\hat{2}} \quad H^{(i,j)}_{1} \quad G^{(i)}_{1\hat{2}} \quad \tilde{G}^{(i,j)}_{1\hat{2}} \quad K^{(i)}_{1\hat{2}}. \tag{2.61}
$$

With one bulk and one defect operator it is impossible to construct a cross-ratio. The final form of the correlator is,

$$
(Z_1^{\lambda_1} \cdot \partial^{\lambda_1}_{\Theta_1})(Z_2^{\lambda_{\hat{2}}} \cdot \partial^{\lambda_{\hat{2}}}_{\Theta_2})(W_2^{\bar{\lambda}_{\hat{3}}} \cdot \partial^{\bar{\lambda}_{\hat{3}}}_{\Phi_2}) \frac{T^a_{BD} b_a}{(-2P_1 \bullet P_2)^{\hat{\Delta}} (P_1 \circ P_1)^{(\Delta - \hat{\Delta})/2}}, \tag{2.62}
$$

where,

$$
T^a_{BD} = \big(H^{(i,j)}_{1\hat{2}}\big)^{a_{ij}} \big(H^{i,j}_{1}\big)^{b_{ij}} \big(G^{i}_{1\hat{2}}\big)^{c_i} \big(\tilde{G}^{(i,j)}_{1\hat{2}}\big)^{d_{ij}} \big(K^{i}_{1\hat{2}}\big)^{e_i}. \tag{2.63}
$$

T^a_{BD} refers to tensor structures and b_a are the coefficients (bulk-to-defect) associated with each tensor structure. The derivatives are present to impose symmetrization on the tensor structures. Each invariant has a power associated with it,

$$
H^{(i,j)}_{1\hat{2}} \to a_{ij}, \quad H^{i,j}_{1} \to b_{ij}, \quad G^{(i)}_{1\hat{2}} \to c_i, \quad \tilde{G}^{(i,j)}_{1\hat{2}} \to d_{ij}, \quad K^{(i)}_{1\hat{2}} \to e_i. \tag{2.64}
$$

We will set up some quick notations,

$$
\begin{aligned}
n^C_1 &= \text{ number of columns of } O \qquad & h^{(i)}_1 &= \text{ length of i-th column of } O \\
n^C_{\hat{2}} &= \text{ number of columns of } \hat{O} \text{ (parallel)} \quad & h^{(i)}_{\hat{2}} &= \text{ length of i-th column of } \hat{O} \text{ (parallel)} \\
\bar{n}^C_{\hat{2}} &= \text{ number of columns of } \hat{O} \text{ (transverse)} \quad & \bar{h}^{(i)}_{\hat{2}} &= \text{ length of i-th column of } \hat{O} \text{ (transverse)}.
\end{aligned}
\tag{2.65}
$$

The powers are subject to following conditions :

$$
\begin{aligned}
h_1^{(i)} &= \sum_j^{n_{\hat{2}}^C} a_{ij} + \sum_j^{n_1^C} b_{ij} + \sum_j^{\bar{n}_{\hat{2}}^C} d_{ij} + e_i, \\
h_{\hat{2}}^{(i)} &= \sum_j^{n_1^C} a_{ji}, \\
\bar{h}_{\hat{2}}^{(i)} &= c_i + \sum_j^{n_1^C} d_{ji}.
\end{aligned}
\tag{2.66}
$$

These equations have been determined by matching homogeneity of the invariants with that of the operators in the correlator. The solution for each variable has to be a non-negative integer and can be worked out easily. *Mathematica* has a Reduce command which solves for integer solutions. We list down the relevant systems of equations for other correlators in the appendix. The system of equations can have multiple solutions. Each solution corresponds to a different tensor structure which can appear with a different coefficient. Once the tensor structures have been computed, they need to be acted on by the appropriate symmetrization derivatives.

Let us consider a concrete example:

$$
\langle O_{\Delta_1,\lambda_1}(P_1,\Theta_1)\hat{O}_{\hat{\Delta},\lambda_2,\hat{\lambda}_2}(P_2,\Phi_2)\rangle . \tag{2.67}
$$

We consider a two-point correlator between a bulk vector and a defect operator with spin-1 orthogonal to the defect,

$$
\lambda_1 = \square \qquad \lambda_{\hat{2}} = \bullet \qquad \bar{\lambda}_{\hat{2}} = \square .
$$

Plugging $h_1^{(1)} = 1$, $h_{\hat{2}}^{(1)} = 0$ and $\bar{h}_{\hat{2}}^{(1)} = 1$ in (2.66) we obtain two tensor structures,

$$
\langle O_{\lambda_1}(P_1,\Theta_1)\hat{O}_{\lambda_{\hat{2}},\bar{\lambda}_{\hat{2}}}(P_{\hat{2}},\Phi_{\hat{2}})\rangle = \frac{b_1 \tilde{G}_{1\hat{2}} + b_2 K_{1\hat{2}} G_{1\hat{2}}}{(-2P_1 \bullet P_{\hat{2}})^{\hat{\Delta}} (P_1 \circ P_1)^{(\Delta-\hat{\Delta})/2}} . \tag{2.68}
$$

We can further demand that the bulk operator is a conserved spin-1 current with dimension $\Delta_1 =$

$d-1$. Conservation condition implies,

$$\partial^M D_M \langle O_{\lambda_1}(P_1, \Theta_1) \hat{O}_{\lambda_{\hat{2}}, \bar{\lambda}_{\hat{2}}}(P_{\hat{2}}, \Phi_{\hat{2}}) \rangle = 0. \tag{2.69}$$

This results in a relation between the coefficients b_1 and b_2:

$$b_1(q-1) + b_2(q-d+\hat{\Delta}) = 0. \tag{2.70}$$

We will now list down the representations that can occur in the decomposition of different bulk operators.

2.4.1.1 Scalar Bulk Operator

We consider all possible two-point correlators with a bulk scalar. The correlator is non-zero in the following case only,

$$\langle O_\Delta(P_1) \hat{O}_{\hat{\Delta},0,s}(P_2, W_2) \rangle. \tag{2.71}$$

where s is a symmetric traceless quantum number of the $SO(q)$ representation. This indicates that a bulk scalar decomposes into defect local operators transforming as symmetric traceless tensors under $SO(q)$ while being scalars under the $SO(p+1,1)$ group. Schematically this can be represented as,

$$O \sim \hat{O} + \hat{O}^i + \hat{O}^{(ij)} + \dots \tag{2.72}$$

2.4.1.2 Spin-ℓ Bulk Operator

The defect decomposition of a spin-ℓ bulk operator yields defect operators in the following representations. Spin-J represents the spin of the bulk operator, spin-j represents the spin of the defect operator parallel to the defect and last column represents the maximum height of the $SO(q)$ representation of the defect operator. For a spin-ℓ bulk primary, we find that the defect operators appearing in the defect expansion are spinning fields under the $SO(p+1,1)$ group while the maximum height of the representation under $SO(q)$ is restricted by ℓ (Table 2.2). The height of

Spin-J	Spin-j	Height of $\lambda_{\hat{2}}$
	Spin-ℓ	1
Spin-ℓ	Spin ℓ-1	ℓ
	$\vdots$	ℓ
	0	ℓ

Table 2.2: Spin-J bulk operator decomposition into defect operators.

the $SO(q)$ representation is also limited by the co-dimension of the defect. It can have a maximum height of q (irrespective of ℓ). If the co-dimension of the defect is 1, then the only operators occurring would transform in the traceless symmetric representation of $SO(q)$.

2.4.2 Bulk-Bulk

We will now consider bulk-bulk two-point correlators. The conformal symmetry does not completely fix the position dependence of the correlator. The following two conformal cross-ratios [23] can be constructed:

$$\xi_1 = \frac{2P_1 \bullet P_2}{(P_1 \circ P_1)^{1/2}(P_2 \circ P_2)^{1/2}}, \qquad \xi_2 = \frac{2P_1 \circ P_2}{(P_1 \circ P_1)^{1/2}(P_2 \circ P_2)^{1/2}}. \tag{2.73}$$

With these two cross-ratios, the bulk-bulk two-point correlator can be written as:

$$\langle O_{\Delta_1,\lambda_1}(P_1, \boldsymbol{\Theta}_1) O_{\Delta_2,\lambda_2}(P_2, \boldsymbol{\Theta}_2)\rangle = \sum_n \frac{T^{(n)}_{BB} f_n(\xi_1, \xi_2)}{(P_1 \circ P_1)^{\Delta_1/2}(P_2 \circ P_2)^{\Delta_2/2}}, \tag{2.74}$$

where $T^{(n)}_{BB}$ are the different tensor structures compatible with the representation of the operators and the functions $f_n(\xi_1, \xi_2)$ can be expanded in terms of bulk-channel conformal blocks. In case of only bulk operators in a correlation function, the invariants that can appear are of the form:

$$\begin{aligned} & H_a^{(i,j)} = \frac{C_a^{(i)AI} C_{aAI}^{(j)}}{(P_a \circ P_a)}, \\ S_{ab}^{(i,j)} = \frac{C_a^{(i)AI} C_b^{(j)BI} P_{aA} P_{bB}}{(P_a \circ P_a)(P_b \circ P_b)}, \qquad & \bar{S}_{ab}^{(i,j)} = \frac{C_a^{(i)AI} C_b^{(j)AJ} P_{aI} P_{bJ}}{(P_a \circ P_a)(P_b \circ P_b)}, \\ K_{ab}^{(i)} = \frac{C_a^{(i)AI} P_{aA} P_{bI}}{(P_a \circ P_a)(P_b \circ P_b)^{1/2}}, \qquad & \bar{K}_{ab}^{(i)} = \frac{C_a^{(i)AI} P_{bA} P_{bI}}{(P_a \circ P_a)^{1/2}(P_b \circ P_b)}, \end{aligned} \tag{2.75}$$

with $a \neq b$ in all the above invariants. The above invariants have the following properties:

$$\begin{aligned} H_a^{(i,j)} &= H_a^{(j,i)}, \\ S_{(ab)}^{(i,j)} &= S_{(ba)}^{(j,i)}, \\ \bar{S}_{(ab)}^{(i,j)} &= \bar{S}_{(ba)}^{(j,i)}. \end{aligned} \tag{2.76}$$

It is also possible to construct additional invariants like,

$$\frac{C_a^{(i)AI} P_{bA} P_{cI}}{(P_a \circ P_a)^{1/2}(P_b \circ P_b)^{1/2}(P_c \circ P_c)^{1/2}} \quad \text{where } (a \neq b \neq c)\,. \tag{2.77}$$

However, the above invariant can be shown to be a linear combination of the invariants already defined in (2.75) using identities listed in $(A.3)$. The list of independent invariants is:

$$H_1^{(i,j)}, H_2^{(i,j)}, S_{12}^{(i,j)}, \bar{S}_{12}^{(i,j)}, K_{12}^{(i)}, K_{21}^{(i)}, \bar{K}_{12}^{(i)}, \bar{K}_{21}^{(i)}. \tag{2.78}$$

Depending on the representation of bulk operators (including the i-index in the above equation), the total number of invariants is (we refer the reader to $(A.1)$ for notations),

$$\frac{1}{2}(l_1^{(1)} + l_2^{(1)})(l_1^{(1)} + l_2^{(1)} + 3) + l_1^{(1)} l_2^{(1)}. \tag{2.79}$$

The two-point correlator is non-zero only for identical operators in an ordinary CFT. This is no longer true in a defect CFT and two-point correlators between arbitrary operators can be non-zero.

We will discuss two examples for the bulk-bulk two-point correlators. The system of equations to evaluate the tensor structures for a given two-point correlator is listed in the appendix ($A.4.1$). We first consider a two-point correlator between a two-form and a vector.

$$\lambda_1 = \begin{array}{|c|}\hline \\ \hline \\ \hline \end{array} \qquad \lambda_2 = \begin{array}{|c|}\hline \\ \hline \end{array}$$

Using the invariants (2.75), and applying the equations of ($A.4.1$) with $h_1^{(1)} = 2$ and $h_2^{(1)} = 1$ we get the following tensor structures:

$$\begin{aligned}\sum_n T^{(n)}_{BB} f_n(\xi_1,\xi_2) =& K^{(1)}_{12}\bar{K}^{(1)}_{12}K^{(1)}_{21} f_1(\xi_1,\xi_2) + K^{(1)}_{12}\bar{K}^{(1)}_{12}\bar{K}^{(1)}_{21} f_2(\xi_1,\xi_2) + S^{(1,1)}_{12}K^{(1)}_{12} f_3(\xi_1,\xi_2) \\ &+ S^{(1,1)}_{12}\bar{K}^{(1)}_{12} f_4(\xi_1,\xi_2) + \bar{S}^{(1,1)}_{12}K^{(1)}_{12} f_5(\xi_1,\xi_2) + \bar{S}^{(1,1)}_{12}\bar{K}^{(1)}_{12} f_6(\xi_1,\xi_2).\end{aligned} \tag{2.80}$$

The next step is to apply derivatives to complete the symmetrization,

$$\begin{aligned}\left(Z^{(1)}_1.\partial_{\Theta^{(1)}_1}\right)\left(Z^{(2)}_1.\partial_{\Theta^{(1)}_1}\right)\sum_n T^{(n)}_{BB} f_n(\xi_1,\xi_2) =& \left(K^{(2z)}_{12}\bar{K}^{(1z)}_{12}K^{(1)}_{21} - K^{(1z)}_{12}\bar{K}^{(2z)}_{12}K^{(1)}_{21}\right) f_1(\xi_1,\xi_2) \\ &+ \left(K^{(2z)}_{12}\bar{K}^{(1z)}_{12}\bar{K}^{(1)}_{21} - K^{(1z)}_{12}\bar{K}^{(2z)}_{12}\bar{K}^{(1)}_{21}\right) f_2(\xi_1,\xi_2) \\ &+ \left(S^{(2z,1)}_{12}K^{(1z)}_{12} - S^{(1z,1)}_{12}K^{(2z)}_{12}\right) f_3(\xi_1,\xi_2) \\ &+ \left(S^{(2z,1)}_{12}\bar{K}^{(1z)}_{12} - S^{(1z,1)}_{12}\bar{K}^{(2z)}_{12}\right) f_4(\xi_1,\xi_2) \\ &+ \left(\bar{S}^{(2z,1)}_{12}K^{(1z)}_{12} - \bar{S}^{(1z,1)}_{12}K^{(2z)}_{12}\right) f_5(\xi_1,\xi_2) \\ &+ \left(\bar{S}^{(2z,1)}_{12}\bar{K}^{(1z)}_{12} - \bar{S}^{(1z,1)}_{12}\bar{K}^{(2z)}_{12}\right) f_6(\xi_1,\xi_2).\end{aligned} \tag{2.81}$$

The application of derivatives results in a lot of terms. Although this is correct, it is not required as the operators under consideration are not symmetric in their indices. When operators do not have symmetry (anti-symmetry), the result in $\boldsymbol{\Theta}$-basis ($\boldsymbol{Z}$-basis) is sufficient.

Let us look at another example involving a hook and a scalar operator.

$$\lambda_1 = \ydiagram{2,1} \qquad \lambda_2 = \bullet$$

We again use $(A.4.1)$ with $h_1^{(1)} = 2$, $h_1^{(2)} = 1$ and $h_{\hat{2}}^{(1)} = 0$ to find the tensor structures,

$$\begin{aligned}\sum_n T_{BB}^{(n)} f_n(\xi_1, \xi_2) &= H_1^{(1,2)} K_{12}^{(1)} f_1(\xi_1, \xi_2) + H_1^{(1,2)} \bar{K}_{12}^{(1)} f_2(\xi_1, \xi_2) \\ &\quad + K_{12}^{(1)} \bar{K}_{12}^{(1)} K_{12}^{(2)} f_3(\xi_1, \xi_2) + K_{12}^{(1)} \bar{K}_{12}^{(1)} \bar{K}_{12}^{(2)} f_4(\xi_1, \xi_2).\end{aligned} \tag{2.82}$$

We apply the derivatives to symmetrize the tensor structures,

$$\begin{aligned}&\left(Z_1^{(2)}.\partial_{\Theta_1^{(1)}}\right)\left(Z_1^{(1)}.\partial_{\Theta_1^{(1)}}\right)\left(Z_1^{(1)}.\partial_{\Theta_1^{(2)}}\right)\sum_n T_{BB}^{(n)} f_n(\xi_1, \xi_2) \\ &\qquad = \left(H_1^{(1z,1z)} K_{12}^{(2z)} - H_1^{(2z,1z)} K_{12}^{(1z)}\right) f_1(\xi_1, \xi_2) \\ &\qquad + \left(H_1^{(1z,1z)} \bar{K}_{12}^{(2z)} - H_1^{(2z,1z)} \bar{K}_{12}^{(1z)}\right) f_2(\xi_1, \xi_2) \\ &\qquad + \left(K_{12}^{(1z)} \bar{K}_{12}^{(2z)} K_{12}^{(1z)} - K_{12}^{(2z)} \bar{K}_{12}^{(1z)} K_{12}^{(1z)}\right) f_3(\xi_1, \xi_2) \\ &\qquad + \left(K_{12}^{(1z)} \bar{K}_{12}^{(2z)} \bar{K}_{12}^{(1z)} - K_{12}^{(2z)} \bar{K}_{12}^{(1z)} \bar{K}_{12}^{(1z)}\right) f_4(\xi_1, \xi_2).\end{aligned} \tag{2.83}$$

This is the final result for a two-point correlator involving a hook and a scalar operator. All the symmetries and anti-symmetries of the hook operator are made explicit after the action of derivative.

2.4.3 Defect-Defect

We finally study two-point correlators of defect local operators,

$$\langle \hat{O}_{\lambda_1, \hat{\lambda}_1}(P_{\hat{1}}, \mathbf{\Theta}_1, \mathbf{\Phi_1}) \hat{O}_{\lambda_2, \hat{\lambda}_2}(P_{\hat{2}}, \mathbf{\Theta}_2, \mathbf{\Phi_2}) \rangle. \tag{2.84}$$

We find new invariants constructed by the contraction of Θ and Φ among themselves:

$$
\begin{aligned}
H_{\hat{a}\hat{b}}^{(i,j)} &= \frac{C_{\hat{a}}^{(i)AB} C_{\hat{b}}^{(j)AB}}{P_{\hat{a}} \bullet P_{\hat{b}}}, \\
\tilde{H}_{\hat{a}\hat{b}}^{(i,j)} &= \Phi_{\hat{a}}^{(i)} \circ \Phi_{\hat{b}}^{(j)}.
\end{aligned}
\tag{2.85}
$$

Since we are considering defect operators, the condition $\hat{a} \neq \hat{b}$ is automatically implied. The possible invariants are $H_{\hat{1}\hat{2}}^{(i,j)}$ and $\tilde{H}_{\hat{1}\hat{2}}^{(i,j)}$ and this implies that the defect operators should have the same representation for both sectors.

$$
\lambda_{\hat{1}} = \lambda_{\hat{2}}, \qquad \bar{\lambda}_{\hat{1}} = \bar{\lambda}_{\hat{2}}. \tag{2.86}
$$

This has to be true since defect local operators behave like operators of an ordinary CFT. There is no cross-ratio in this case as the conformal symmetry completely fixes the form of the correlator.

2.5 Three-Point Correlators

Crossing equations involving three-point correlators constrain the data-set of a defect CFT. These are analogous to four-point crossings in an ordinary CFT.

2.5.1 Bulk-Bulk-Bulk

No additional invariants appear for bulk three-point correlators and the ones listed in (2.75) are sufficient. The total number of invariants in this case is 21 from (2.44) and we list them below:

$$
\begin{aligned}
&H_1^{(i,j)}, H_2^{(i,j)}, H_3^{(i,j)}, \\
&S_{12}^{(i,j)}, S_{23}^{(i,j)}, S_{31}^{(i,j)}, \\
&\bar{S}_{12}^{(i,j)}, \bar{S}_{23}^{(i,j)}, \bar{S}_{31}^{(i,j)}, \\
&K_{12}^{(i)}, K_{21}^{(i)}, K_{23}^{(i)}, K_{32}^{(i)}, K_{31}^{(i)}, K_{13}^{(i)}, \\
&\bar{K}_{12}^{(i)}, \bar{K}_{21}^{(i)}, \bar{K}_{23}^{(i)}, \bar{K}_{32}^{(i)}, \bar{K}_{31}^{(i)}, \bar{K}_{13}^{(i)}.
\end{aligned}
\tag{2.87}
$$

Depending on the representation of the bulk operators we determine the number of invariants (taking into account i-index) to be:

$$\frac{1}{2}(l_1^{(1)} + l_2^{(1)} + l_3^{(1)})(l_1^{(1)} + l_2^{(1)} + l_3^{(1)} + 7) + l_1^{(1)} l_2^{(1)} + l_2^{(1)} l_3^{(1)} + l_3^{(1)} l_1^{(1)}. \tag{2.88}$$

Consider a three-point correlator,

$$\langle O_{\lambda_1}(P_1, \mathbf{\Theta}_1) O_{\lambda_2}(P_2, \mathbf{\Theta}_2) O_{\lambda_3}(P_3, \mathbf{\Theta}_3)\rangle = \sum_n \frac{f_{123}^{(n)} T_{BBB}^{(n)} f_n(\xi_1, ..., \xi_6)}{(P_{11})^{\Delta_1/2}(P_{22})^{\Delta_2/2}(P_{33})^{\Delta_3/2}}. \tag{2.89}$$

Here $T_{BBB}^{(n)}$ are three-point tensor structures and functions $f_n(\xi_1, ..., \xi_6)$ can be expanded in terms of three-point conformal blocks. The conformal blocks are functions of the cross-ratios. Six cross-ratios can be constructed out of three bulk operators:

$$\begin{aligned}
\xi_1 &= \frac{2P_1 \bullet P_2}{(P_{11})^{1/2}(P_{22})^{1/2}}, & \xi_2 &= \frac{2P_1 \circ P_2}{(P_{11})^{1/2}(P_{22})^{1/2}} \\
\xi_3 &= \frac{2P_2 \bullet P_3}{(P_{22})^{1/2}(P_{33})^{1/2}}, & \xi_4 &= \frac{2P_2 \circ P_3}{(P_{22})^{1/2}(P_{33})^{1/2}} \\
\xi_5 &= \frac{2P_3 \bullet P_1}{(P_{33})^{1/2}(P_{11})^{1/2}}, & \xi_6 &= \frac{2P_3 \circ P_1}{(P_{33})^{1/2}(P_{11})^{1/2}}.
\end{aligned} \tag{2.90}$$

As an example, let us consider three-point correlator of a 2-form and two scalars.

$$\lambda_1 = \begin{array}{|c|}\hline \\ \hline \\ \hline \end{array} \qquad \lambda_2 = \bullet \qquad \lambda_3 = \bullet$$

We use the system of equations (obtained from homogeneity constraints) in $(A.4.2)$ with $h_1^{(1)} = 2$ and $h_2^{(1)} = h_3^{(1)} = 0$ to obtain the tensor structures,

$$\begin{aligned}
\sum_n f_{123}^{(n)} T_{BBB}^{(n)} f_n(\xi) =& f_{123}^{(1)} K_{12} K_{13} f_1(\xi) + f_{123}^{(2)} K_{12} \bar{K}_{12} f_2(\xi) + f_{123}^{(3)} K_{12} \bar{K}_{13} f_3(\xi) \\
& + f_{123}^{(4)} K_{13} \bar{K}_{12} f_4(\xi) + f_{123}^{(5)} K_{13} \bar{K}_{13} f_5(\xi) + f_{123}^{(6)} \bar{K}_{12} \bar{K}_{13} f_6(\xi).
\end{aligned} \tag{2.91}$$

$f_{123}^{(n)}$ are three-point coefficients associated to each tensor structure.

2.5.2 Bulk-Bulk-Defect

Three-point correlators involving two bulk and one defect operators are important for bootstrap as pointed out in [34]. We encounter one new invariant in this case,

$$N^{(i)}_{\hat{c},1b} = \frac{C^{(i)AB}_{\hat{c}} P_{1A} P_{bB}}{(P_{\hat{c}} \bullet P_1)^{1/2} (P_1 \bullet P_b)^{1/2} (P_b \bullet P_{\hat{c}})^{1/2}} \quad (1 \neq b). \tag{2.92}$$

We determine the number of invariants to be 17 by plugging in ($n_1 = 2$ and $n_2 = 1$) in (2.44). We list them below,

$$\begin{aligned}
&G^{(i)}_{1\hat{3}}, G^{(i)}_{2\hat{3}}, \\
&H^{(i,j)}_{1}, H^{(i,j)}_{2}, \\
&\bar{K}^{(i)}_{12}, K^{(i)}_{12}, \bar{K}^{(i)}_{21}, K^{(i)}_{21}, \\
&\tilde{G}^{(i,j)}_{1\hat{3}}, \tilde{G}^{(i,j)}_{2\hat{3}}, H^{(i,j)}_{1\hat{3}}, H^{(i,j)}_{2\hat{3}}, \\
&S^{(i,j)}_{12}, \bar{S}^{(i,j)}_{12}, \\
&K^{(i)}_{1\hat{3}}, K^{(i)}_{2\hat{3}}, \\
&N^{(i)}_{\hat{3},12}.
\end{aligned} \tag{2.93}$$

There are three independent cross-ratios in this case. The two bulk operators yield two cross-ratios which we already encountered before ξ_1 and ξ_2. Including the defect operator yields an additional cross-ratio,

$$\chi = \frac{(P_{\hat{3}} \bullet P_1)(P_2 \bullet P_2)^{1/2}}{(P_{\hat{3}} \bullet P_2)(P_1 \bullet P_1)^{1/2}}. \tag{2.94}$$

A three-point correlator involving two bulk and one defect operator has the following structure:

$$\langle O_1 O_2 \hat{O}_3 \rangle = \sum_n \frac{T^{(n)}_{BBD} f_n(\xi_1, \xi_2, \chi)}{(P_{12})^{\frac{\Delta_1+\Delta_2-\Delta_3}{2}} (P_{1\hat{3}})^{\frac{\Delta_1+\hat{\Delta}_3-\Delta_2}{2}} (P_{2\hat{3}})^{\frac{\Delta_2+\hat{\Delta}_3-\Delta_1}{2}}}. \tag{2.95}$$

As an example, let us consider a three-point correlator involving a vector, a scalar and a defect operator which is a 2-form along the defect and a scalar orthogonal to the defect.

$$\lambda_1 = \begin{array}{|c|}\hline \\ \hline\end{array} \qquad \lambda_2 = \bullet \qquad \lambda_{\hat{3}} = \begin{array}{|c|}\hline \\ \hline \\ \hline\end{array} \qquad \bar{\lambda}_{\hat{3}} = \bullet$$

Using the system of equations listed in $(A.4.3)$ and taking $h_1^{(1)} = 1$, $h_2^{(1)} = 0$, $h_{\hat{3}}^{(1)} = 2$ and $\bar{h}_{\hat{3}}^{(1)} = 0$, we obtain only one possible tensor structure:

$$\langle O_1(P_1, \Theta_1) O_2(P_2) \hat{O}_3(P_{\hat{3}}, \Theta_3) \rangle = \frac{H_{1\hat{3}}^{11} N_{\hat{3},12}^{1} f_1(\xi_1, \xi_2, \chi)}{(P_{12})^{\frac{\Delta_1+\Delta_2-\Delta_3}{2}} (P_{1\hat{3}})^{\frac{\Delta_1+\hat{\Delta}_3-\Delta_2}{2}} (P_{2\hat{3}})^{\frac{\Delta_2+\hat{\Delta}_3-\Delta_1}{2}}}. \tag{2.96}$$

2.5.3 Defect-Defect-Bulk

The three-point correlator involving two defect and one bulk operator is not interesting by itself as it does not yield a crossing relation. However, we encounter an additional invariant in this case,

$$\tilde{N}_{\hat{a}a}^{(i)} = \frac{C_{\hat{a}}^{iAB} P_{(\hat{a}+1)A} P_{aB}}{(P_{a\hat{a}})^{1/2} (P_{\hat{a}(\hat{a}+1)})^{1/2} (P_{a(\hat{a}+1)})^{1/2}}. \tag{2.97}$$

Combining this new invariant with the previously known ones we obtain the following list of invariants:

$$\begin{aligned}
&H_3^{(i,j)}, \\
&H_{3\hat{1}}^{(i,j)}, H_{3\hat{2}}^{(i,j)}, \\
&G_{3\hat{1}}^{(i,j)}, G_{3\hat{2}}^{(i,j)}, \tilde{G}_{3\hat{1}}^{(i,j)}, \tilde{G}_{3\hat{2}}^{(i,j)}, \\
&H_{\hat{1}\hat{2}}^{(i,j)}, \tilde{H}_{\hat{1}\hat{2}}^{(i,j)}, \\
&K_{3\hat{1}}^{i}, K_{3\hat{2}}^{i}, \\
&\tilde{N}_{\hat{1}3}^{(i)}, \tilde{N}_{\hat{2}3}^{(i)}.
\end{aligned} \tag{2.98}$$

Only one cross-ratio can be constructed out of two defect and one bulk operators,

$$\zeta = \frac{(P_{\hat{1}} \bullet P_{\hat{2}})(P_3 \bullet P_3)}{(P_{\hat{1}} \bullet P_3)(P_{\hat{2}} \bullet P_3)}. \tag{2.99}$$

2.5.4 Defect-Defect-Defect

The last ingredients for implementing three-point bootstrap are three-point correlators of defect local operators. For three defect operators it is impossible to construct a cross-ratio. In addition to invariants appearing in (2.85), an additional invariant can be constructed,

$$\tilde{K}^{(i)}_{\hat{a}\hat{b}} = \frac{C^{(i)AB}_{\hat{a}} P_{\hat{a}+1,A} P_{\hat{b}B}}{(P_{\hat{a}(\hat{a}+1)})^{1/2} (P_{(\hat{a}+1)\hat{b}})^{1/2} (P_{\hat{a}\hat{b}})^{1/2}} \quad \hat{b} \neq \hat{a}, \hat{a}+1. \tag{2.100}$$

Using $n_2 = 3$ in (2.44), we determine the total number of invariants to be 9:

$$H^{(i,j)}_{\hat{1}\hat{2}}, H^{(i,j)}_{\hat{2}\hat{3}}, H^{(i,j)}_{\hat{3}\hat{1}}, \tilde{H}^{(i,j)}_{\hat{1}\hat{2}}, \tilde{H}^{(i,j)}_{\hat{2}\hat{3}}, \tilde{H}^{(i,j)}_{\hat{3}\hat{1}}, \tilde{K}^{(i)}_{\hat{1}\hat{3}}, \tilde{K}^{(i)}_{\hat{2}\hat{1}}, \tilde{K}^{(i)}_{\hat{3}\hat{2}}. \tag{2.101}$$

We will consider an example of a three-point correlator with a 2-form, a vector, and a scalar.

$$\lambda_{\hat{1}} = \ydiagram{1,1} \qquad \lambda_{\hat{2}} = \ydiagram{1} \qquad \lambda_{\hat{3}} = \bullet$$

When all the quantum numbers of the defect operators are parallel to the defect, it acts like a correlator in an ordinary CFT. We list the result below,

$$\langle \hat{O}_{\hat{\Delta}_1}(P_{\hat{1}}, \Theta_1) \hat{O}_{\hat{\Delta}_2}(P_{\hat{2}}, \Theta_2) \hat{O}_{\hat{\Delta}_3}(P_{\hat{3}}) \rangle = \hat{f}_{\hat{O}_1\hat{O}_2\hat{O}_3} \frac{H^{(1,1)}_{\hat{1}\hat{2}} \tilde{K}^{(1)}_{\hat{1}\hat{3}}}{P_{\hat{1}\hat{2}}^{\frac{\hat{\Delta}_1+\hat{\Delta}_2-\hat{\Delta}_3}{2}} P_{\hat{2}\hat{3}}^{\frac{\hat{\Delta}_2+\hat{\Delta}_3-\hat{\Delta}_1}{2}} P_{\hat{3}\hat{1}}^{\frac{\hat{\Delta}_3+\hat{\Delta}_1-\hat{\Delta}_2}{2}}}. \tag{2.102}$$

We can impose symmetrization by applying $Z\partial_\Theta$ derivatives (2.12) to the above expression. However, it is redundant in this case as there is no symmetry in any of the operator representations and **Θ**-basis serves us fine. Since parallel quantum numbers behave as a regular CFT, our result matches with that of [29]. If all the spins and forms are in the direction orthogonal to the defect, only one invariant is possible: $\tilde{H}^{(i,j)}_{\hat{1}\hat{2}}$. However with just this invariant it is impossible to construct a tensor structure for the given operators.

$$\langle \hat{O}_{\hat{\Delta}_1}(P_{\hat{1}},\Phi_1)\hat{O}_{\hat{\Delta}_2}(P_{\hat{2}},\Phi_2)\hat{O}_{\hat{\Delta}_3}(P_{\hat{3}})\rangle = 0 \tag{2.103}$$

We obtain different results depending on whether the spin and forms are aligned parallel or orthogonal to the defects. Mixed symmetric correlator between operators carrying both (parallel and orthogonal) quantum numbers can be computed in a similar manner.

2.6 n-Point Correlators

In this section, we will briefly comment on n-point ($n = n_1 + n_2$) correlators involving n_1 bulk and n_2 defect operators. The three-point correlators exhausted all possible invariants. No additional invariant can appear for higher point correlators and all the tensor structures have to be constructed out of the previously known invariants. We list all the invariants down together with their number,

$$\begin{aligned}
&H_a^{(i,j)} \to n_1 \quad \text{where } i \neq j \quad || \quad H_{a\hat{a}}^{(i,j)} \to n_1 n_2 \\
&G_{a\hat{a}}^{(i)} \to n_1 n_2 \quad || \quad \tilde{G}_{a\hat{a}}^{(i,j)} \to n_1 n_2 \quad || \quad K_{a\hat{a}}^{i} \to n_1 n_2 \\
&S_{ab}^{(i,j)} \to \frac{n_1(n_1-1)}{2} \text{ where } a \neq b \text{ and } S_{(ab)}^{(i,j)} = S_{(ba)}^{(j,i)} \\
&\bar{S}_{ab}^{(i,j)} \to \frac{n_1(n_1-1)}{2} \text{ where } a \neq b \text{ and } \bar{S}_{(ab)}^{(i,j)} = \bar{S}_{(ba)}^{(j,i)} \\
&K_{ab}^{(i)} \to n_1^2 - n_1 \text{ where } a \neq b \quad || \quad \bar{K}_{ab}^{(i)} \to n_1^2 - n_1 \text{ where } a \neq b \\
&H_{\hat{a}\hat{b}}^{(i,j)} \to \frac{n_2(n_2-1)}{2} \text{ where } \hat{a} \neq \hat{b} \quad || \quad \tilde{H}_{\hat{a}\hat{b}}^{(i,j)} \to \frac{n_2(n_2-1)}{2} \text{ where } \hat{a} \neq \hat{b} \\
&N_{\hat{k},1b}^{(i)} \to n_2(n_1-1) \text{ where } b \neq 1 \\
&\tilde{K}_{\hat{a}\hat{b}}^{(i)} \to n_2(n_2-2) \text{ where } \hat{b} \neq \hat{a}, \hat{a}+1 \\
&\tilde{N}_{\hat{a}a}^{(i)} \to n_1 n_2 .
\end{aligned} \tag{2.104}$$

Tensor structures for n-point correlators have to be constructed out of these invariants while respecting the homogeneity constraints. There is a slight subtlety involved with the last three invariants. $N_{\hat{c}1b}$, $\tilde{N}_{\hat{a}a}$ and $\tilde{K}_{\hat{a}\hat{b}}$ are all independent at the three-point level. However, they are not all independent for a higher-point correlator as $N_{\hat{c}1b}$ can be generated from $\tilde{N}_{\hat{a}a}$ $(A.3)$. Depending on n_1 and n_2, the independence of $N_{\hat{c}1b}$, $\tilde{N}_{\hat{a}a}$ and $\tilde{K}_{\hat{a}\hat{b}}$ varies. We list down the different cases and the independent invariants associated to those cases:

$$\begin{aligned}
&n_1 \geq 2 \quad \& \quad n_2 = 1 \qquad \rightarrow N_{\hat{c}ab} \\
&n_1 \geq 1 \quad \& \quad n_2 = 2 \qquad \rightarrow \tilde{N}_{\hat{a}a} \\
&n_1 = 0 \quad \& \quad n_2 \geq 3 \qquad \rightarrow \tilde{K}_{\hat{a}\hat{b}} \\
&n_1 \geq 1 \quad \& \quad n_2 \geq 3 \qquad \rightarrow \tilde{N}_{\hat{a}a}, \tilde{K}_{\hat{a}\hat{b}}.
\end{aligned} \tag{2.105}$$

In all other cases, $N_{\hat{c}ab}$, $\tilde{N}_{\hat{a}a}$ and $\tilde{K}_{\hat{a}\hat{b}}$ do not appear. We quote the equation for the total number of invariants (2.44) again for convenience,

$$3n_1^2 - 2n_1 + 2n_2^2 - 3n_2 + 5n_1n_2. \tag{2.106}$$

Taking into account (2.105), the sum of all invariants listed in (2.104) becomes,

$$\begin{aligned}
&n_1 \geq 2 \quad \& \quad n_2 = 1 \qquad \rightarrow 3n_1^2 - 2n_1 + n_2^2 - 2n_2 + 5n_1n_2 \\
&n_1 \geq 1 \quad \& \quad n_2 = 2 \qquad \rightarrow 3n_1^2 - 2n_1 + n_2^2 - n_2 + 5n_1n_2 \\
&n_1 = 0 \quad \& \quad n_2 \geq 3 \qquad \rightarrow 3n_1^2 - 2n_1 + 2n_2^2 - 3n_2 + 4n_1n_2 \\
&n_1 \geq 1 \quad \& \quad n_2 \geq 3 \qquad \rightarrow 3n_1^2 - 2n_1 + 2n_2^2 - 3n_2 + 5n_1n_2.
\end{aligned} \tag{2.107}$$

Except for the last case, this result does not seem to match with (2.106). The deviation from (2.106) can be calculated by subtracting our result from (2.106),

$$\begin{aligned}
&n_1 \geq 2 \quad \& \quad n_2 = 1 \qquad \rightarrow n_2^2 - n_2 = 0 \implies n_2 = 1 \\
&n_1 \geq 1 \quad \& \quad n_2 = 2 \qquad \rightarrow n_2^2 - 2n_2 = 0 \implies n_2 = 2, 0 \\
&n_1 = 0 \quad \& \quad n_2 \geq 3 \qquad \rightarrow n_1n_2 = 0 \implies n_1 = 0 \\
&n_1 \geq 1 \quad \& \quad n_2 \geq 3 \qquad \rightarrow 0.
\end{aligned} \tag{2.108}$$

We see that all the polynomials in (2.107) yield the same result as (2.106) as they are various limits of the same equation (2.106) at different n_1 and n_2.

The number of independent cross-ratios for n_1 bulk and n_2 defect operators were calculated in [35] and the number is,

$$n_1(n_1+1)+n_2(n_1+1)+\frac{n_2(n_2+1)}{2}. \tag{2.109}$$

For the purpose of bootstrap in a defect CFT, higher (greater than three)-point correlators provide no new information. All of the defect CFT data is already accounted at three-point crossing level.

For a purely bulk n-point correlator, tensor structures can be constructed out of the invariants in (2.75). When we count the total number of independent invariants keeping in mind each invariant has $i, j, \ldots$ indices labelling the columns of Young representation as well, we get

$$\frac{1}{2}\Big(\sum_a^n l_a^{(1)}\Big)\Big(\sum_a^n l_a^{(1)}+2n-\frac{3}{2}\Big)+\sum_{a>b} l_a^{(1)} l_b^{(1)}. \tag{2.110}$$

2.7 Parity Analysis

In our analysis so far, we have restricted to parity-even structures. In this section, we will consider parity-odd tensor structures. Parity entails a flip in one of the spatial directions. This implies that any Lorentz contraction would always be parity invariant. The Levi-Civita tensor ϵ is required to construct a tensor structure that is parity-odd. The ϵ-tensor with all its indices contracted gives a contribution from each direction. Hence, the structures made out of ϵ are always parity odd. For the bulk operators which transforms under $O(d+1,1)$ representation, the epsilon tensor is the full $d+2$ dimensional one. Let us consider a spin-1 operator in the presence of a co-dimension 2 defect:

$$\langle O_\Delta(P,Z)\rangle = a_O \frac{\epsilon_{01\cdots p+2IJ} P^I Z^J}{(P\circ P)^{\frac{\Delta+1}{2}}}. \tag{2.111}$$

The spin-1 correlator was zero in the parity-even case while it is non-zero here with parity-odd structure. In a similar manner, one-point correlators of completely anti-symmetric tensors (or forms) which were previously vanishing are non-zero using parity-odd structures. The following one-point correlators are possible for forms in the presence of a q co-dimension defect:

$$\langle O_{(q-1)\text{-form}}(P,\Theta)\rangle = \frac{\epsilon_{01\cdots p+2I_1\cdots I_q}P^{I_1}\Theta^{I_2}\cdots\Theta^{I_q}}{(P\circ P)^{\frac{\Delta+1}{2}}}, \tag{2.112}$$

$$\langle O_{(p+1)\text{-form}}(P,\Theta)\rangle = \frac{\epsilon_{A_1\cdots A_{p+2}12\cdots q}P^{A_1}\Theta^{A_2}\cdots\Theta^{A_{p+2}}}{(P\circ P)^{\frac{\Delta+1}{2}}}, \tag{2.113}$$

$$\langle O_{q\text{-form}}(P,\Theta)\rangle = \frac{(P\circ P)(\epsilon_{01\cdots p+2I_1\cdots I_q}\Theta^{I_1}\cdots\Theta^{I_q}) - q(P\circ\Theta)(\epsilon_{01\cdots p+2I_1\cdots I_q}P^{I_1}\Theta^{I_2}\cdots\Theta^{I_q})}{(P\circ P)^{(\Delta+2)/2}} \tag{2.114}$$

$$\langle O_{(p+2)\text{-form}}(P,\Theta)\rangle = \frac{(P\bullet P)(\epsilon_{A_1\cdots A_{p+2}12\cdots q}\Theta^{A_1}\cdots\Theta^{A_{p+2}}) - (p+2)(P\bullet\Theta)(\epsilon_{A_1\cdots A_{p+2}12\cdots q}P^{A_1}\Theta^{A_2}\cdots\Theta^{A_{p+2}})}{(P\circ P)^{(\Delta+2)/2}}. \tag{2.115}$$

We find that $(q-1)$, (q), $(p+1)$ and (p)-forms can have a non-zero one-point correlator in the presence of a q co-dimension defect. Once again we get a check of the defect duality (2.57). A defect of co-dimension $d+2-q$ gives a non-zero value to the same forms as a q co-dimension defect. The structure of the above one-point correlators imply,

$$\partial^M D_M\langle O_{n\text{-form}}(P,\Theta)\rangle = 0, \tag{2.116}$$

trivially. We do not obtain any constraints on the scaling dimension of the bulk operator from the above equation. The case for a non-zero expectation value of $(q-1)$-form and $(p+1)$-form has a clear physical picture. A defect CFT could have a p-form gauge potential A_p sitting on the defect:

$$S_{CFT} = S' + \int_{\mathcal{M}_p} A_p. \tag{2.117}$$

Here S' refers to other terms in the CFT action and the gauge potential A_p is integrated over the entire defect. In such cases, the $(p+1)$-form field strength dA_p can have a non-zero expectation value. The Hodge dual of the field strength $*dA_p$ is a $(m-1)$-form and it would also have a non-zero expectation value. Equation (2.116) can be explained by the fact that d^2A_p and $d*dA_p$ vanish trivially.

Similarly, it is possible to construct parity-odd tensor structures for defect local operators. Defect operators have two quantum numbers, one for the parallel group and one for the transverse. This implies the defect operators can be parity-odd with respect to either. This is implemented by considering two separate ϵ-tensors.

$$\epsilon_{AB\cdots p+2} \quad \text{and} \quad \epsilon_{IJ\cdots q} \tag{2.118}$$

Tensor structures constructed out of these two ϵ-tensors will be parity-odd.

2.8 Components

Embedding space also simplifies the computation of conformal blocks. We would like to be able to carry out the conformal bootstrap program for defects directly in embedding space following the program initiated in [36, 37]. For completeness, we briefly mention the strategy to project down to physical space (d-dimensions) the results of previous sections. Only projections in the presence of flat defects are considered in this section. For a detailed review of component calculations for both spherical and flat cases we point the reader to [23]. To recover indices from a polynomial expression, the expression needs to be acted on by *component derivatives*. These derivatives are constructed to remove the auxiliary vectors while maintaining the required symmetry or anti-symmetry. It is important to note that the form of these derivatives is operator-representation dependent. The derivatives listed below only work with symmetric traceless operators and forms.

$$\begin{aligned}
D_z^a &= (\frac{p-2}{2} + z^b \frac{\partial}{\partial z^b})\frac{\partial}{\partial z^a} - \frac{1}{2} z_a \frac{\partial^2}{\partial z^b \partial z_b}, \\
D_w^i &= (\frac{q-2}{2} + w^j \frac{\partial}{\partial w^j})\frac{\partial}{\partial w^i} - \frac{1}{2} w_i \frac{\partial^2}{\partial w^j \partial w_j}, \\
D_\theta^a &= \frac{p-2}{2}\frac{\partial}{\partial \theta^a} + \theta^b \frac{\partial}{\partial \theta^b}\frac{\partial}{\partial \theta^a}, \\
D_\phi^i &= \frac{q-2}{2}\frac{\partial}{\partial \phi^i} + \phi^j \frac{\partial}{\partial \phi^j}\frac{\partial}{\partial \phi^i}.
\end{aligned} \tag{2.119}$$

We have used (a, i) to label physical space directions parallel and orthogonal to the defect. Projections to the Poincaré section for bulk operator in the presence of a flat defect are:

$$\begin{aligned}
&Z^{A(i)}|_x = (0, 2x^m z_m^{(i)}, x^a), \qquad Z^{I(i)}|_x = z^{(i)i}, \\
&\Theta^{A(i)}|_x = (0, 2x^m \theta_m^{(i)}, x^a), \qquad \Theta^{I(i)}|_x = \theta^{(i)i}, \\
&P^A|_x = (1, x^m x_m, x^a), \qquad P^I|_x = x^i.
\end{aligned} \tag{2.120}$$

While the projections to Poincaré section for a defect operator are:

$$\begin{aligned}
&Z^{A(i)}|_x = (0, 2x^a z_a^{(i)}, x^a), \quad Z^I|_x = 0, \quad W^A|_x = 0, \quad W^{I(i)}|_x = w^{(i)i}, \\
&\Theta^{A(i)}|_x = (0, 2x^a \theta_a^{(i)}, x^a), \quad \Theta^I|_x = 0, \quad \Phi^A|_x = 0, \quad \Phi^{I(i)}|_x = \phi^{(i)i}, \\
&P^A|_x = (1, x^a x_a, x^a) \text{ and } \quad P^I|_x = 0.
\end{aligned} \tag{2.121}$$

Using these results, we can project the contractions between different vectors in physical space:

$$\begin{aligned}
&Z_1^{(i)} \bullet Z_2^{(j)} \to z_1^{(i)a} z_2^{(j)b} \eta_{ab}, \quad P_m \bullet Z_n^{(j)} = x_{mn}^a z_n^{a(j)} - x_n^i z_n^{i(j)} \\
&-2P_m \bullet P_n = |x_{mn}^a|^2 + |x_m^i|^2 + |x_n^i|^2, \\
&\Theta_1^{(i)} \bullet \Theta_2^{(j)} \to \theta_1^{(i)a} \theta_2^{(j)b} \eta_{ab}, \quad P_m \bullet \Theta_n^{(j)} = x_{mn}^a \theta_n^{a(j)} - x_n^i \theta_n^{i(j)},
\end{aligned} \tag{2.122}$$

where $x_{mn} = x_m - x_n$. We are now in a position to list down the steps to implement component calculation:

1. For a correlator in embedding space, all the coordinates must be projected to the Poincaré patch and dot products evaluated via (2.122).

2. Depending on the correlator required component derivatives (2.119) must be acted accordingly.

As an example, we will obtain the physical space result for a bulk two-point correlator involving a 2-form and a vector. Our goal is to compute $\langle O_1^{[ab]}(x_1)O_2^c(x_2)\rangle$ from (2.80). We will directly work in $\boldsymbol{\theta}$-basis for components as there is no symmetry in the correlator indices. To obtain the correct correlator, the terms in (2.80) containing $\theta_1^a\theta_1^b\theta_2^c$ are required. Only one tensor structure contains the required terms.

$$\bar{S}_{12}^{(1,1)}\bar{K}_{12}^{(1)} = -\frac{(\Theta_1 \bullet \Theta_2)(P_1 \circ P_1)(P_1 \circ P_2)(P_2 \circ P_2)(P_2 \bullet \Theta_1)}{(P_1 \circ P_1)^{3/2}(P_2 \circ P_2)^2} \tag{2.123}$$

Projecting down to d-dimensions we obtain,

$$\bar{S}_{12}^{(1,1)}\bar{K}_{12}^{(1)}| = \frac{(\theta_1^e\theta_2^f\eta_{ef})(x_{21}^g\theta_1^h\eta_{gh} - \theta_1^i x_2^i)(x_1^i x_2^i)}{|x_1^i||x_2^i|^2}. \tag{2.124}$$

The structure of the required correlator suggests the form of the derivatives to be $D^c_{\theta_2}D^b_{\theta_1}D^a_{\theta_1}$. The antisymmetry in the indices a, b is manifest due to anti-commutation among θ_1s.

$$\begin{aligned}
&D^c_{\theta_2}D^b_{\theta_1}D^a_{\theta_1}(\theta_1^e\theta_2^f\eta_{ef})(x_{21}^g\theta_1^h\eta_{gh})\frac{x_1^i x_2^i}{|x_1^i||x_2^i|^2} \\
&= (\alpha^3 - \alpha^2)(\eta^{ac}x_{21}^b - \eta^{bc}x_{21}^a)\frac{x_1^i x_2^i}{|x_1^i||x_2^i|^2} \qquad \text{where } \alpha = (\frac{p-2}{2})
\end{aligned} \tag{2.125}$$

This result has the desired antisymmetry in a and b. The full correlator in physical space is,

$$\langle O_1^{[ab]}(x_1)O_2^c(x_2)\rangle = (\alpha^3 - \alpha^2)\frac{(\eta^{ac}x_{21}^b - \eta^{bc}x_{21}^a)(x_1^i x_2^i)}{|x_1^i|^{\Delta_1}|x_2^i|^{2+\Delta_2}}f_6(\xi_1, \xi_2). \tag{2.126}$$

Even though this procedure for obtaining components is universal and works for arbitrary representations, the form of the derivative operators (2.119) is quite complicated for representations involving multiple Zs or Θs per operator. In those complicated cases, the procedure for calculating components has been given in [38]. Our goal is to work in embedding space itself so we will not follow this path.

2.9 Defects in Arbitrary Representation of $SO(q)$

In previous sections, we had considered defects transforming as singlets under the global $SO(q)$ group. In this section, we will consider correlators of operators in the presence of a defect transforming in arbitrary representations of $SO(q)$. The defect will also have indices (symmetric, anti-symmetric, or mixed symmetric). We will contract defect indices with a Θ-basis anti-symmetric auxiliary vector χ^I while demanding that χ^I is transverse. Schematically this looks like:

$$D^q(P_\alpha)_{I_1\cdots I_n}\chi^{I_1}\cdots\chi^{I_n}. \tag{2.127}$$

We have defined χs to be transverse by construction. χs have the following property,

$$\chi^{(i)}\circ\chi^{(j)}=0. \tag{2.128}$$

For defects indices we use Y as a $\boldsymbol{Z}$-basis vector of the orthogonal group. We will only consider parity-even tensor structures of one and two-point correlators. We give an analogous formula (2.44) to count the number of invariants (ignoring the $i-index$ of defect and operators):

$$3n_1^2+2n_2^2-2n_2+5n_1n_2. \tag{2.129}$$

Dipole moments can be considered as vector-defects in a quantum field theory. In a conformal theory, defect in arbitrary representations under $SO(q)$ can be constructed by integrating an operator in the same representation of $SO(q)$ over the entire hyperplane of the defect. Schematically this looks like:

$$D^q(P_\alpha,\chi)=\int_Y O(Y,\Phi)|_Y\ d^qY, \tag{2.130}$$

where $O(Y,\Phi)$ has support only on the hyperplane.

2.9.1 One-Point Correlator

The new invariants that can appear in a one-point correlator of a bulk operator are the following,

$$\begin{aligned}\mathcal{P}_a^{(i)} &= \frac{P_a \circ \chi^{(i)}}{(P_{aa})^{1/2}},\\ \mathcal{R}_a^{(i,j)} &= \frac{C_a^{AI(i)} P_a^A \chi^{(j)}}{(P_{aa})}.\end{aligned} \tag{2.131}$$

We obtain the following invariants (including the previously known invariants),

$$H_1^{(i,j)}, \mathcal{R}_1^{(i,j)}, \mathcal{P}_1^{(i)}. \tag{2.132}$$

The singlet defect case had only one invariant (2.47), whereas now there are three. As an example, let us consider a vector in the presence of a one-form (or vector) defect. Only one tensor structure can be constructed,

$$\langle O(\Theta)\rangle_{D(\chi)} = \frac{\mathcal{R}_1^{11}}{(X\circ X)^{\Delta/2}}. \tag{2.133}$$

It is interesting to find that the vector operator has a non-zero one-point correlator. In the singlet defect case the one-point correlator of the vector vanishes.

2.9.2 Two-Point Correlators

2.9.2.1 Bulk-Bulk

In addition to the invariants listed in (2.75) and (2.131), it might also be possible to construct the following invariant:

$$\mathcal{T}_{ab}^{(i,j,k)} = \frac{C_a^{(i)AI} C_b^{(j)AJ} P_{aI} \chi_J^{(k)}}{P_{aa}(P_{bb})^{1/2}}. \tag{2.134}$$

However this is not independent and it can be related to previously known invariants:

$$(P_1\circ P_1)(P_2\circ P_2)^{1/2}(P_1\bullet P_2)\mathcal{T}_{12} = (C_2^{AI}P_1^A\chi^I)(C_1^{AI}P_2^A P_1^I) + \frac{C_1^{AB}C_{2AB}}{2}(P_1\circ P_1)(P_2\circ\chi). \tag{2.135}$$

Combining all the invariants together, any tensor structure has to be constructed out of the following invariants:

$$
\begin{aligned}
&H_1^{(i,j)}, H_2^{(i,j)}, S_{12}^{(i,j)},\\
&\bar{S}_{12}^{(i,j)}, K_{12}^{(i)}, K_{21}^{(i)}, \bar{K}_{12}^{(i)}, \bar{K}_{21}^{(i)},\\
&\mathcal{P}_1^{(i)}, \mathcal{P}_2^{(i)},\\
&\mathcal{R}_1^{(i,j)}, \mathcal{R}_2^{(i,j)}.
\end{aligned}
\tag{2.136}
$$

For a defect in symmetric traceless representation, we can again use the trick of replacing all χ^i-vector with a single Y-auxiliary vector. Tensor structures can be constructed out of these invariants for two-point correlators by equating homogeneity of the bulk operators with that of the product of invariants.

2.9.2.2 Defect-Defect

Only one new invariant appears in this case,

$$\bar{\mathcal{R}}_{\hat{a}}^{(i,j)} = \Phi_{\hat{a}}^{(i)} \circ \chi^{(j)}. \tag{2.137}$$

Including the previously known invariants, the list of invariants in this case is:

$$H_{\hat{1}\hat{2}}^{(i,j)}, \tilde{H}_{\hat{1}\hat{2}}^{(i,j)}, \bar{\mathcal{R}}_1^{(i,j)}, \bar{\mathcal{R}}_2^{(i,j)}. \tag{2.138}$$

If the defect operators only carry parallel quantum numbers, all correlators vanish. This is because the defect index is in the orthogonal direction and it needs another orthogonal index to contract with. The defect CFT becomes trivial in this case. It is necessary for defect local operators to carry orthogonal quantum numbers to have non-zero correlation functions in the case of defects with spin.

2.9.2.3 *Bulk-Defect*

No new invariants can be constructed at this level. The possible invariants for a two-point correlator involving a bulk operators and a defect operator are,

$$\begin{aligned}&\mathcal{R}_1^{(i,j)}, \mathcal{P}_1^i, \bar{\mathcal{R}}_{\hat{2}}^{(i,j)}\\&H_{1\hat{2}}^{(i,j)}, H_1^{i,j}, G_{1\hat{2}}^i, \tilde{G}_{1\hat{2}}^{(i,j)}, K_{1\hat{2}}^i.\end{aligned} \tag{2.139}$$

As an example, we would like to know the bulk scalar decomposition in the presence of a defect transforming as a m-form under $SO(q)$. In this case the only invariants that we can use are $\mathcal{P}_1^i, G_{1\hat{2}}^i, \bar{\mathcal{R}}_{\hat{2}}^i$. We find that only defect operators whose representation (under $SO(q)$) has a height less or equal to $m+1$ appear in the decomposition. When the m-form defect is a 0-form (singlet) the maximum height of defect operator-representation is one, the same as shown in (2.72).

3. RESUMMATION AT FINITE CONFORMAL SPIN*

In this chapter we follow up on the computation of anomalous dimensions and OPE corrections for double-twist operators from the inversion formula [19, 39] initiated in [40] by including all the sub-leading residues. This results in an analytically continued closed form expression valid at any value of the conformal spin and in arbitrary dimension. This chapter is based on [41] by the author and his collaborators.

3.1 Introduction

The lightcone limit of crossing equation for four-point function provides us with a particular amenable analytical region that contains important physical information. This limit is controlled by large spin operators which allows one to develop a systematic perturbative expansion of the crossing relation in terms of inverse spin [42, 43, 44, 45, 46].

The inversion formula developed in [19, 39] (and reviewed in the Introduction) can be used to re-sum the expansion in large spin, providing access to anomalous dimension and OPE coefficients at finite values of the conformal spin, as has been done recently in four dimensions [40, 47, 48]. Previously, an analogous expansion for the large spin was computed in the series of works [49] and applied to holographic CFTs in four dimensions, large $N-$theories in three dimensions and for $\mathcal{N} = 4$ SYM. Some expressions in arbitrary dimensions were also given in [40], which even though resumming the large sum expansion, are only valid asymptotically. The reason is that in [40] the contribution coming from the residues in Mellin space which were subleading in large β (conformal spin) were neglected.

We will consider the correlation function of four conformal primary scalar operators given by conformal invariance as,

$$\langle \mathcal{O}_4(x_4)\cdots\mathcal{O}_1(x_1)\rangle = \frac{1}{(x_{12}^2)^{\frac{1}{2}(\Delta_1+\Delta_2)}(x_{34}^2)^{\frac{1}{2}(\Delta_3+\Delta_4)}}\left(\frac{x_{14}^2}{x_{24}^2}\right)^a\left(\frac{x_{14}^2}{x_{13}^2}\right)^b\mathcal{G}(z,\bar{z})\,, \tag{3.1}$$

*Reprinted with permission from "Resummation at finite conformal spin" by C. Cardona, S. Guha, S. K. Kanumlli and K. Sen, 2018, *JHEP* 2019 : 01, Copyright [2019] by the authors.

where $a = \frac{1}{2}(\Delta_2 - \Delta_1)$, $b = \frac{1}{2}(\Delta_3 - \Delta_4)$, and z, $\bar{z}$ are conformal cross-ratios given by,

$$u = z\bar{z} = \frac{x_{12}^2 x_{34}^2}{x_{13}^2 x_{24}^2}, \qquad v = (1-z)(1-\bar{z}) = \frac{x_{23}^2 x_{14}^2}{x_{13}^2 x_{24}^2}\,. \tag{3.2}$$

Henceforth, we will be using $(z, \bar{z})$ coordinates instead of (u, v). The function $\mathcal{G}(z, \bar{z})$ has the following *s-channel* conformal block expansion representation,

$$\mathcal{G}(z, \bar{z}) = \sum_{J,\Delta} f_{12\mathcal{O}} f_{43\mathcal{O}}\, G_{\Delta,J}(z, \bar{z})\,, \tag{3.3}$$

where the sum runs over the exchanged primary operators with spin J and dimension Δ. $G_{\Delta,J}$ are the conformal blocks eigenfunctions of the quadratic and quartic Casimir invariants of the conformal group and which can be conveniently represented by the following spectral representation [50],

$$\mathcal{G}(z, \bar{z}) = 1 + \sum_{J=0}^{\infty} \int_{d/2-i\infty}^{d/2+i\infty} \frac{d\Delta}{2\pi i}\, c(J, \Delta)\, f_{\Delta,J}(z, \bar{z})\,. \tag{3.4}$$

The function $f_{J,\Delta}$ is given in terms of a linear combination of conformal blocks plus its shadow respectively as,

$$f_{\Delta,J}(u, v) = \frac{1}{k_{d-\Delta,J}} \frac{\gamma_{\lambda_1,a}}{\gamma_{\bar{\lambda}_1,b}} G_{\Delta,J}(u, v) + \frac{1}{k_{\Delta,J}} \frac{\gamma_{\bar{\lambda}_1,a}}{\gamma_{\lambda_1,a}} G_{d-\Delta,J}(u, v)\,, \tag{3.5}$$

with coefficients defined in appendix B.1. The appropriate normalization for the integral representation, to match with the physical conformal block is given in (B.10) of appendix B.1[1]. For each operator exchange, labelled by (Δ, J), the contour integral representation of $f_{\Delta,J}(u, v)$ given in (B.1), picks up the physical and shadow poles to give the linear combination on the *rhs* of (3.5).

Our main tool in this work is the Lorentzian OPE inversion formula [19, 39], which allows us

[1]Note that $\gamma_{a,b}$ used in the normalization is different from the $\gamma_{12}^{J,\Delta}$ used for the notation of the anomalous dimension. We have used the notations of [51].

to extract $C(J,\Delta)$ from the discontinuities of the four-point function.

$$C^t(J,\Delta) = \frac{\kappa_{J+\Delta}}{4}\int_0^1 dz d\bar{z}\, \mu(z,\bar{z})\, G_{J+d-1,\Delta+1-d}(z,\bar{z})\, \mathrm{dDisc}\big[\mathcal{G}(z,\bar{z})\big]\,, \tag{3.6}$$

where the conformal invariant measure is given by,

$$\mu(z,\bar{z}) = \left|\frac{z-\bar{z}}{z\bar{z}}\right|^{d-2} \frac{\big((1-z)(1-\bar{z})\big)^{a+b}}{(z\bar{z})^2}\,. \tag{3.7}$$

The partial wave coefficient is given as,

$$C(J,\Delta) = C^t(J,\Delta) + (-1)^J C^u(J,\Delta)\,. \tag{3.8}$$

The u-channel contribution C^u is computed from the same integral (3.6) but with 1 and 2 interchanged and the integration ranging from $-\infty$ to 0 and the double discontinuity taken around $z=\infty$. In practice, the OPE coefficients can be extracted from the $\bar{z}$ integration as a power expansion in small z. At leading order in small z (3.6) is approximated by,

$$C^t(J,\Delta) = \int_0^1 \frac{dz}{2z} z^{\frac{\tau}{2}}\, C^t(z,\beta)\,, \tag{3.9}$$

where the following "generating function" has been defined,

$$C^t(z,\beta) \equiv \int_z^1 \frac{d\bar{z}\,(1-\bar{z})^{a+b}}{\bar{z}^2} \kappa_\beta\, k_\beta(\bar{z}) \mathrm{dDisc}[\mathcal{G}(z,\bar{z})]\,, \tag{3.10}$$

with

$$k_{2h}(z) = z^h {}_2F_1\left[\begin{matrix} h,\ h \\ 2h \end{matrix}; z\right]. \tag{3.11}$$

The usual conformal twist and spin are respectively $\tau = \Delta - J$ and $\beta = \Delta + J$. We are interested in studying the contributions to (3.10) coming from a single exchange, so by using the $t-$channel block decomposition of the four-point point function $\mathcal{G}(z,\bar{z})$ we can compute the contribution:

$$C^t(z,\beta)|_{J,\Delta} \;=\; f_{14(J,\Delta)}f_{23(J,\Delta)}\kappa_\beta\int_z^1 d\bar{z}\,\frac{(1-\bar{z})^{a+b}}{\bar{z}^2}k_\beta(\bar{z})\mathrm{dDisc}\left[\frac{(z\bar{z})^{\frac{\Delta_3+\Delta_4}{2}}G_{\Delta,J}(1-z,1-\bar{z})}{[(1-z)(1-\bar{z})]^{\frac{\Delta_2+\Delta_3}{2}}}\right], \tag{3.12}$$

where $f_{i\,j(J,\Delta)}$ corresponds to the OPE structure constant between the external scalars i and j and the exchanged operator.

At small z the generating function (4.43) can be written as a power expansion in z, whose contribution at the leading term from a single exchange will be given by

$$C^t(z,\beta)|_{J,\Delta} \sim C(\beta)z^{\frac{\tau}{2}+\frac{1}{2}\gamma_{12}(\beta)}\,, \tag{3.13}$$

where $C(\beta)$ and $\gamma_{12}(\beta)$ corresponds to the square OPE coefficient and anomalous dimension of the double twist operator having $\tau=-(\Delta_1+\Delta_2)$. If the anomalous dimension $\gamma_{12}(\beta)$ and correction to OPE coefficients $\delta P_{\Delta,J}(\beta)$ are small, we can write

$$C(\beta)=C_0(\beta)[1+\delta P_{\Delta,J}(\beta)]\,, \tag{3.14}$$

so that,

$$C^t(z,\beta)|_{J,\Delta} \sim z^{\frac{\tau}{2}}C_0(\beta)\bigg(\delta P_{\Delta,J}(\beta)+\frac{1}{2}\gamma_{12}(\beta)\log(z)\bigg)\,. \tag{3.15}$$

We similarly need to expand the RHS of (4.43) at small z, where the conformal blocks develop log-terms and regular terms, as reviewed in the Appendix. Therefore we can see that the anomalous dimension will be related to the log terms, whereas the OPE coefficients will be given by the regular terms. In this paper we will restrict to the four point function of identical scalars ϕ ($\Delta_1=\Delta_2=\Delta_3=\Delta_4=\Delta_\phi$). We focus on the anomalous dimensions and corrections to the OPE coefficients for double twist operators of the form $[\phi\phi]_J=\phi\partial_{\mu_1}\ldots\partial_{\mu_J}\phi$.

3.2 Warming Up

In four and two dimensions the conformal blocks can be represented by combinations of Gauss hypergeometric functions through (3.11). Respectively we have,

$$G_{\Delta,J}(z,\bar{z}) = \frac{k_{\Delta-J}(z)k_{\Delta+J}(\bar{z}) + k_{\Delta+J}(z)k_{\Delta-J}(\bar{z})}{1+\delta_{J,0}}\,, \quad \text{2D} \tag{3.16}$$

$$G_{\Delta,J}(z,\bar{z}) = \frac{z\bar{z}}{\bar{z}-z}\left[k_{\Delta-J-2}(z)k_{\Delta+J}(\bar{z}) - k_{\Delta+J}(z)k_{\Delta-J-2}(\bar{z})\right], \quad \text{4D}\,. \tag{3.17}$$

Hence in the small$-z$ limit, the building-block integral we need to perform is of the form,

$$J_0 \equiv \int_0^1 \frac{dz}{z^2}\Big(\frac{z}{1-z}\Big)^p k_h(z)k_g(1-z). \tag{3.18}$$

This integral is a special case of a Jacobi transform, which has been studied in detail recently in the context of one dimensional Conformal Field Theories in [52][2]. (3.18) computes the crossing kernel in the lightcone limit even in higher dimensions, because of the factorization property of the blocks as we see from (3.16). This type of integrals are hard to perform in position space, but as we are going to see, they are straightforward in Mellin space. We will evaluate this simple example in detail as it captures all the conceptual details involved in the more complicated integrals dealt later in the text.

We follow the same strategy as in [52]. First we will expand both $k_h(z)$ functions in the more convenient variable $\frac{z}{1-z}$, by using the following identity of the hypergeometric functions,

$${}_2F_1(h,h,2h,z) = (1-z)^h {}_2F_1(h,h,2h,\frac{z}{z-1}). \tag{3.19}$$

Then representing the hypergeometrics using the Mellin-Barnes representation we will be able to

[2] In the lightcone limit, the conformal blocks factorise and the kernel for the inversion formula can be written in terms of one dimensional integrals as in (3.18).

perform the z integral first. The Mellin-Barnes form of hypergeometric is given by,

$$ {}_2F_1(a,b;c;z) = \frac{\Gamma(c)}{\Gamma(a)\Gamma(b)} \int_{-i\infty}^{i\infty} \frac{\Gamma(a+s)\Gamma(b+s)\Gamma(-s)}{\Gamma(c+s)} (-z)^s \, ds. \tag{3.20} $$

Using 3.44 and 3.20 , the integral 3.18 becomes,

$$ J_0 = \frac{\Gamma(2h)\Gamma(2g)}{\Gamma(h)^2\Gamma(g)^2} \int_{\mathcal{C}} ds \int_{\mathcal{C}} dt \int_0^1 dz \frac{z^{p+s-t+h-g-2}}{(1-z)^{p+s-t+h-g}} \frac{\Gamma(-s)\Gamma(h+s)^2\Gamma(-t)\Gamma(t+g)^2}{\Gamma(2h+s)\Gamma(2g+t)} \tag{3.21} $$

$\mathcal{C}$ refers to the contour going from $-i\infty$ to $+i\infty$ and encircling the right half of the plane. The contribution of the semi-circular arc at ∞ vanishes. The z-integral is log-divergent, so we need to regularize it. To perform it we follow the prescription of [52] and deform one of the hypergeometrics in the following way,

$$ k_h(z) = z^h z^\epsilon {}_2F_1\left[\begin{matrix} h,\ h \\ 2h+\epsilon \end{matrix}; z\right]. \tag{3.22} $$

Now the z-integral becomes a simple beta function and the Mellin integration over s can be performed by means of the Barnes' second lemma:

$$ \begin{aligned} &\int_{-i\infty}^{i\infty} \frac{\Gamma(a+s)\Gamma(b+s)\Gamma(c+s)\Gamma(1-d-s)\Gamma(-s)}{\Gamma(e+s)} ds = \\ &\qquad \frac{\Gamma(a)\Gamma(b)\Gamma(c)\Gamma(1-d+a)\Gamma(1-d+b)\Gamma(1-d+c)}{\Gamma(e-a)\Gamma(e-b)\Gamma(e-c)}, \end{aligned} \tag{3.23} $$

where we should take,

$$ a = h \quad b = h \quad c = -1+p-t+h-g+\epsilon \quad d = p-t+h-g \quad e = 2h+\epsilon\,. \tag{3.24} $$

This gives us the following result:

$$ \frac{\Gamma(2h+\epsilon)\Gamma(2g)}{\Gamma(g)^2} \int_{-i\infty}^{i\infty} dt \, \frac{\Gamma(-1+p-t+h-g+\epsilon)\Gamma(1-p+t+g)\Gamma(1-p+t+g)\Gamma(-t)\Gamma(g+t)^2}{\Gamma(h+\epsilon)^2\Gamma(2h+1-p+t-h+g)\Gamma(2g+t)}. \tag{3.25} $$

Notice that the divergence in $1/\epsilon$ automatically cancels and now we can safely take the $\epsilon \to 0$

limit. What remains is doing the contour over the t-variable. By closing the contour to the right, there are two sets of poles for the t-variable,

$$t \in \mathbb{N} \qquad t \in -1+p+h-g+\mathbb{N} \tag{3.26}$$

Summing up these two series of residues, we get the following result,

$$\begin{aligned} J_0 =& \frac{\Gamma(2h)\Gamma(1+g-p)^2\Gamma(-1+h-g+p)}{\Gamma(h)^2\Gamma(1+h+g-p)} {}_4F_3\left[\begin{matrix} g,\ g,\ 1+g-p,\ 1+g-p \\ 2g,\ 2-h+g-p,\ 1+h+g-p \end{matrix};1\right] \\ &+ \frac{\Gamma(2g)\Gamma(1-h+g-p)\Gamma(-1+h+p)^2}{\Gamma(g)^2\Gamma(-1+h+g+p)} {}_4F_3\left[\begin{matrix} h,\ h,\ -1+h+p,\ -1+h+p \\ 2h,\ h-g+p,\ -1+h+g+p \end{matrix};1\right] \end{aligned} \tag{3.27}$$

An observation from this example which we will apply to the remaining cases considered below is in order. Naively, we could have started by trying to compute the integral (3.18) by using the usual series expansion of the hypergeometric function. However, since this is only convergent in the region $|z| < 1$, this will produce an asymptotic expansion valid only for large values of h, as that is the regime controlled by the small z region. Continuing to finite h involves re-suming additional contributions from the lower limit of the z integral[3]. The Mellin-Barnes form in (3.20), makes these additional contributions explicit, in terms of the second pair of poles in (3.26).

3.3 Anomalous Dimension

In this section we calculate the contribution to anomalous dimension of a double-twist operator from a single block exchange of a four-point correlation function of identical operators, by using the integral representation of conformal block. So for our case $\tau = -(\Delta_1 + \Delta_2) = -2\Delta_\phi$ and the conformal spin $\beta = \Delta + J$ defined for the double twist operators in the $s-$channel. The anomalous dimensions $\gamma_{12}^{J,\Delta}(\beta)$ are the corrections to the dimensions of operators $[\phi\phi]_J \equiv \phi\partial_{\mu_1}\ldots\partial_{\mu_J}\phi$, given by,

$$\Delta_{[\phi\phi]_J} = 2\Delta_\phi + J + 1/2\gamma_{12}^{J,\Delta}\,, \tag{3.28}$$

[3]The lower limit of the z integral is not convergent and gives rise to additional contributions discussed in [47].

due to exchange of operators of dimension Δ and spin J in the crossed (t) channel. We restrict ourselves to corrections to the double twist operators $\sim z^{\frac{\Delta_1+\Delta_2}{2}}\log z$ which comes only from the leading $\log z$ term *i.e* the leading twist contributions in the crossed (t) channel. Please note that we refer to τ for the double twist operators and not the twist of the $t-$channel exchanges. Also for clarification, we move back and forth between the notations $d/2$ and $h = d/2$ in what follows.

3.3.1 Scalar Exchange

When the anomalous dimension is small, contribution from the exchange can be computed as [19]:

$$\gamma_{12}^{0,\Delta}(\beta) = \frac{1}{C_0(\beta)}\int_0^1 \frac{d\bar{z}}{\bar{z}^2}\kappa_\beta k_\beta(\bar{z})\mathrm{dDisc}\left[\left(\frac{1-\bar{z}}{\bar{z}}\right)^{\frac{\tau}{2}} G^t_{\Delta,0}|_{\log}\right]. \tag{3.29}$$

In the above equation, $G^t_{\Delta,0}|_{\log}$ stands for the log term in the $z \to 0$ expansion of t-channel conformal block. First contribution to the OPE coefficient comes from unity block and is given by [53, 54, 55],

$$C_0(\beta) = \frac{\Gamma\left(\frac{\beta}{2}\right)^2\Gamma\left(\frac{1}{2}(\beta-\tau-2)\right)}{\Gamma(\beta-1)\Gamma\left(-\frac{\tau}{2}\right)^2\Gamma\left(\frac{1}{2}(\beta+\tau+2)\right)}. \tag{3.30}$$

In the second part we will be dealing with the corrections to these coefficients from conformal bock exchanges. The constant κ_β is,

$$\kappa_\beta = \frac{\Gamma\left(\frac{\beta}{2}\right)^4}{2\pi^2\Gamma(\beta-1)\Gamma(\beta)}. \tag{3.31}$$

Our starting point will be the Mellin transform integral representation for the scalar conformal block in the t-channel detailed in the Appendix B.1,

$$G^t_{\Delta,0}|_{\log} = -\frac{\Gamma(\Delta)\Gamma(-h+\Delta+1)}{\Gamma\left(\frac{\Delta}{2}\right)^3\Gamma\left(-h+\frac{\Delta}{2}+1\right)}\int_C ds\left(\frac{1-\bar{z}}{\bar{z}}\right)^{\frac{\Delta}{2}+s}\Gamma(-s)\frac{\Gamma(s+\frac{\Delta}{2})\Gamma(1-h+s+\frac{\Delta}{2})}{\Gamma(1-h+\Delta+s)}, \tag{3.32}$$

where and we have included the global factor from the crossing equation. We can immediately check that by picking up $s = n$ poles for the s-integral and summing over residues, we get the well known log-term for the scalar block [56, 51],

$$-\frac{(1-\bar{z})^{\frac{\Delta}{2}+\tau/2}}{\bar{z}^{\frac{\Delta}{2}+\tau/2}}\frac{\Gamma(\Delta)}{\Gamma(\frac{\Delta}{2})^2}\,{}_2F_1(1-\frac{d}{2}+\frac{\Delta}{2},\frac{\Delta}{2},1-\frac{d}{2}+\Delta,\frac{\bar{z}-1}{\bar{z}})\,, \tag{3.33}$$

thus confirming that (3.32) is the correct representation to be used.

Taking the double discontinuity over expression (3.32) produces the following additional phase

$$2\sin^2\left[\pi\left(\lambda_2+\frac{\tau}{2}+s\right)\right]\,. \tag{3.34}$$

Note however that in the inversion formula (3.10), we are considering the discontinuities of individual physical blocks in $t-$channel. These physical blocks are reproduced by the $s=n$ poles in (3.32) for $n\in\mathbb{I}_{\geq 0}$ respectively. Hence the phase factor corresponding to the entire block simply multiplies the whole integral by $\sin^2\left[\pi\left(\lambda_2+\frac{\tau}{2}\right)\right]$. Considering this phase and plugging in the representation (3.33) into (3.29), the contribution to the anomalous dimension coming from the scalar exchange is then given by,

$$\begin{aligned}\gamma^{0,\Delta}=&-4\sin^2\left[\pi\left(\frac{\Delta+\tau}{2}\right)\right]\frac{\kappa_\beta}{C_0(\beta)}\frac{\Gamma(\beta)\Gamma(\Delta)\Gamma(-h+\Delta+1)}{\Gamma\left(\frac{\beta}{2}\right)^2\Gamma\left(\frac{\Delta}{2}\right)^3\Gamma\left(-h+\frac{\Delta}{2}+1\right)}\\&\int_{\mathcal{C}}ds\,dt\int_0^1\frac{d\bar{z}}{\bar{z}^2}\left(\frac{\bar{z}}{1-\bar{z}}\right)^{\frac{\beta-\Delta-\tau}{2}-s+t}\Gamma(-t)\frac{\Gamma\left(\frac{\beta}{2}+t\right)^2}{\Gamma\left(\beta+t\right)}\Gamma(-s)\frac{\Gamma(s+\frac{\Delta}{2})\Gamma(1-h+s+\frac{\Delta}{2})}{\Gamma(1-h+\Delta+s)}.\end{aligned} \tag{3.35}$$

This is essentially the same integral (3.21) that we have dealt with in section 3.2 and hence the same steps follows, leading us to,

$$\gamma^{0,\Delta} = -4\frac{\kappa_\beta\,\Gamma(\Delta)\sin^2\left(\frac{\Delta+\tau}{2}\pi\right)}{\pi^2\Gamma\left(\frac{\Delta}{2}\right)^3 C_0(\beta)}$$
$$\times\left(\frac{\Gamma(\beta)\Gamma\left(\frac{\Delta}{2}\right)\Gamma\left(\frac{\Delta+\tau+2}{2}\right)^2\Gamma\left(\frac{\beta-\Delta-\tau-2}{2}\right)}{\Gamma\left(\frac{\beta}{2}\right)^2\Gamma\left(\frac{\beta+\Delta+\tau+2}{2}\right)}\,{}_4F_3\left[\begin{matrix}1-h+\frac{\Delta}{2},\frac{\Delta}{2},\frac{\Delta+\tau}{2}+1,\frac{\Delta+\tau}{2}+1\\1-h+\Delta,2-\frac{\beta-\Delta-\tau}{2},\frac{\beta+\Delta+\tau}{2}+1\end{matrix};1\right]\right.$$
$$\left.+\frac{\Gamma\left(\frac{\beta-\tau-2}{2}\right)\Gamma(-h+\Delta+1)\Gamma\left(\frac{-\beta+\Delta+\tau+2}{2}\right)\Gamma\left(\frac{-2h+\beta-\tau}{2}\right)}{\Gamma\left(\frac{-2h+\Delta+2}{2}\right)\Gamma\left(\frac{-2h+\beta+\Delta-\tau}{2}\right)}\,{}_4F_3\left[\begin{matrix}\frac{\beta}{2},\frac{\beta}{2},\frac{\beta-\tau}{2}-1,\frac{\beta-\tau}{2}-h\\\beta,\frac{\beta-\Delta-\tau}{2},-h+\frac{\beta+\Delta-\tau}{2}\end{matrix};1\right]\right). \tag{3.36}$$

The first Hypergeometric comes from summing over residues at $s = n$ pole series and second from those at $s = \frac{\beta-\Delta-\tau}{2} - 1 + n$. In four dimensions (i.e. $h = 2$), this expression matches with (3.56) of [47]. Following [52], we can write (3.36) in terms of more compact Wilson function ϕ_α [57] as,

$$\gamma^{0,\Delta} = -4\frac{\kappa_\beta}{C_0(\beta)}\frac{\sin^2\left(\left(\frac{\Delta+\tau}{2}\right)\pi\right)}{\Gamma\left(\frac{\Delta}{2}\right)^2}\Gamma(\beta)\Gamma(\Delta)\Gamma(1-h+\Delta)\Gamma\left(\frac{\beta-\tau}{2}-1\right)$$
$$\times\Gamma\left(\frac{\beta-\tau}{2}-h\right)\Gamma\left(1+\frac{\Delta+\tau}{2}\right)^2\phi_\alpha\left(\beta;a,b,c,d\right)\,, \tag{3.37}$$

where

$$\begin{aligned} a &= \frac{\Delta}{2}+\frac{1}{2}+\frac{\tau}{4}, & b &= \frac{1}{2}+\frac{\Delta}{2}-\frac{\tau}{4}-h\,, & c &= \frac{\beta}{2}+\frac{\tau}{4}+\frac{1}{2}\,,\\ d &= \frac{\beta}{2}-\frac{\tau}{4}-\frac{1}{2}\,, & \alpha &= \frac{h}{2}+\frac{\tau}{4}\,, & \beta &= \frac{1}{2}+\frac{\tau}{4}\,. \end{aligned} \tag{3.38}$$

We can rewrite the scalar contribution to the anomalous dimension as a ${}_7F_6$ hypergeometric:

$$\gamma^{0,\Delta} = -4\frac{\kappa_\beta}{C_0(\beta)}\frac{\sin^2\left[\left(\frac{\Delta+\tau}{2}\right)\pi\right]\Gamma(\Delta)\Gamma\left(\frac{\beta-\tau}{2}-1\right)\Gamma(\beta)\Gamma\left(\frac{\beta-\tau}{2}-h\right)\Gamma\left(1+\frac{\Delta+\tau}{2}\right)^2\Gamma\left(-h+\frac{\beta}{2}+\Delta+1\right)}{\Gamma(\frac{\beta}{2})\Gamma\left(\frac{\Delta}{2}\right)^2\Gamma\left(\frac{\beta+\Delta}{2}\right)\Gamma\left(\frac{\beta+\Delta+\tau}{2}+1\right)\Gamma\left(1-h+\frac{\beta+\Delta}{2}\right)\Gamma\left(\frac{\beta+\Delta-\tau}{2}-h\right)}$$
$${}_7F_6\left[\begin{matrix}\frac{\beta}{2},1-h+\frac{\Delta}{2},1-\frac{h}{2}+\frac{\beta}{4}+\frac{\Delta}{2},\frac{\Delta}{2},-h+\frac{\beta}{2}+\Delta,-h+\frac{\Delta-\tau}{2},1+\frac{\Delta+\tau}{2}\\-\frac{h}{2}+\frac{\beta}{4}+\frac{\Delta}{2},\frac{\beta+\Delta}{2},1-h+\frac{\beta+\Delta}{2},1-h+\Delta,-h+\frac{\beta+\Delta-\tau}{2},1+\frac{\beta+\Delta+\tau}{2}\end{matrix};1\right]. \tag{3.39}$$

The same kind of ${}_7F_6$ function also appears in the context of the $\epsilon-$expansion, which is recently discussed in [58].

3.3.2 Spin Exchange

The computation of the contribution to the anomalous dimension from a scalar can be straightforwardly upgraded to the spinning exchange, which is the topic of this section. We start with the integral representation of the log term for the conformal block, as discussed in the Appendix B.1,

$$\begin{aligned} G_{\Delta,J}(1-z,1-\bar{z}) = &-\frac{\Gamma(2\lambda_1)}{\Gamma(\lambda_1)^2(d-2)_J}\log z\sum_{m=0}^{J}(-1)^m\frac{A_m(J,\Delta)}{(\lambda_1-m)_m^2} \\ &\times\int_{\mathcal{C}}ds\left(\frac{1-\bar{z}}{\bar{z}}\right)^{s+\lambda_1-m}\Gamma(-s)\frac{(\lambda_1-m)_s(1-\bar{\lambda}_2)_s}{(1+\lambda_2-\bar{\lambda}_2)_{s+J-m}}\,. \end{aligned} \tag{3.40}$$

Using the spin block (3.40) instead of the scalar block in (3.29) and evaluating the sum over residues at the poles $s=n$ and $s=\frac{\beta-\Delta-J-\tau}{2}+m-1+n$ we get

$$\begin{aligned} \gamma^{J,\Delta} = &\,4\frac{\kappa_\beta}{C_0(\beta)}\sum_{m=0}^{J}\frac{(-1)^{m+1}}{(d-2)_J}\frac{A_m(J,\Delta)}{(\lambda_1-m)_m^2}\frac{\Gamma(-h+\Delta+1)\Gamma(2\lambda_1)}{\Gamma\left(\lambda_1\right)^2\Gamma\left(\lambda_1-m\right)}\sin^2\left(\frac{1}{2}\pi(\Delta+J+\tau)\right) \\ &\left(\frac{\Gamma(\beta)\Gamma\left(\lambda_1-m\right)\Gamma\left(\frac{\tau+2}{2}+\lambda_1-m\right)^2\Gamma\left(\frac{\beta-\tau-2}{2}-\lambda_1+m\right)}{\Gamma\left(\frac{\beta}{2}\right)^2\Gamma(-h-m+2\lambda_1+1)\Gamma\left(\frac{\beta+\tau+2}{2}+\lambda_1-m\right)}\right. \\ &\times{}_4F_3\left[\begin{matrix}1-h+\lambda_1,\lambda_1-m,\frac{\tau}{2}+\lambda_1-m+1,\frac{\tau}{2}+\lambda_1-m+1\\ -h+2\lambda_1-m+1,\frac{-\beta+\tau}{2}+\lambda_1-m+2,\frac{\beta+\tau}{2}+\lambda_1-m+1\end{matrix};1\right] \\ &\left.+\frac{\Gamma\left(\frac{\beta-\tau-2}{2}\right)\Gamma\left(\frac{-2h+2m+\beta-\tau}{2}\right)\Gamma\left(\frac{2-\beta+\tau}{2}+\lambda_1-m\right)}{\Gamma\left(\frac{-2h+2}{2}+\lambda_1\right)\Gamma\left(\frac{\beta-2h-\tau}{2}+\lambda_1\right)}\,{}_4F_3\left[\begin{matrix}\frac{\beta}{2},\frac{\beta}{2},\frac{\beta-\tau}{2}-1,\frac{\beta-\tau}{2}-h+m\\ \beta,\frac{\beta-\tau}{2}-\lambda_1+m,-h+\frac{\beta-\tau}{2}+\lambda_1\end{matrix};1\right]\right). \end{aligned} \tag{3.41}$$

Which as in the scalar case can be written more compactly in terms of a Wilson function as,

$$\gamma^{J,\Delta} = 4\frac{\kappa_\beta}{C_0(\beta)}\sum_{m=0}^{J}\frac{(-1)^{m+1}}{(d-2)_J}\frac{A_m(J,\Delta)}{(\lambda_1-m)_m^2}\frac{\Gamma(\beta)\Gamma(2\,\lambda_1)\Gamma\left(\frac{\beta-\tau}{2}-1\right)\Gamma\left(\frac{\beta-\tau}{2}-h+m\right)\Gamma\left(\frac{\tau}{2}+\lambda_1-m+1\right)^2}{\Gamma\left(\frac{\beta}{2}\right)\Gamma\left(\lambda_1\right)^2\Gamma\left(\frac{\beta}{2}+\lambda_1+1-h\right)\Gamma\left(\frac{\beta}{2}+\lambda_1-m\right)}$$
$$\frac{\sin^2\left(\pi\left(\frac{\tau}{2}+\lambda_1-m\right)\right)\Gamma\left(-h+2\lambda_1-m+\frac{\beta}{2}+1\right)\Gamma(-h+\Delta+1)}{\Gamma\left(\frac{\beta-\tau}{2}-h+\lambda_1\right)\Gamma\left(\frac{\beta+\tau}{2}+\lambda_1-m+1\right)\Gamma(-h-m+2\lambda_1+1)}$$
$${}_7F_6\left[\begin{matrix}\frac{\beta}{2},\lambda_1-h+1,\lambda_1-m,\frac{\beta}{4}+\lambda_1-\frac{h+m}{2}+1,\frac{\beta}{2}+2\lambda_1-h-m,\lambda_1-h-\frac{\tau}{2},\lambda_1-m+\frac{\tau}{2}+1\\ \frac{\beta}{4}+\lambda_1-\frac{h+m}{2},\frac{\beta}{2}+\lambda_1-h+1,\frac{\beta}{2}+\lambda_1-m,2\lambda_1-h-m+1,\frac{\beta-\tau}{2}+\lambda_1-h,\frac{\beta+\tau}{2}+\lambda_1-m+1\end{matrix};1\right].\tag{3.42}$$

3.4 Corrections to OPE Coefficients

Similarly as the contribution to the anomalous dimension at leading order in the light-cone limit is given by the $\log(z)$ factors, the OPE coefficient corrections corresponding to the given exchanges can be computed by performing the same exercise on the remaining non-log terms coming from the double poles at $t=0$ in the integral representation of the conformal blocks. In the following we shall compute such contributions. Corrections to the OPE have the following form,

$$\delta P_{\Delta,J} = \frac{1}{C_0(\beta)}\int_0^1\frac{d\bar{z}}{\bar{z}^2}\kappa_\beta k_\beta(\bar{z})\mathrm{dDisc}\left[\left(\frac{1-\bar{z}}{\bar{z}}\right)^{\frac{\tau}{2}}G^t_{\Delta,J}|_{\text{reg}}\right].\tag{3.43}$$

We will consider a general spin-J exchange case. Our starting point would be the integral representation of the regular terms of the conformal block calculated in ($B.24$). For both the anomalous dimension (3.29) and OPE correction (3.43), there are three sets of integrals : a) the $\bar{z}$ integral, b) kernel integral in Mellin Barnes, and c) the integral coming from the t-channel conformal block representation ($B.23$,$B.24$).To maintain uniformity we will transform the kernel in $\frac{\bar{z}-1}{\bar{z}}$ variable using,

$${}_2F_1(h,h,2h,z) = (1-z)^h{}_2F_1\left[h,h,2h,\frac{z}{z-1}\right].\tag{3.44}$$

After this transformation we will write the kernel hypergeometric as a Mellin-Barnes integral (3.20) in the t-variable. Now we are ready to perform the entire $\bar{z}$ integral involving spins. Collecting all powers of $\bar{z}$ from the kernel and the conformal block the $\bar{z}$ integral becomes,

$$\int_0^1 \frac{d\bar{z}}{\bar{z}^2}\bar{z}^{\epsilon}\left(\frac{\bar{z}}{1-\bar{z}}\right)^{\frac{\beta-\Delta-J-\tau}{2}+m-s+t} = \frac{\Gamma(\alpha+\epsilon+t)\Gamma(-\alpha-t)}{\Gamma(\epsilon)}\,, \tag{3.45}$$

with $\alpha = \frac{\beta-\tau}{2} - \lambda_1 + m - 1 - s$. The gamma functions contain terms that are mixed in s and t integral variables. The t-integral can be performed using the second Barnes' lemma (3.23). Just like before the t-integral generates a $\Gamma(\epsilon)$, which cancels the one generated by the $\bar{z}$-integral above. Now that the divergences have canceled, we can smoothly take the $\epsilon \to 0$ limit. Applying this to the OPE correction case (3.43), we will split the contribution into two parts (one coming from Mack polynomial term and one from Mack derivative term). The final expression involves the remaining integral in s,

$$\begin{aligned}\delta P^{(1)}_{\Delta,J} =&\alpha_J \sum_{m=0}^{J} \frac{(-1)^{m+1}}{(\lambda_1-m)_m^2} A_m(J,\Delta)\\ &\times \int_{\mathcal{C}} ds \Gamma(-s)\frac{(\lambda_1-m)_s(1-\bar{\lambda}_2)_s}{(1+\lambda_2-\bar{\lambda}_2)_{s+J-m}}\frac{\Gamma(\frac{\beta-\tau}{2}-\lambda_1+m-1-s)\Gamma(\frac{\tau}{2}+\lambda_1-m+1+s)^2}{\Gamma(\frac{\beta+\tau}{2}+\lambda_1-m+1+s)}\\ &\times\left[(H_{s+\lambda_1-m-1} - \pi\cot\pi(s+\lambda_1-m) - H_{s-\bar{\lambda}_2} + H_{-\lambda_2-J+m} + H_{-\bar{\lambda}_2})\right].\end{aligned} \tag{3.46}$$

The Mack derivative term is,

$$\begin{aligned}\delta P^{(2)}_{\Delta,J} =&\frac{\alpha_J}{(d-\Delta-1)_J}\sum_{m=0}^{J}\sum_{n=0}^{J-m}\frac{(-1)^{m+n+1}}{(\lambda_1-m-n)^2_{m+n}}B_{m,n}(J,\Delta)\\ &\times \int_{\mathcal{C}} ds\Gamma(-s)\frac{(\lambda_1-m-n)_s(1-\bar{\lambda}_2)_s}{(1+\lambda_2-\bar{\lambda}_2)_{s+J-m-n}}\frac{\Gamma(\frac{\beta-\tau}{2}-\lambda_1+m+n-1-s)\Gamma(\frac{\tau}{2}+\lambda_1-m-n+1+s)^2}{\Gamma(\frac{\beta+\tau}{2}+\lambda_1-m-n+1+s)}\,.\end{aligned} \tag{3.47}$$

In the above equations we have defined α_J as,

$$\alpha_J = 2\sin^2\left[\left(\frac{\tau}{2}+\lambda_2\right)\pi\right]\frac{\kappa_\beta}{C_0(\beta)}\frac{\Gamma(2\lambda_1)\Gamma(\beta)}{\Gamma(\lambda_1)^2\Gamma(\frac{\beta}{2})^2}\frac{1}{(d-2)_J}. \tag{3.48}$$

The $2\sin^2\left[\left(\frac{\tau}{2}+\lambda_2\right)\pi\right]$ term comes from the double-discontinuity of the conformal block and its pre-factor: $\left(\frac{1-\bar{z}}{\bar{z}}\right)^{\frac{\tau}{2}} G^{t}_{\Delta,J}|_{\text{reg}}$. Now we will proceed with the s-integral.

3.4.1 Terms with Mack Polynomial

For simplicity of calculation we will split (3.46) into three parts. I_1 contains the integral with Harmonic numbers that depend on s,

$$I_1 = \alpha_J \sum_{m=0}^{J} (-1)^{m+1} \frac{A_m(J,\Delta)}{(\lambda_1 - m)^2_m} \int_{\mathcal{C}} ds \Gamma(-s) \frac{(\lambda_1 - m)_s (1-\bar{\lambda}_2)_s}{(1+\lambda_2-\bar{\lambda}_2)_{s+J-m}} \frac{\Gamma(\frac{\beta-\tau}{2} - \lambda_1 + m - 1 - s)}{\Gamma(\frac{\beta+\tau}{2} + \lambda_1 - m + 1 + s)} \times \Gamma(\frac{\tau}{2} + \lambda_1 - m + 1 + s)^2 \left[H_{s+\lambda_1-m-1} - H_{s-\bar{\lambda}_2}\right]. \tag{3.49}$$

I_2 is an integral involving the Cotangent term,

$$\begin{aligned} I_2 =& \alpha_J \pi \sum_{m=0}^{J} \frac{(-1)^m}{(\lambda_1 - m)^2_m} A_m(J,\Delta) \\ & \int_{\mathcal{C}} ds \Gamma(-s) \frac{(\lambda_1 - m)_s (1-\bar{\lambda}_2)_s}{(1+\lambda_2-\bar{\lambda}_2)_{s+J-m}} \frac{\Gamma(\frac{\beta-\tau}{2} - \lambda_1 + m - 1 - s)\Gamma(\frac{\tau}{2} + \lambda_1 - m + 1 + s)^2}{\Gamma(\frac{\beta+\tau}{2} + \lambda_1 - m + 1 + s)} \\ & \times \cot \pi(s + \lambda_1 - m). \end{aligned} \tag{3.50}$$

I_3 is the integral involving the remaining pieces,

$$\begin{aligned} I_3 =& \alpha_J \sum_{m=0}^{J} \frac{(-1)^{m+1}}{(\lambda_1 - m)^2_m} A_m(J,\Delta) \left[H_{-\lambda_2-J+m} + H_{-\bar{\lambda}_2}\right] \\ & \times \int_{\mathcal{C}} ds \Gamma(-s) \frac{(\lambda_1 - m)_s (1-\bar{\lambda}_2)_s}{(1+\lambda_2-\bar{\lambda}_2)_{s+J-m}} \frac{\Gamma(\frac{\beta-\tau}{2} - \lambda_1 + m - 1 - s)\Gamma(\frac{\tau}{2} + \lambda_1 - m + 1 + s)^2}{\Gamma(\frac{\beta+\tau}{2} + \lambda_1 - m + 1 + s)}. \end{aligned} \tag{3.51}$$

We will perform these integrals separately and then add the contributions up together. Closing the contour to the right half plane gives rise to two series of poles in s,

$$s \in \mathbb{N} \qquad s \in \frac{\beta - \tau}{2} - \lambda_1 + m - 1 + \mathbb{N} \tag{3.52}$$

These two infinite sum over residues again give rise to two ${}_4F_3$ hypergeometrics. The integral in I_1 involves Harmonic numbers therefore the sum over residues would involve Harmonic numbers in sum as well. To perform this sum we will employ the trick given in appendix (B.2). The final result is,

$$\begin{aligned}
I_1 =&\alpha_J \sum_{m=0}^{J} \frac{(-1)^{m+1}}{(\lambda_1-m)_m^2} A_m(J,\Delta) \frac{\Gamma(1+\lambda_2-\bar{\lambda}_2)}{\Gamma(\lambda_1-m)\Gamma(1-\bar{\lambda}_2)} \\
&\Bigg[C_m(J,\Delta) \Bigg({}_4F_3\left[\begin{matrix} 1-h+\lambda_1, \lambda_1-m, \frac{\tau}{2}+\lambda_1-m+1, \frac{\tau}{2}+\lambda_1-m+1 \\ -h+2\lambda_1-m+1, \frac{-\beta+\tau}{2}+\lambda_1-m+2, \frac{\beta+\tau}{2}+\lambda_1-m+1 \end{matrix}; 1\right] \\
&(H_{\frac{J+\Delta}{2}-m-1} - H_{-h+\frac{J+\Delta}{2}}) - \mathcal{G}_1 \Bigg) \\
&+ D_m(J,\Delta) \Bigg({}_4F_3\left[\begin{matrix} \frac{\beta}{2}, \frac{\beta}{2}, \frac{\beta-\tau}{2}-1, \frac{\beta-\tau}{2}-h+m \\ \beta, \frac{\beta-\tau}{2}-\lambda_1+m, -h+\frac{\beta-\tau}{2}+\lambda_1 \end{matrix}; 1\right] (H_{\frac{\beta-\tau}{2}-2} - H_{\frac{\beta-\tau}{2}-h+m-1}) + \mathcal{G}_2 \Bigg) \Bigg],
\end{aligned} \tag{3.53}$$

where we have defined,

$$\begin{aligned}
C_m(J,\Delta) =& \frac{\Gamma(\lambda_1-h+1)\Gamma(\lambda_1-m)\Gamma\left(\frac{\tau}{2}+\lambda_1+1-m\right)^2 \Gamma\left(m-1+\frac{\beta-\tau}{2}-\lambda_1\right)}{\Gamma(-h-m+2\lambda_1+1)\Gamma\left(\frac{\beta+\tau}{2}+\lambda_1-m+1\right)}, \\
D_m(J,\Delta) =& \frac{\Gamma\left(\frac{\beta}{2}\right)^2 \Gamma\left(\frac{\beta-\tau}{2}-1\right)\Gamma\left(-h+m+\frac{\beta-\tau}{2}\right)\Big)\Gamma\left(\frac{\tau-\beta}{2}+\lambda_1-m+1\right)}{\Gamma(\beta)\Gamma\left(\frac{\beta-\tau}{2}+\lambda_1-h\right)},
\end{aligned} \tag{3.54}$$

to make these expressions more compact. The functions $\mathcal{G}_1$ and $\mathcal{G}_2$ are the Kampé de Fériet-like functions defined in (B.39).

For the remaining terms, performing the integral is straightforward and we obtain,

$$
\begin{aligned}
I_2 =&\pi\alpha_J \sum_{m=0}^{J} \frac{(-1)^m}{(\lambda_1-m)_m^2} A_m(J,\Delta) \frac{\Gamma(1+\lambda_2-\bar{\lambda}_2)}{\Gamma(\lambda_1-m)\Gamma(1-\bar{\lambda}_2)} \Bigg(C_m(J,\Delta)\ \cot\left[\pi\left(\lambda_1-m\right)\right] \\
&\times_4 F_3\left[\begin{matrix} 1-h+\lambda_1, \lambda_1-m, \frac{\tau}{2}+\lambda_1-m+1, \frac{\tau}{2}+\lambda_1-m+1 \\ -h+2\lambda_1-m+1, \frac{-\beta+\tau}{2}+\lambda_1-m+2, \frac{\beta+\tau}{2}+\lambda_1-m+1 \end{matrix}; 1\right] \\
&+ D_m(J,\Delta)\ \cot\left[\pi\left(\frac{\beta-\tau}{2}\right)\right]\ {}_4F_3\left[\begin{matrix} \frac{\beta}{2}, \frac{\beta}{2}, \frac{\beta-\tau}{2}-1, \frac{\beta-\tau}{2}-h+m \\ \beta, \frac{\beta-\tau}{2}-\lambda_1+m, -h+\frac{\beta-\tau}{2}+\lambda_1 \end{matrix}; 1\right]\Bigg),
\end{aligned} \tag{3.55}
$$

and,

$$
\begin{aligned}
I_3 =&\alpha_J \sum_{m=0}^{J} \frac{(-1)^{m+1}}{(\lambda_1-m)_m^2} A_m(J,\Delta) \frac{\Gamma(1+\lambda_2-\bar{\lambda}_2)}{\Gamma(\lambda_1-m)\Gamma(1-\bar{\lambda}_2)} \left[H_{-\lambda_2-J+m}+H_{-\bar{\lambda}_2}\right] \\
&\Bigg[C_m(J,\Delta)\ \ {}_4F_3\left[\begin{matrix} 1-h+\lambda_1, \lambda_1-m, \frac{\tau}{2}+\lambda_1-m+1, \frac{\tau}{2}+\lambda_1-m+1 \\ -h+2\lambda_1-m+1, \frac{-\beta+\tau}{2}+\lambda_1-m+2, \frac{\beta+\tau}{2}+\lambda_1-m+1 \end{matrix}; 1\right] \\
&+ D_m(J,\Delta)\ \ {}_4F_3\left[\begin{matrix} \frac{\beta}{2}, \frac{\beta}{2}, \frac{\beta-\tau}{2}-1, \frac{\beta-\tau}{2}-h+m \\ \beta, \frac{\beta-\tau}{2}-\lambda_1+m, -h+\frac{\beta-\tau}{2}+\lambda_1 \end{matrix}; 1\right]\Bigg].
\end{aligned} \tag{3.56}
$$

3.4.2 Terms with Derivative of Mack Polynomial

Performing the s-integral in (3.47) results in the following piece of the correction,

$$
\begin{aligned}
\delta P^{(2)}_{\Delta,J} =& \frac{\alpha_J}{(d-\Delta-1)_J} \sum_{m+n\leq J} \frac{(-1)^{m+n+1}}{(\lambda_1-m-n)_{m+n}^2} B_{m,n}(J,\Delta) \frac{\Gamma(1+\lambda_2-\bar{\lambda}_2)}{\Gamma(\lambda_1-m-n)\Gamma(1-\bar{\lambda}_2)} \\
&\times \Bigg(C_{m+n}(J,\Delta)\ \ {}_4F_3\left[\begin{matrix} 1-h+\lambda_1, \lambda_1-m, \frac{\tau}{2}+\lambda_1-m+1, \frac{\tau}{2}+\lambda_1-m+1 \\ -h+2\lambda_1-m+1, \frac{-\beta+\tau}{2}+\lambda_1-m+2, \frac{\beta+\tau}{2}+\lambda_1-m+1 \end{matrix}; 1\right] \\
&+ D_{m+n}(J,\Delta)\ \ {}_4F_3\left[\begin{matrix} \frac{\beta}{2}, \frac{\beta}{2}, \frac{\beta-\tau}{2}-1, \frac{\beta-\tau}{2}-h+m \\ \beta, \frac{\beta-\tau}{2}-\lambda_1+m, -h+\frac{\beta-\tau}{2}+\lambda_1 \end{matrix}; 1\right]\Bigg).
\end{aligned} \tag{3.57}
$$

This term has a double sum in m and n variables with the constraint that $m + n < J$.

3.4.3 Total Correction to OPE Coefficients

The net contribution to the OPE correction for a general spin-J exchange is the sum of all the above terms,

$$\begin{aligned}\delta P_{\Delta,J} &= \delta P^{(1)}_{\Delta,J} + \delta P^{(2)}_{\Delta,J} \\ &= I_1 + I_2 + I_3 + \delta P^{(2)}_{\Delta,J}\end{aligned} \tag{3.58}$$

We can recover the scalar exchange OPE correction by setting $m = J = 0$ in the above equation. From (3.53) we obtain,

$$\begin{aligned}I_1 = -\alpha_0 \frac{\Gamma(1-h+\Delta)}{\Gamma(1-h+\frac{\Delta}{2})\Gamma(\frac{\Delta}{2})} &\Bigg(C_0(0,\Delta) \Bigg[{}_4F_3 \left[\begin{matrix} \frac{\Delta}{2},\ 1-h+\frac{\Delta}{2},\ 1+\frac{\Delta+\tau}{2},\ 1+\frac{\Delta+\tau}{2} \\ 1-h+\Delta,\ 2-\frac{\beta-\Delta-\tau}{2},\ 1+\frac{\beta+\Delta+\tau}{2} \end{matrix} ;1 \right] \\ &\times (H_{\frac{\Delta}{2}-1} - H_{-h+\frac{\Delta}{2}}) - \mathcal{G}_1 \Bigg] + D_0(0,\Delta) \\ &\times \Bigg[{}_4F_3 \left[\begin{matrix} \frac{\beta}{2},\ \frac{\beta}{2},\ -1+\frac{\beta+\tau}{2},\ -h+\frac{\beta+\tau}{2} \\ \beta,\ \frac{\beta-\tau-\Delta}{2},\ -h+\frac{\beta+\Delta-\tau}{2} \end{matrix} ;1 \right] (H_{\frac{\beta-\tau}{2}-2} - H_{\frac{\beta-\tau}{2}-h-1}) + \mathcal{G}_2 \Bigg] \Bigg)\end{aligned} \tag{3.59}$$

In the above equation $\mathcal{G}_1$ and $\mathcal{G}_2$ are (B.39) with $m = J = 0$. The result for the cotangent contribution is,

$$\begin{aligned}I_2 =& \pi\alpha_0 \frac{\Gamma(1-h+\Delta)}{\Gamma(1-h+\frac{\Delta}{2})\Gamma(\frac{\Delta}{2})} \left(D_0(0,\Delta) \cot\left(\frac{\pi(\beta-\tau)}{2}\right) {}_4F_3 \left[\begin{matrix} \frac{\beta}{2},\ \frac{\beta}{2},\ -1+\frac{\beta+\tau}{2},\ -h+\frac{\beta+\tau}{2} \\ \beta,\ \frac{\beta-\tau-\Delta}{2},\ -h+\frac{\beta+\Delta-\tau}{2} \end{matrix} ;1 \right] \right. \\ &\left. + C_0(0,\Delta) \cot\left(\frac{\pi\Delta}{2}\right) {}_4F_3 \left[\begin{matrix} \frac{\Delta}{2},\ 1-h+\frac{\Delta}{2},\ 1+\frac{\Delta+\tau}{2},\ 1+\frac{\Delta+\tau}{2} \\ 1-h+\Delta,\ 2-\frac{\beta-\Delta-\tau}{2},\ 1+\frac{\beta+\Delta+\tau}{2} \end{matrix} ;1 \right] \right).\end{aligned} \tag{3.60}$$

The constant terms are,

$$
\begin{aligned}
I_3 = &-\alpha_0 \frac{\Gamma(1-h+\Delta)}{\Gamma(1-h+\frac{\Delta}{2})\Gamma(\frac{\Delta}{2})}\Bigg(D_0(0,\Delta)\ {}_4F_3\left[\begin{matrix}\frac{\beta}{2},\ \frac{\beta}{2},\ -1+\frac{\beta+\tau}{2},\ -h+\frac{\beta+\tau}{2} \\ \beta,\ \frac{\beta-\tau-\Delta}{2},\ -h+\frac{\beta+\Delta-\tau}{2}\end{matrix};1\right] \\
&+ C_0(0,\Delta){}_4F_3\left[\begin{matrix}\frac{\Delta}{2},\ 1-h+\frac{\Delta}{2},\ 1+\frac{\Delta+\tau}{2},\ 1+\frac{\Delta+\tau}{2} \\ 1-h+\Delta,\ 2-\frac{\beta-\Delta-\tau}{2},\ 1+\frac{\beta+\Delta+\tau}{2}\end{matrix};1\right]\Bigg) \\
&\times (H_{-\frac{\Delta}{2}} + H_{\frac{\Delta}{2}-h})\,.
\end{aligned} \tag{3.61}
$$

Putting all the pieces together we obtain the total correction to the OPE coefficient to be,

$$
\delta P^{t}_{\Delta,0} = I_1 + I_2 + I_3. \tag{3.62}
$$

There is no Mack derivative term $\delta P^{(2)}_{\Delta,0}$ for the scalar exchange case. Thus for the scalar the correction to the OPE coefficient essentially comes from the finite part (excluding the $\log$ term) of the measure. For spin case, the additional contribution comes from $\delta P^{(2)}_{\Delta,J}$ part.

3.4.4 Special Cases

The expression for OPE coefficients undergo simplifications in even dimensions. The terms involving Kampé de Fériet-like double sums reduce to ${}_4F_3$ Hypergeometrics. Since those terms are generated by the I_1 integral, their reduction can be easily seen from the integral representation of I_1,

$$
\begin{aligned}
I_1 = \alpha_J \sum_{m=0}^{J} \frac{(-1)^{m+1}}{(\lambda_1-m)_m^2} \int_{\mathcal{C}} ds \Gamma(-s) \frac{(\lambda_1-m)_s(1-\bar{\lambda}_2)_s}{(1+\lambda_2-\bar{\lambda}_2)_{s+J-m}} \frac{\Gamma(\frac{\beta-\Delta-J-\tau}{2}+m-1-s)\Gamma(\frac{\Delta+J+\tau}{2}-m+1+s)^2}{\Gamma(\frac{\beta+\Delta+J+\tau}{2}-m+1+s)} \\
\times A_m(J,\Delta)\left[H_{s+\lambda_1-m-1} - H_{s-\bar{\lambda}_2}\right].
\end{aligned} \tag{3.63}
$$

The double sums were generated by the derivatives of ${}_4F_3$ hypergeometric with respect to their parameters. In even dimensions the Harmonic number parameters are integer separated,

$$
H_{s+\lambda_1-m-1} - H_{s-\bar{\lambda}_2} \to H_{s+\frac{\Delta+J}{2}-m-1} - H_{s+\frac{\Delta+J}{2}-h}\,, \tag{3.64}
$$

In the above equation m is an integer while h is an integer in even dimensions. In this case, the difference of Harmonic numbers reduces to a simple functions of s using the Harmonic number recursion relations. For simplicity we will consider the case of scalars where ($m = J = 0$). The difference (3.64) vanishes in two dimensions and in four dimensions it simplifies to,

$$H_{s+\frac{\Delta}{2}-1} - H_{s+\frac{\Delta}{2}-2} = \frac{1}{s+\frac{\Delta}{2}-1}\,. \tag{3.65}$$

3.4.4.1 Two Dimensions

Since h=1 the integral for I_1 vanishes in two dimensions,

$$I_1^{2d} = 0 \tag{3.66}$$

For the other integrals (I_2 and I_3) we can directly take the final result for the scalar case from (3.60) and (3.61) and substitute the values of h. Let us first define the following functions:

$$f_1(h) = \frac{\Gamma(1-h+\Delta)}{\Gamma(1-h+\frac{\Delta}{2})\Gamma(\frac{\Delta}{2})}C_0(0,\Delta) = \frac{\Gamma\left(\frac{\Delta+\tau+2}{2}\right)^2\Gamma\left(\frac{\beta-\Delta-\tau-2}{2}\right)}{\Gamma\left(\frac{\beta+\Delta+\tau+2}{2}\right)}\,, \tag{3.67}$$

$$\begin{aligned} f_2(h) =& D_0(0,\Delta)\frac{\Gamma(1-h+\Delta)}{\Gamma(1-h+\frac{\Delta}{2})\Gamma(\frac{\Delta}{2})} \\ =& \frac{\Gamma\left(\frac{\beta}{2}\right)^2\Gamma(-h+\Delta+1)\Gamma\left(\frac{-\beta+\Delta+\tau+2}{2}\right)\Gamma\left(\frac{+\beta-\tau-2}{2}\right)\Gamma\left(\frac{-2h+\beta-\tau}{2}\right)}{\Gamma(\beta)\Gamma\left(\frac{\Delta}{2}\right)\Gamma\left(\frac{-2h+\Delta+2}{2}\right)\Gamma\left(\frac{-2h+\beta+\Delta-\tau}{2}\right)}\,. \end{aligned} \tag{3.68}$$

The correction to OPE coefficient for a scalar in two dimension becomes,

$$\delta P^{2d}_{\Delta,0} = \alpha_0\Big(f_2(1)\,{}_4F_3\left[\begin{matrix}\frac{\beta}{2},\ \frac{\beta}{2},\ -1+\frac{\beta+\tau}{2},\ -1+\frac{\beta+\tau}{2}\\ \beta,\ \frac{\beta-\tau-\Delta}{2},\ -1+\frac{\beta+\Delta-\tau}{2}\end{matrix};1\right](\pi\cot(\pi\Delta/2)-H_{-\frac{\Delta}{2}}-H_{\frac{\Delta}{2}-1})$$
$$+ f_1(1)\,{}_4F_3\left[\begin{matrix}\frac{\Delta}{2},\ \frac{\Delta}{2},\ 1+\frac{\Delta+\tau}{2},\ 1+\frac{\Delta+\tau}{2}\\ \Delta,\ 2-\frac{\beta-\Delta-\tau}{2},\ 1+\frac{\beta+\Delta+\tau}{2}\end{matrix};1\right](\pi\cot(\pi(\beta-\tau)/2)-H_{-\frac{\Delta}{2}}-H_{\frac{\Delta}{2}-1})\Big)\,, \tag{3.69}$$

3.4.4.2 Four Dimensions

For four dimensions, the I_1 integral simplifies to,

$$I_1^{4d} = -\alpha_0\int_{\mathcal{C}} ds\Gamma(-s)\frac{(\lambda_1)_s(1-\bar{\lambda}_2)_s}{(1+\lambda_2-\bar{\lambda}_2)_s}\frac{\Gamma(\frac{\beta-\Delta-\tau}{2}-1-s)\Gamma(\frac{\Delta+\tau}{2}+1+s)^2}{\Gamma(\frac{\beta+\Delta+\tau}{2}+1+s)}\frac{1}{s+\frac{\Delta}{2}-1}\,. \tag{3.70}$$

This integral can be easily evaluated and results in two ${}_4F_3$ hypergeometric functions only and no Kampé de Fériet-like double sums.

$$\delta P^{4d}_{\Delta,0} = \alpha_0\Big(f_1(2)\,{}_4F_3\left[\begin{matrix}\frac{\Delta}{2},\ -1+\frac{\Delta}{2},\ 1+\frac{\Delta+\tau}{2},\ 1+\frac{\Delta+\tau}{2}\\ -1+\Delta,\ 2-\frac{\beta-\Delta-\tau}{2},\ 1+\frac{\beta+\Delta+\tau}{2}\end{matrix};1\right](\pi\cot(\pi\Delta/2)-H_{-\frac{\Delta}{2}}-H_{\frac{\Delta}{2}-1})$$
$$- f_1(2)\,{}_4F_3\left[\begin{matrix}-1+\frac{\Delta}{2},\ -1+\frac{\Delta}{2},\ 1+\frac{\Delta+\tau}{2},\ 1+\frac{\Delta+\tau}{2}\\ -1+\Delta,\ 2-\frac{\beta-\Delta-\tau}{2},\ 1+\frac{\beta+\Delta+\tau}{2}\end{matrix};1\right](\frac{2}{\Delta-2})$$
$$+ f_2(2)\,{}_4F_3\left[\begin{matrix}\frac{\beta}{2},\ \frac{\beta}{2},\ -1+\frac{\beta+\tau}{2},\ -2+\frac{\beta+\tau}{2}\\ \beta,\ \frac{\beta-\tau-\Delta}{2},\ -2+\frac{\beta+\Delta-\tau}{2}\end{matrix};1\right](\pi\cot(\pi(\beta-\tau)/2)-H_{-\frac{\Delta}{2}}-H_{\frac{\Delta}{2}-1})$$
$$- f_2(2)\,{}_4F_3\left[\begin{matrix}\frac{\beta}{2},\ \frac{\beta}{2},\ -2+\frac{\beta+\tau}{2},\ -2+\frac{\beta+\tau}{2}\\ \beta,\ \frac{\beta-\tau-\Delta}{2},\ -2+\frac{\beta+\Delta-\tau}{2}\end{matrix};1\right](\frac{2}{\beta-\tau-4})\Big)\,. \tag{3.71}$$

The extra ${}_4F_3$ hypergeometrics in the four dimensions case compared to two dimensions are generated from the I_1 integral (which vanished in 2d).

In this chapter, we aim to understand whether (and to what extent) there exists a connection between the basis of functions $f_{i,j}(z,\bar{z})$ and the functions appearing in diagrammatic perturbation theory of massless ϕ^4 theories. To sum up, we recast the expansion of $\mathrm{dDisc}\,\mathcal{G}^t(z,\bar{z})$ in terms of functions inspired from the integrals found in diagrammatic massless ϕ^4 theory.

4.1 Introduction

The ϵ-expansion technique of Wilson and Kogut [25, 26] and innumerable followups demonstrated an effective way to compute the corrections to dynamical quantities (dimensions, coupling etc.) along the RG flow. Recently, [59, 60] developed tools to compute the same quantities from the bootstrap program. Equivalently, using the inversion formula of [19] in the light-cone limit $(1-\bar{z} \ll z \ll 1)$,

$$C(\beta) = \int d^2z\ \mu(z,\bar{z})\ k_\beta(\bar{z})\ \mathrm{dDisc}\left[\mathcal{G}^t(z,\bar{z})\right]_{\mathrm{LC}} + (t \to u)\,, \tag{4.1}$$

[24, 61, 62] demonstrated that the tower of large spin double twist operators in the direct channel ($\beta = \tau_\ell + 2\ell$), is controlled by the perturbative expansion of the crossed channel correlator around a Wilson-Fisher fixed point in $d = 4-\epsilon$ dimensions[1]. The quantity of specific interest is $\mathrm{dDisc}\left(\mathcal{G}^t(z,\bar{z})\right)$ expanded around the WF fixed point,

$$\mathrm{dDisc}\left[\mathcal{G}^t(z,\bar{z})\right]_{\mathrm{LC}} = \mathrm{dDisc}\left[\frac{(z\bar{z})^{\Delta_\phi}}{(1-\bar{z})^{\Delta_\phi}}\sum_{\mathcal{O}} C_{\phi\phi\mathcal{O}}G_{\Delta_{\mathcal{O}},\ell}(1-z,1-\bar{z})\right]_{\mathrm{LC}}\,, \tag{4.2}$$

where $\mathcal{O}$ is the traceless symmetric exchange in the OPE of $\phi\times\phi$ around the perturbative fixed point and $G_{\Delta_{\mathcal{O}},\ell}$ is the conformal block. We have the following perturbative expansion for the

[1] See also [63, 49, 64, 65] for useful applications related to large spin expansion and inversion formula.

scaling dimensions and three-point coefficients,

$$\begin{aligned}
\Delta_\phi &= \Delta_\phi^0 + g^2\gamma_\phi + \dots\,, \\
\Delta_{\mathcal{O}} &= 2\Delta_\phi + \ell + \begin{cases} g\gamma_{\mathcal{O}}\,, \ell = 0 \\ g^2\gamma_{\mathcal{O}}\,, \ell > 0 \end{cases} + \dots\,, \\
C_{\phi\phi\mathcal{O}} &= C^0_{\phi\phi\mathcal{O}} + gC^1_{\phi\phi\mathcal{O}} + \dots\,,
\end{aligned} \tag{4.3}$$

where we treat g and ϵ to be independent for now. We represent the double-discontinuity as,

$$\text{dDisc}\left[\mathcal{G}^t(z,\bar{z})\right]_{\text{LC}} = \text{dDisc}\left[(1-\bar{z})^{\gamma/2}\right] \sum_{i+j=n} g^i \epsilon^j f_{i,j}(z,\bar{z})\,,\; n \geq 0\,, \tag{4.4}$$

where γ is the anomalous dimension given in (4.3). This is either $O(g)$ or $O(g^2)$ depending on scalar and higher spin exchanges respectively. Due to the perturbative expansion leading ($\tau = 2$) scalar contributes to lowest orders upto $O(g^3)$ while $O(g^4)$ onwards scalars mix with other higher spin operators.

4.2 Scalar Block Expansion

To expand the conformal block we first start with the integral representation of the block with scalar exchange[56, 51, 66]. We expand it in the $z \to 0$ limit and obtain (see -C.2 for details),

$$\begin{aligned}
&G_{\Delta,0}(1-z,1-\bar{z}) \\
&= \frac{(1-\bar{z})^{\Delta/2}}{\bar{z}} \frac{\Gamma(1+\Delta-h)\Gamma(\Delta)}{\Gamma(\frac{\Delta}{2})^3\Gamma(\frac{\Delta}{2}-h+2)}\bigg[(\Delta/2-(h-1-\Delta/2)\bar{z}) \\
&\times \int_0^1 dx\, \mathcal{I}_1^{\Delta,h}(x,0,1-\bar{z})\left(2H_{\Delta/2-1} + \log\frac{z\bar{z}}{(1-x(1-\bar{z}))^2}\right) \\
&+ (1-\bar{z})\int_0^1 dx\, \mathcal{I}_2^{\Delta,h}(x,0,1-\bar{z})\left(2 + (h-2-\Delta/2)(2H_{\Delta/2-1} + \log\frac{z\bar{z}}{(1-x(1-\bar{z}))^2})\right)\bigg]\,.
\end{aligned} \tag{4.5}$$

In this expansion we plug in the parameters,

$$d = 4 - \epsilon\,,\ \Delta_\phi = (d-2)/2 + \gamma_\phi(g)\,,\ \Delta = 2\Delta_\phi + \gamma_\Delta(g) = d - 2 + \gamma(g)\,, \tag{4.6}$$

where $\gamma = 2\gamma_\phi + \gamma_\Delta$ and $h = d/2$. γ_Δ and γ_ϕ are respectively,

$$\gamma_\Delta(g) = g\,,\ \ \gamma_\phi(g) = \frac{g^2}{12} - \frac{g^3}{8} + \frac{11}{144}g^2\epsilon + \dots\,. \tag{4.7}$$

Even though $g = f(\epsilon)$, [2]for now we will consider these two parameters as being independent. Using (4.6), we expand (4.5) to get,

$$\begin{aligned}
\mathcal{G}_{\Delta,0}(1-z,1-\bar{z}) &= \left(\frac{z\bar{z}}{1-\bar{z}}\right)^{\Delta_\phi} G_{\Delta,0}(1-z,1-\bar{z}) \\
&= (z\bar{z})^{\Delta_\phi}\frac{(1-\bar{z})^{g/2}}{\bar{z}}\frac{\Gamma(2-\epsilon+\gamma(g))\Gamma(1-\epsilon/2+\gamma(g))}{\Gamma(1+\frac{\gamma(g)-\epsilon}{2})^3\Gamma(1+\gamma(g)/2)}\Bigg[(1-\bar{z})\int_0^1 dx\mathcal{I}_2^{\gamma(g),\epsilon}(x,1-\bar{z}) \\
&\qquad + (1+(\gamma(g)-\epsilon)/2+\gamma(g)/2\ \bar{z})\int_0^1 dx\mathcal{I}_1^{\gamma(g),\epsilon}(x,1-\bar{z})\Bigg]\,.
\end{aligned} \tag{4.8}$$

where,

$$\begin{aligned}
\mathcal{I}_1^{\gamma(g),\epsilon}(x,1-\bar{z}) &= \frac{x^{\frac{\gamma(g)-\epsilon}{2}}(1-x)^{\gamma(g)/2}}{(1-x(1-\bar{z}))^{1+\frac{\gamma(g)-\epsilon}{2}}}\left[2H_{\frac{\gamma(g)-\epsilon}{2}} + \log\frac{z\bar{z}}{(1-x(1-\bar{z}))^2}\right]\,, \\
\mathcal{I}_2^{\gamma(g),\epsilon}(x,1-\bar{z}) &= \frac{x^{1+\frac{\gamma(g)-\epsilon}{2}}(1-x)^{\gamma(g)/2}}{(1-x(1-\bar{z}))^{1+\frac{\gamma(g)-\epsilon}{2}}}\left[2-(1+\gamma(g)/2)\left(2H_{\frac{\gamma(g)-\epsilon}{2}} + \log\frac{z\bar{z}}{(1-x(1-\bar{z}))^2}\right)\right]\,.
\end{aligned} \tag{4.9}$$

We utilize the following identity of harmonic numbers,

$$H_{\frac{\gamma(g)-\epsilon}{2}} = \sum_{n=1}^{\infty}(-1)^{n-1}\zeta_{n+1}\left(\frac{\gamma(g)-\epsilon}{2}\right)^n\,, \tag{4.10}$$

[2]Obtained by setting the $\beta-$function to zero order by order in usual perturbative QFT.

and,

$$\frac{x^{\frac{\gamma(g)-\epsilon}{2}}(1-x)^{\gamma(g)/2}}{(1-x(1-\bar{z}))^{\frac{\gamma(g)-\epsilon}{2}}}=\sum_{m,n=0}^{\infty}\frac{(\frac{\gamma(g)}{2})^m(\frac{\epsilon}{2})^n}{m!n!}\log^m\frac{x(1-x)}{1-x(1-\bar{z})}\log^n\frac{1-x(1-\bar{z})}{x}\,. \tag{4.11}$$

Using the expansion of anomalous dimension [67],

$$\gamma(g)=g+\alpha_1 g^2+\alpha_2 g^3+\alpha_3 g^2\epsilon+\dots\,,\quad \alpha_1=\frac{1}{6}\,,\ \alpha_2=-\frac{1}{4}\,,\ \alpha_3=\frac{11}{72}\,, \tag{4.12}$$

we rewrite (4.8) in terms of the known integrals [68],

$$I_{\chi_1}(\chi_2,\chi_3,\chi_4,1-\bar{z})=\int_0^1\frac{x^{\chi_1}\log^{\chi_2}x\log^{\chi_3}(1-x)\log^{\chi_4}(1-x(1-\bar{z}))}{1-x(1-\bar{z})}\,, \tag{4.13}$$

where, for our purposes $\chi_1=0,1$. Finally we obtain,

$$\mathrm{dDisc}[G_{\Delta,0}(1-z,1-\bar{z})]=(z\bar{z})^{\Delta_\phi^{cl}}\left(\sum_{n=2}^{\infty}\frac{g^n}{2^n n!}\log^n(1-\bar{z})\right)\sum_{\alpha=0}^{\infty}\sum_{i+j=\alpha}g^i\epsilon^j f_{i,j}(z,\bar{z})\,. \tag{4.14}$$

The dDisc starts from $n\geq 2$. The details of $f_{i,j}(z,\bar{z})$ are given in appendix C.2.3 and we intend to put these functions in a basis. In the following section, we perform the same analysis for twist-2 higher spin ($\ell\geq 2$) operators.

4.3 Twist-2 Operators

In the $z\to 0$ limit, the twist-2 block is given by (refer to (C.29) of C.2),

$$\begin{aligned}\mathcal{G}_2(z,\bar{z})=&(z\bar{z})^{\Delta_\phi}[(1-\bar{z})(1-z)]^{\lambda_2-\Delta_\phi}\int_0^1 dx\frac{(x(1-x))^{d/2-2}}{(z+x(1-z))^{d/2-1}(\bar{z}+x(1-\bar{z}))^{d/2-1}}\\&\times\frac{\Gamma(d-3)}{\Gamma(d/2-1)^2}\sum_{\ell=2}^{\infty}\frac{(d-3+2\ell)}{\ell^2(\ell+1)^2}C_\ell^{(d-3)/2}(1-2x)\,.\end{aligned} \tag{4.15}$$

For the order we are interested in, $\Gamma(d-3)/\Gamma(d/2-1)^2=1$. For twist$-2$ operators the scaling dimensions are $\Delta=2\Delta_\phi+\ell+g^2\gamma_\ell$ and hence $\lambda_2=(\Delta-\ell)/2=\Delta_\phi+g^2/2\gamma_\ell$ and $\Delta_\phi=1-\epsilon/2$.

To perform the sum over spin we consider a generalization of the form,

$$\sum_{\ell=2}^{\infty}\frac{(2\lambda+2\ell)}{(J_\lambda^2)^m}C_\ell^\lambda(x)=F_{m,\lambda}(x)\,, \tag{4.16}$$

where for twist-2 operators $J_\lambda^2=(\ell+\lambda+1/2)(\ell+\lambda-1/2)$, $\lambda=(d-3)/2$ and $d=4-\epsilon$. Using the differential equation [49] for $C_\ell^\lambda(x)$,

$$D_\lambda\equiv(1-x^2)d_x^2-(2\lambda+1)xd_x-(\lambda^2-1/4)\,,\ D_\lambda C_\ell^\lambda(x)=-J_\lambda^2C_\ell^\lambda(x)\,,\ d_x\equiv d/dx\,, \tag{4.17}$$

we can write,

$$D_\lambda F_{m,\lambda}(x)=-F_{m-1,\lambda}(x)\,,\ \ \forall\, m\geq 1\,, \tag{4.18}$$

as the generalization of the leading contribution. First we determine $F_{0,\lambda}(x)$ and obtain the boundary conditions for $F_{1,\lambda}$ and $F_{2,\lambda}$ and plug the lower order solutions in the *rhs* to determine the $m+1$-th terms. Regarding the boundary conditions one can show that,

$$F'_{m,\lambda}(x=0)=0\,. \tag{4.19}$$

Using the integral representation of $C_\ell^\lambda(x)$,

$$\begin{aligned}C_\ell^\lambda(x)&=\oint dz(1-2xz+z^2)^{-\lambda}z^{-1-\ell}\,,\\ F_{0,\lambda}(x)&=\sum_{\ell=2}^{\infty}(2\lambda+2\ell)C_\ell^\lambda(x)=-2\lambda\,.\end{aligned} \tag{4.20}$$

Solving for the first order we find,

$$F_{1,\lambda}(x)=a_{0,0}-\frac{1}{2}\log(1-x^2)+\frac{\epsilon}{8}(8a_{0,1}+2(a_{0,0}+1)\log(1-x^2)-\log^2(1-x)-\log^2(1+x))\,, \tag{4.21}$$

where,

$$F_{1,\lambda}(0)=a_{0,0}+\epsilon\, a_{0,1}\,, \tag{4.22}$$

and the constrants $a_{0,0}$ and $a_{0,1}$ can be determined from solving (4.20) at $x = 0$ and expanding in $\lambda = (1-\epsilon)/2$. For $m = 2$ a direct evaluation as a function of λ can be challenging, hence we separate,

$$F_{2,\lambda}(x) = g(x) + \epsilon\, h(x)\,, \tag{4.23}$$

where,

$$\begin{aligned} g(x) =& b_{0,0} + \frac{1+a_{0,0}}{2}\log(1-x^2) - \frac{1}{2}\log(1-x)\log(1+x)\,, \\ h(x) =& \frac{1}{24}\Bigg[6\tanh^{-1}x\left(\zeta_2 - 2\mathrm{Li}_2\frac{x-1}{x+1}\right) - 3\log^2(1-x)\log(1+x) - \log^3(1+x) \\ & - 12\mathrm{Li}_3\frac{x-1}{x+1} + 3\log^2(1-x^2)(1+a_{0,0}) + 6\log(1-x^2)(2a_{0,1}+b_{0,0}) + 24b_{0,1} - 9\zeta_3\Bigg]\,. \end{aligned} \tag{4.24}$$

We also have,

$$F_{2,\lambda}(0) = b_{0,0} + \epsilon\, b_{0,1}\,. \tag{4.25}$$

Here $b_{0,0}$ and $b_{0,1}$ are constants to be detemined by plugging in (4.18) in (4.20) and expanding at $x = 0$ around $\lambda = (1-\epsilon)/2$. We will use the representation,

$$\tanh^{-1}x = \frac{1}{2}\log\frac{1+x}{1-x}\,. \tag{4.26}$$

In terms of these decompostions, we can write (C.29) in the form (putting $d = 4-\epsilon$),

$$\begin{aligned} \mathcal{G}_2(z,\bar{z}) =& (z\bar{z})^{\Delta_\phi}((1-\bar{z})(1-z))^{g^2/2}\int_0^1 \frac{dx}{(z+x(1-z))(\bar{z}+x(1-\bar{z}))} \\ & \times\left(1+\frac{\epsilon}{2}\log\frac{(z+x(1-z))(\bar{z}+x(1-\bar{z}))}{x(1-x)}\right)[g(1-2x)+\epsilon h(1-2x)]\,, \\ =& (z\bar{z})^{\Delta_\phi^{\mathrm{cl}}}((1-\bar{z})(1-z))^{g^2/2}(F_0(z,\bar{z})+\epsilon F_1(z,\bar{z}))\,. \end{aligned} \tag{4.27}$$

The individual parts are,

$$
\begin{aligned}
F_0(z,\bar z) &= \int_0^1 dx \frac{g(1-2x)}{(z+x(1-z))(\bar z+x(1-\bar z))}\,,\\
F_1(z,\bar z) &= \int_0^1 \frac{dx}{(z+x(1-z))(\bar z+x(1-\bar z))}\left(h(1-2x)+\frac{g(1-2x)}{2}\log\frac{(z+x(1-z))(\bar z+x(1-\bar z))}{z\bar z[x(1-x)]}\right).
\end{aligned}
\tag{4.28}
$$

We see from (4.27) that the double discontinuities start from $O(g^4)$. F_0 appears at $O(g^4)$ and F_1 appears at $O(g^4\epsilon)$. We can put F_1 in the following format,

$$
\begin{aligned}
&h(1-2x)+\frac{g(1-2x)}{2}\log\frac{(z+x(1-z))(\bar z+x(1-\bar z))}{z\bar z[x(1-x)]}\\
=&\frac{1}{24}\Bigg[C_0+3(C_1+2\zeta_2-4)\log x(1-x)+3\zeta_2\log\frac{1-x}{x}+6(2-\zeta_2)\log((z+x(1-z))(\bar z+x(1-\bar z)))\\
&-6\log x\log(1-x)\log((z+x(1-z))(\bar z+x(1-\bar z)))-\log^3(1-x)-3\log(1-x)\log^2 x\\
&+6\log x\log(1-x)\log x(1-x)-6\left(\log\frac{1-x}{x}\mathrm{Li}_2\left(\frac{x}{x-1}\right)+2\mathrm{Li}_3\left(\frac{x}{x-1}\right)\right)\Bigg]-\frac{\log z\bar z}{2}g(1-2x)\,,
\end{aligned}
\tag{4.29}
$$

and the constants,

$$
\begin{aligned}
C_0 &= 24b_{0,1}+24a_{0,1}\log 2+6\log 2(2-\zeta_2)+2\log^3 2-9\zeta_3\,,\\
C_1 &= 4a_{0,1}-\zeta_2+2+\log^2 2\,.
\end{aligned}
\tag{4.30}
$$

Most of the integrals above can be split into a general form as discussed in appendix C.2.4, where we provide a list of such integrals. For the $O(1)$ contribution, we know $a_{0,0}=\log 2-1$ and $b_{0,0}=1-\zeta_2/2-\log^2 2/2$, so that $g(x)$ in (4.23) becomes,

$$
g(1-2x)=1-\frac{\zeta_2}{2}-\frac{\log x\log(1-x)}{2}\,. \tag{4.31}
$$

In terms of the integrals we thus have,

$$
F_0(z,\bar z)=\left(1-\frac{\zeta_2}{2}\right)\mathcal{I}_{0,0,0}(z,\bar z)-\frac{1}{2}\mathcal{I}_{1,1,0}(z,\bar z)\,, \tag{4.32}
$$

while for $O(g^4\epsilon)$, we can write,

$$F_1(z,\bar{z}) = \frac{1}{24}(C_0\mathcal{I}_{0,0,0} + 3(C_1 + 2\zeta_2 - 4)(\mathcal{I}_{1,0,0} + \mathcal{I}_{0,1,0}) + 3\zeta_2(\mathcal{I}_{0,1,0} - \mathcal{I}_{1,0,0}) - \mathcal{I}_{0,3,0} \\ + 3\mathcal{I}_{2,1,0} + 6\mathcal{I}_{1,2,0} + 6((2-\zeta_2)\mathcal{J}_1 + \mathcal{J}_2 - \mathcal{J}_3)) - \frac{\log z\bar{z}}{2}F_0(z,\bar{z})\,. \tag{4.33}$$

We will eventually take the $z \to 0$ limit so that,

$$\lim_{z\to 0} F_0(z,\bar{z}) = -\frac{1}{2\bar{z}}\left((\zeta_2-2)\log z + 2\log\bar{z} + \frac{1}{6}\log^3\bar{z} + \mathrm{Li}_3(1-\bar{z}) - \mathrm{Li}_3\left(\frac{\bar{z}-1}{\bar{z}}\right) - \zeta_3\right). \tag{4.34}$$

which matches with B.1 of [24] modulo overall factors. For the first sub-leading term (including the first order expansion of $\bar{z}^{\Delta_\phi}F_0(z,\bar{z})$),

$$\lim_{z\to 0} F_1(z,\bar{z}) = \frac{1}{24\bar{z}}\Bigg[3(8-\log^2\bar{z})\mathrm{Li}_2(1-\bar{z}) - 3\mathrm{Li}_2(1-\bar{z})^2 + 6\log\bar{z}\,\mathrm{Li}_3\left(\frac{\bar{z}-1}{\bar{z}}\right) \\ + 3(\zeta_2-2)(\log^2 z + 4\log z\log\bar{z} - 6\log^2\bar{z}) - 6\log^2\bar{z} - 12\zeta_2\mathrm{Li}_2(1-\bar{z}) \\ - \log^4\bar{z} + 9\zeta_4 - 6S_{2,2}(1-\bar{z})\Bigg] + C_0\frac{\log\bar{z} - \log z}{24\bar{z}} \\ + \frac{C_1 + 2\zeta_2 - 4}{4\bar{z}}(\zeta_2 - \mathrm{Li}_2(1-\bar{z})) + (4 - \zeta_2 - C_1)\frac{\log^2\bar{z} - \log^2 z}{16\bar{z}}\,. \tag{4.35}$$

The above two equations are the main results of this section. (4.34) is the twist-2 contribution at $O(g^4)$ and (4.35) is the contribution of twist-2 at $O(g^4\epsilon)$.

4.4 Generating Function

A large portion (if not all) of the functional basis for the conformal block expansion can be generated by a "*generating function*" of the form,

$$\mathfrak{I}_{(g_1,g_2,g_3)}(z,\bar{z}) = \mathrm{Disc}\left[\int \frac{d^4x_6}{x_{16}^{2+2g_1\delta}\,x_{26}^{2+2g_2\delta}\,x_{36}^{2+2g_3\delta}\,x_{46}^{2-2(g_1+g_2+g_3)\delta}}\right]_{z\to 0}, \tag{4.36}$$

where $z\bar{z} = (x_{12}^2 x_{34}^2)/(x_{13}^2 x_{24}^2)\,, (1-z)(1-\bar{z}) = (x_{14}^2 x_{23}^2)/(x_{13}^2 x_{24}^2)$. We expand the generating function in δ (using HypExp MATHEMATICA package) and at each order we can consider,

$$I^n_{(g_1,g_2,g_3)}(z,\bar{z}) = \partial^n_\delta \mathfrak{I}_{g_1,g_2,g_3}(z,\bar{z})\Big|_{\delta=0}\,. \tag{4.37}$$

For example, $I^0_{0,0,0} = \log z - \log \bar{z} = B_0$ which is the basis function at the zeroth order. As we will demonstrate, both the diagrammatic perturbation and the conformal correlator expansion can be written in terms of the functions derived from $\mathfrak{I}_{(g_1,g_2,g_3)}$. The set $\{g_i\}$, provides considerable freedom for construction. However for our purposes,

$$\text{I) } g_1 = g_3 \;\&\; g_1 = -g_2\,,\ \text{II) } g_1 = -g_2 \;\&\; g_3 = (2-\sqrt{3})g_1\,. \tag{4.38}$$

covers most of the expense. For $n \geq 1$, we denote the two classes as[3],

$$I^n_{(1,-1,1)} = B_n \qquad I^n_{(1,-1,2-\sqrt{3})} = H_n\,. \tag{4.39}$$

The evaluation of the integral (4.36) is listed in appendix-(C.3.1). We will write the results of this till first order,

$$\begin{aligned}
&= \log(1-\bar{z})\left(\frac{\log(z)-\log(\bar{z})}{\bar{z}}\right) \\
&\Big(\log(1-\bar{z})\big(\frac{\mathrm{Li}_2(1-\bar{z})-\zeta_2}{\bar{z}}\big) + \log(1-\bar{z})^2\big(\frac{\log(\bar{z})-\log(z)}{2\bar{z}}\big)\Big)\delta\,.
\end{aligned} \tag{4.40}$$

At each δ^n, the power of $\log(1-\bar{z})$ goes from unity to $n+1$. However at each n, the new addition to the basis comes from the functional coefficient accompanying $\log(1-\bar{z})$. All the higher powers of $\log(1-\bar{z})$ are accompanied by functions which already appeared at lower order in n. Thus, we will construct our basis from the lowest order discontinuity. For class I), we find to few lowest

[3]We would like to stress that while the choice is not unique, it suffices our purpose.

orders,

$$
\begin{aligned}
&B_0 = \log(z) - \log(\bar{z})\,, B_1 = \mathrm{Li}_2(1-\bar{z}) - \zeta_2\,,\\
&B_2 = -6\zeta_3 + 6\mathrm{Li}_3(1-\bar{z}) - 6\mathrm{Li}_3\left(\frac{\bar{z}-1}{\bar{z}}\right) + 3\mathrm{Li}_2(1-\bar{z})\log(z\bar{z}) + 9\zeta_2(\log(z)-\log(\bar{z})) + \log^3(\bar{z})\,,\\
&B_3 = 21\zeta_4 - 24\mathrm{Li}_4(1-\bar{z}) - 6\mathrm{Li}_3(1-\bar{z})(\log(z)-\log(\bar{z})) + 12S_{2,2}(1-\bar{z}) + 6\zeta_3(\log(z)-\log(\bar{z}))\\
&\qquad - 12\zeta_2(\mathrm{Li}_2(1-\bar{z}) - \zeta_2)\,,
\end{aligned}
\tag{4.41}
$$

while for class II),

$$
\begin{aligned}
&H_0 = B_0\,, H_1 = B_1\,,\\
&H_2 = 12\zeta_3 + 3\mathrm{Li}_2(1-\bar{z})\log(z\bar{z}) - 12\mathrm{Li}_3(1-\bar{z}) - 6\mathrm{Li}_3\left(\frac{\bar{z}-1}{\bar{z}}\right) + 3\zeta_2(\log(z)-\log(\bar{z})) + \log^3(\bar{z})\,.
\end{aligned}
\tag{4.42}
$$

Now we will try to argue why the generating function (4.43) seems a plausible choice.

4.4.1 Connection to Loop Integrals

The generating function we advocate is inspired by the class of integrals used to represent loop diagrams [69, 70, 71] A particular class of integrals can be used to represent a large subset of loop diagrams (rings, sunsets etc. see appendix C.3)[4]. This class of integrals are,

$$
\begin{aligned}
&\text{even-loop: } I_L = \lim_{\delta\to 0}\left(\frac{x_{23}^2}{x_{14}^2}\right)^{\delta/2} f(\delta)^{L/2} f(-\delta)^{L/2} \int \frac{d^4x_6}{x_{16}^{2-\delta}\,x_{46}^{2-\delta}\,x_{26}^{2+\delta}\,x_{36}^{2+\delta}}\,,\\
&\text{odd-loop: } I_L = \lim_{\delta\to 0}\left(\frac{x_{23}^2}{x_{14}^2}\right)^{\delta/2} f(\delta)^{(L+1)/2} f(-\delta)^{(L-1)/2} \int \frac{d^4x_6}{x_{16}^{2-\delta}\,x_{46}^{2-\delta}\,x_{26}^{2+\delta}\,x_{36}^{2+\delta}}\,,
\end{aligned}
\tag{4.43}
$$

where,

$$
f(\delta) = \frac{\Gamma(\delta)\Gamma(1-\frac{\delta}{2})^2}{\Gamma(1+\frac{\delta}{2})^2\Gamma(2-\delta)}\,. \tag{4.44}
$$

Apart from the pre-factors, the final integral that needs to be done is the same. For $\delta \to 0$, the finite piece is obtained by expanding the integral in δ which cancels the poles (in δ) coming from

[4] There are other class of integrals for ladder diagrams and convolutions of these integrals therein.

the prefactor.

As a check of the generating function we can rewrite the loop integrals in appendix C.3 using the basis above. For tree level and one-loop we find,

$$\text{tree} = \log(1-\bar{z})\frac{B_0}{4}\,, \quad \text{1-loop} = \log^2(1-\bar{z})\left(\frac{B_0}{4}\right) + \log(1-\bar{z})\left(B_0 - \frac{B_1}{2}\right)\,. \tag{4.45}$$

For two-loop ring,

$$\text{2-loop} = \log^3(1-\bar{z})\left(-\frac{B_0}{24}\right) + \log^2(1-\bar{z})\left(\frac{B_1}{4}\right) - \log(1-\bar{z})\left(\frac{B_2}{12} + (1-\frac{\zeta_2}{2})B_0\right)\,. \tag{4.46}$$

To conclude the section, note that (4.36) is a generalization of the class of integrals in (4.43), where we extended the notion of expansion to multiple parameters $\{g_i\}$ to allow for considerable freedom to construct a basis. The correspondence between loop expansion and conformal correlator expansion suggests that the dDisc at $O(L+2)$ from the correlator expansion associates with Disc at $O(L)-$ diagrams. For example, the leading dDisc at $O(g^2)$ term of the CFT correlator associates with $O(g)$ term in the tree level, $O(g^3)$ connects with $1-$loop and so on.

4.5 Conformal Correlator Expansion

In this section we show that the conformal correlator expansion (4.14) can be cast in terms of the basis obtained in the previous section. We will split the contributions into three types - pure g terms, $g^2\epsilon^n$ terms and everything else. Pure g terms corresponds to expansion at fixed $d = 4$ and we find that these can be obtained from ring-diagrams evaluated at $d = 4$. In the comparisons we will always ignore the overall $\bar{z}$ factor. In particular for all order-4 terms ($O(g^4)$,$O(g^3\epsilon)$ and $O(g^2\epsilon^2)$) in the conformal correlator expansion the generating function (4.43) should be sufficient as we will see in the next section. We further refine our statement by saying that all the basis can be generated by very small number of generating functions for any given order. In fact we see that till $O(4)$ (4.36) suffices while an additional generating function is required at the next order[5].

[5]The additional generating function is associated with the ladder diagrams.

4.5.1 Pure g

We first list down the pure g contributions of the correlator,

$$
\begin{aligned}
O(g^2) &: -\log(1-\bar{z})^2\left(\frac{\log(z)-\log(\bar{z})}{4\bar{z}}\right)\,,\\
O(g^3) &: \log(1-\bar{z})^2\frac{\mathrm{Li}_2(1-\bar{z})-\zeta_2}{4\bar{z}}-\log(1-\bar{z})^3\left(\frac{\log(z)-\log(\bar{z})}{24\bar{z}}\right),\\
O(g^4) &: \log(1-\bar{z})^2\Bigg(\frac{6\zeta_3-6\mathrm{Li}_3(1-\bar{z})+6\mathrm{Li}_3\left(\frac{\bar{z}-1}{\bar{z}}\right)-3\mathrm{Li}_2(1-\bar{z})\log(z\bar{z})+3\zeta_2(\log(\bar{z})-\log(z))-\log^3(\bar{z})}{48\bar{z}}\\
&\quad+\frac{-\zeta_2+\mathrm{Li}_2(1-\bar{z})}{24\bar{z}}-\frac{1}{48\bar{z}}\log(z\bar{z})(\log(z)-\log(\bar{z}))+\frac{22\log(z)-22\log(\bar{z})}{48\bar{z}}\Bigg)\\
&\quad+\log(1-\bar{z})^3(\frac{\mathrm{Li}_2(1-\bar{z})-\zeta_2}{24\bar{z}})-\log(1-\bar{z})^4(\frac{\log(z)-\log(\bar{z})}{192\bar{z}})\,.
\end{aligned}
\tag{4.47}
$$

With the correlator expansion in hand we can now cast then in the basis constructed in (4.41),

$$
\begin{aligned}
&O(g^2): -\log(1-\bar{z})^2\frac{B_0}{4}\,,\;\; O(g^3): \log(1-\bar{z})^2\frac{B_1}{4}-\log(1-\bar{z})^3\frac{B_0}{24}\,,\\
&O(g^4): \log(1-\bar{z})^2\Big(-\frac{1}{48}B_2+\frac{1}{24}B_1+\frac{(11+3\zeta_2)}{24}B_0-\frac{1}{48}\log(z\bar{z})B_0\Big)\\
&\qquad+\log(1-\bar{z})^3\frac{B_1}{24}-\log(1-\bar{z})^4\frac{B_0}{192}\,,\\
&O(g^5): \log(1-\bar{z})^2\Big(\frac{3}{288}B_3-\frac{1}{144}B_2-\frac{(25+6\zeta_2)}{48}B_1+(-\frac{1}{16}-\frac{3}{4}\zeta_3+\frac{1}{24}\zeta_2)B_0+\log(z\bar{z})(\frac{1}{48}B_1+\frac{1}{32}B_0)\Big)\\
&\qquad+\log(1-\bar{z})^3\Big(-\frac{1}{288}B_2+\frac{1}{144}B_1+\frac{(11+3\zeta_2)}{144}B_0-\frac{1}{288}\log(z\bar{z})B_0\Big)\\
&\qquad+\log(1-\bar{z})^4\frac{B_1}{192}-\log(1-\bar{z})^5\frac{B_0}{1920}\,.
\end{aligned}
\tag{4.48}
$$

We notice that in all the comparisons we were able to write the conformal block expansion completely in terms of B-terms. The coefficients were just constants or ζ functions and the $\log(z\bar{z})$ term is an artifact of the kinematic factor. We also observe an interesting pattern, the discontinuities at a given order g^n appear as higher-discontinuities at order g^{n+1} upto overall coefficients. The new information at every order is always contained in its lowest discontinuity (or the coefficient of $\log(1-\bar{z})^2$). The results obtained above are similar to loop diagram results in (4.45,4.46). More specifically we notice that functions that appear at loop-L are the same one that appear in conformal correlator at $O(L+2)$.

4.5.1.1 *Prediction for O(g^6)*

With the observation noted in the previous section we can make a prediction for next order in g,

$$
\begin{aligned}
O(g^6) : \epsilon \log(1-\bar{z})^6 B_0 + \delta \log(1-\bar{z})^5 B_1 + \gamma \log(1-\bar{z})^4 \bigg(B_1 - \frac{1}{2} B_2 + \frac{22 + 6\zeta_2 - \log z\bar{z}}{2} B_0 \bigg) \\
+ \beta \log(1-\bar{z})^3 \bigg(\frac{B_3}{96} - \frac{B_2}{144} - \frac{(25 + 6\zeta_2 - \log z\bar{z})}{48} B_1 + \frac{4\zeta_2 - 72\zeta_3 + 3\log z\bar{z} - 6}{96} B_0 \bigg) \\
+ \alpha \log(1-\bar{z})^2 \bigg(B_4 \cdots \bigg) ,
\end{aligned}
\tag{4.49}
$$

where $(\alpha, \beta, \gamma, \delta, \epsilon)$ are unfixed numerical coefficients. Only the lowest order discontinuity is unknown, however we do know that it is composed of a combination of B_4 and lower order B_is.

4.5.1.2 *Twist-2 Matching*

We will also try to put the twist-2 contribution (4.34) at O(g^4) in terms of our basis. The O(g^4) contribution is,

$$
T_2 = \log^2(1-\bar{z}) \left(\log z \, (\zeta_2 - 2) + 2 \log \bar{z} + \frac{1}{6} \log^3 \bar{z} + \mathrm{Li}_3(1-\bar{z}) - \mathrm{Li}_3 \left(\frac{\bar{z}-1}{\bar{z}} \right) - \zeta_3 \right) . \tag{4.50}
$$

In terms of our basis we can cast this as,

$$
T_2 = \left(\frac{B_2}{6} - (2 + \zeta_2) B_0 - \frac{1}{2} \log(z\bar{z}) B_1 \right) \log^2(1-\bar{z}) . \tag{4.51}
$$

4.5.2 $O(g^2 \epsilon^n)$

Here we will report an interesting observation regarding terms of type $g^2 \epsilon^n$. Since these terms have g^2 they only contain a $\log^2(1-\bar{z})$ discontinuity. In our perturbative diagram computations we have worked in $d = 4$ dimensions instead of $d = 4 - \epsilon$. Working in $d = 4 - \epsilon$ would have given us ϵ corrections to our basis and we believe that this would be the honest way to generate a basis for $O(g^2\epsilon^n)$ terms. However, we can still get away with it because we notice nice pattern in the terms of this type. Since these contributions are simple enough we can cast them in their own basis,

$$\begin{aligned}
O(g^2\epsilon) &: \log^2(1-\bar{z})\left(\frac{B_0}{4}+\frac{\zeta_2}{4}+\log(z)\frac{B_0}{8}\right)\,, \\
O(g^2\epsilon^2) &: \log^2(1-\bar{z})\left(\left(\frac{B_0\zeta_2}{16}+\frac{\zeta_2}{4}-\frac{\zeta_3}{8}\right)+\left(\frac{B_0}{8}+\frac{\zeta_2}{8}\right)\log(z)+\frac{1}{32}B_0\log^2(z)\right)\,, \\
O(g^2\epsilon^3) &: \log^2(1-\bar{z})\Big[-\frac{\zeta_3}{8}+\frac{7\zeta_4}{32}-B_0\left(\frac{\zeta_3}{16}-\frac{\zeta_2}{16}\right)-\left(\frac{B_0\zeta_2}{32}+\frac{1}{2}\left(\frac{\zeta_2}{4}-\frac{\zeta_3}{8}\right)\right)\log(z) \\
&\quad -\frac{1}{192}B_0\log^3(z)+\frac{1}{32}\left(B_0+\zeta_2\right)\log^2(z)\Big]\,.
\end{aligned} \tag{4.52}$$

We noticed a similar pattern appearing as the pure g terms. At each order $g^2\epsilon^n$ there are terms with increasing power of $\log(z)$ which becomes terms of higher powers of $\log(z)$ in the next order. We make a final comment that the basis comprises of terms of form,

$$\equiv \{B_0, \log^n(z)\} + \{\zeta(n+1), \cdots, \zeta(2)\}|_{n\geq 1}\,. \tag{4.53}$$

4.5.3 Remaining Terms

At fourth order there are 3 possible contributions to the conformal block expansion - $O(g^4), O(g^3\epsilon)$ and $O(g^2\epsilon^2)$. We have already cast $O(g^4)$ and $O(g^2\epsilon^2)$ in a basis and are left with $O(g^3\epsilon)$ term whose contribution is,

$$\begin{aligned}
O(g^3\epsilon) &: \log^3(1-\bar{z})\left(\frac{2\zeta_2+(\log(z)+2)(\log(z)-\log(\bar{z}))}{48\bar{z}}\right) \\
&-\frac{\log^2(1-\bar{z})}{48\bar{z}}\Bigg(12\zeta_3+6\mathrm{Li}_2(1-\bar{z})\log(z)+12\mathrm{Li}_2(1-\bar{z})-12\mathrm{Li}_3(1-\bar{z})-6\mathrm{Li}_3\left(\frac{\bar{z}-1}{\bar{z}}\right) \\
&+6\mathrm{Li}_2(1-\bar{z})\log(\bar{z})-6\zeta_2(2\log(z)-\log(\bar{z})+2)+12\log(z)+\log^3(\bar{z})-12\log(\bar{z})\Bigg)\,.
\end{aligned} \tag{4.54}$$

At this point we remind ourself of the second choice of regularization which resulted in an additional basis H_2 (4.42). We have already encountered the $\log^3(1-\bar{z})$ piece before. So here we will focus on only the $\log^2(1-\bar{z})$ term. It can be cast into a basis as follows,

$$O(g^3\epsilon)|_{\log^2(1-\bar{z})} : \frac{1}{48}H_2 + \log(z\bar{z})\frac{B_1}{16} - \zeta_2\frac{B_0}{4} + \frac{B_1+B_0}{4}\,. \tag{4.55}$$

With this result in hand we have been able to show our basis covers the expansion till $O(4)$. This implies that our one generating function (4.43) is sufficient for all terms upto $O(4)$. At the next order we have terms $O(g^5)$, $O(g^4\epsilon)$, $O(g^3\epsilon^2)$ and $O(g^2\epsilon^3)$. While the first and last of the above term already fit in our basis,$O(g^4\epsilon)$ and $O(g^3\epsilon^2)$ (in C.33) has additional $\mathrm{Li}_2^2(1-\bar{z})$ contribution. A similar issue arises for the $O(g^4\epsilon)$ piece of twist-2 block as well. Note that the correspondence we have drawn, suggests that $O(5)$ in conformal block expansion should correspond to $3-$loop diagrams. At $3-$loop level there exists an additional generating function (from ladder diagrams) which accommodates $O(g^4\epsilon)$ and $O(g^3\epsilon^2)$. We have not performed the computation explicitly, but schematically show in Appendix(C.4), how the ladder diagram contributes a factor of $\mathrm{Li}_2^2(1-\bar{z})$.

5. SUMMARY

In this work we have made progress in understanding analytical and structural properties of CFT and defect-CFT. We would like to conclude by summaries each chapter separately.

5.1 Correlators in Defect CFT

In the first chapter we constructed correlators of operators in arbitrary representation in the presence of defects. This was done utilizing embedding formalism for defect CFT. We also identified all possible operators that can appear in the bulk-to-defect OPE of a bulk operator in arbitrary representation. In the process of computing correlators we have computed all defect-conformal invariants that can appear in n-point correlators. To conclude we also discuss one and two-point correlators for spinning-defects.

With these results in hand it would be possible to constrain the defect CFT by studying crossing relation of operators in arbitrary representations. A defect CFT (dCFT) has two sets of CFT data in addition to couplings between the bulk and the defect sector. The total data-set of a dCFT is:

$$\{\Delta, \hat{\Delta}, f_{ijk}, \hat{f}_{ijk}, b_{ij}\}. \tag{5.1}$$

The four-point crossing equation for the theory living on the defect (in principle) fixes all the data of the defect sector. The remaining information about the bulk and the bulk-to-defect couplings are captured by crossing equations of the $\langle O_1 O_2 \rangle$ and $\langle O_1 O_2 \hat{O}_3 \rangle$ correlators. As an example let us consider a two-point correlator of two bulk scalars. The bulk two point function has two expansion channels (Figure 5.1), U and Y [1] . They yield a crossing equation in terms of $\{b_{ij}, f_{ijk}\}$,

$$\sum_{\hat{O}} b^2_{\Phi\hat{O}} F(\hat{\Delta}_{\hat{O}}, \eta) = \sum_{O} f_{\Phi\Phi O} b_{O1} \tilde{F}(\Delta_O, \eta). \tag{5.2}$$

[1] We thank Daniel Robbins for the terminology.

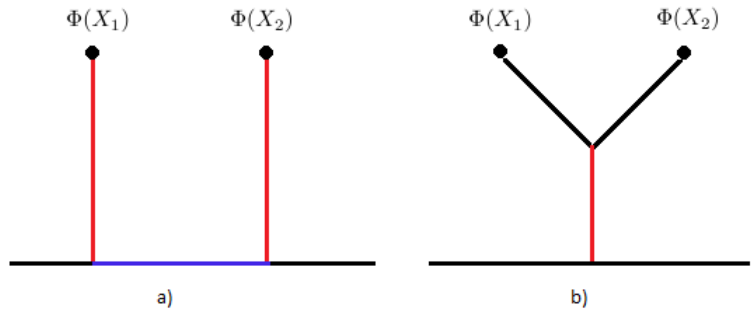

Figure 5.1: Two defect channels: a) U-Channel b) Y-Channel.

F and $\tilde{F}$ are conformal blocks which are functions of scaling dimensions and relevant cross ratios. Their explicit form was calculated in [23, 21]. The crossing equation has been studied both analytically [23, 72] and numerically [34, 22]. This problem is challenging to solve numerically as the right-side (5.2) does not have positive coefficients. This crossing relation does not provide us with the complete information of the dCFT data as we are missing $\hat{f}_{ijk}$. To constrain the remaining data we need crossing arising from three-point correlator involving two bulk and one defect local operator. A three-point crossing involving scalars has the following schematic form:

$$\sum_{\hat{O}_1}\sum_{\hat{O}_2} b_{\Phi_1\hat{O}_1} b_{\Phi_2\hat{O}_2} \hat{f}_{\hat{O}_1\hat{O}_2\hat{O}_3} \tilde{G}(\eta, \hat{\Delta}_1, \hat{\Delta}_2) = \sum_{\tilde{\Phi}} f_{\Phi_1\Phi_2\tilde{\Phi}} b_{\tilde{\Phi}\hat{O}_3} G(\Delta_{\tilde{\Phi}}, \eta). \tag{5.3}$$

Δ and $\hat{\Delta}$ stand for scaling dimensions of operators appearing in the intermediate channels. $\hat{G}$ and $\tilde{G}$ are the conformal blocks, which are functions of cross-ratios. These functions can be determined by acting with the Casimir operator as was done in [23]. These blocks were recently calculated in [73] for the boundary case. We hope that calculations performed in this chapter would come in handy for three-point bootstrap.

5.2 Resummation at Finite Conformal Spin

In this chapter we have considered the single block contributions to the anomalous dimensions and OPE coefficients of operators $[\mathcal{O}\mathcal{O}]_{\Delta,J}$. In order to achieve that, we have used the integral

(Mellin) representation of the blocks which make the analysis and results fairly general. On the one hand it is democratic with respect to space time dimensions, thus making the computation uniform both in even and odd dimensions, specially where the closed form of the conformal blocks is not available. Further, the Mellin integral makes the additional contributions (coming from the lower limit of the z integral) explicit, making it possible to re-sum correctly for any finite β.

The anomalous dimensions and the corrections to the OPE coefficients can be written as an exact function of the conformal spin (β) in terms of Wilson polynomials for each exchange contribution in the $t-$channel. These Wilson polynomials are the generalizations of the residues of the $6j-$symbols recently discussed in [47].

The closed form expressions create a possibility for numerical exploration along with a proper handling of the associated error estimates. The computation for operators $[\mathcal{O}_1(\partial^2)^n\mathcal{O}_2]_{\Delta,J}$ with $\Delta = \Delta_1 + \Delta_2 + J + 2n$ can be handled in the exact same fashion as for the $n = 0$ case. In this case, one needs to consider the descendant contributions from the Mellin representation of the blocks we neglected in this work[2]. Along with the descendant contributions from the block, one also needs to expand the kernel in the inversion formula (3.6). For our case, we considered,

$$\lim_{z\to 0} G_{J+d-1,\Delta+1-d}(z,\bar{z}) \sim z^{\frac{J-\Delta}{2}} k_\beta(\bar{z}) + \dots\,, \tag{5.4}$$

where $\dots$ terms become relevant in the subleading orders (*i.e.* for $n > 0$ cases). As a result, there is a mixing problem involved at the subleading orders. For example z^i term coming from the kernel and z^j term can combine to z^n where $n = i + j$. This can be interpreted in the following way. At any subleading order, we have contributions from the primary $[\mathcal{O}_1(\partial^2)^n\mathcal{O}_2]_{\Delta,J}$ and the $m-$th descendant of the primary $[\mathcal{O}_1(\partial^2)^{n-m}\mathcal{O}_2]_{\Delta,J}$. It would be interesting to see how these contributions can be disentangled[3].

[2]We focused on the $t = 0$ poles. For the descendants, we need to take into account $t = n$ poles in (B.1)

[3]We thank Aninda Sinha for discussion on this point.

5.3 Conformal Correlators and Diagrammatic Expansion

In the final chapter we tried to find relation between the two methods of computing observables in a CFT, perturbative diagrams and conformal correlator expansion.

We explore the possibility that the basis of functions can be derived from a simple generating function systematically. The generating function works well for pure g terms and mixed terms in the expansion upto $O(g^4)$. From $O(g^5)$ onwards a new class of generating functions is additionally required, albeit the number of such class of functions should be finite.

The motivation of the generating function comes from diagrammatic perturbation theory for massless ϕ^4 theory. (4.36) is a generalization of the master integrals for a large subset of loop Feynman diagrams. Further, (4.36) can be deployed to rewrite both the expansion of the conformal correlator and the loop Feynman diagrams in terms of the same basis of functions[4].

Our technique can also be applied to other situations with ϵ-expansion like boundary CFTs [74]. The boundary CFT case is much simpler from the conformal correlator expansion since two-point functions are non-trivial [75, 76] and have conformal blocks associated to them. In addition the crossing equation can be satisfied in boundary CFT with finite number of terms at lower orders in ϵ-expansion.

[4]For the diagrammatic computation, the regularization scheme does not alter the structural properties we are concerned with. Hence, the same building blocks used to rewrite these diagrams.

REFERENCES

[1] D. Simmons-Duffin, *The Conformal Bootstrap*. World-Scientific TASI 2015 lectures, 3 2017.

[2] S. Rychkov, *EPFL Lectures on Conformal Field Theory in D>= 3 Dimensions*. SpringerBriefs in Physics, 1 2016.

[3] D. Poland, S. Rychkov, and A. Vichi, "The Conformal Bootstrap: Theory, Numerical Techniques, and Applications," *Rev. Mod. Phys.*, vol. 91, p. 015002, 2019.

[4] M. S. Costa, J. Penedones, D. Poland, and S. Rychkov, "Spinning Conformal Correlators," *JHEP*, vol. 11, p. 071, 2011.

[5] S. Weinberg, "Six-dimensional Methods for Four-dimensional Conformal Field Theories II: Irreducible Fields," *Phys. Rev. D*, vol. 86, p. 085013, 2012.

[6] P. A. Dirac, "Wave equations in conformal space," *Annals Math.*, vol. 37, pp. 429–442, 1936.

[7] F. Dolan and H. Osborn, "Conformal four point functions and the operator product expansion," *Nucl. Phys. B*, vol. 599, pp. 459–496, 2001.

[8] F. Dolan and H. Osborn, "Conformal partial waves and the operator product expansion," *Nucl. Phys. B*, vol. 678, pp. 491–507, 2004.

[9] R. Rattazzi, V. S. Rychkov, E. Tonni, and A. Vichi, "Bounding scalar operator dimensions in 4D CFT," *JHEP*, vol. 12, p. 031, 2008.

[10] D. Poland, D. Simmons-Duffin, and A. Vichi, "Carving Out the Space of 4D CFTs," *JHEP*, vol. 05, p. 110, 2012.

[11] S. M. Chester, W. Landry, J. Liu, D. Poland, D. Simmons-Duffin, N. Su, and A. Vichi, "Carving out OPE space and precise $O(2)$ model critical exponents," *JHEP*, vol. 06, p. 142, 2020.

[12] F. Kos, D. Poland, D. Simmons-Duffin, and A. Vichi, "Precision Islands in the Ising and $O(N)$ Models," *JHEP*, vol. 08, p. 036, 2016.

[13] F. Kos, D. Poland, D. Simmons-Duffin, and A. Vichi, “Bootstrapping the O(N) Archipelago,” *JHEP*, vol. 11, p. 106, 2015.

[14] S. El-Showk, M. F. Paulos, D. Poland, S. Rychkov, D. Simmons-Duffin, and A. Vichi, “Solving the 3D Ising Model with the Conformal Bootstrap,” *Phys. Rev. D*, vol. 86, p. 025022, 2012.

[15] D. Simmons-Duffin, “The Lightcone Bootstrap and the Spectrum of the 3d Ising CFT,” *JHEP*, vol. 03, p. 086, 2017.

[16] A. Fitzpatrick and J. Kaplan, “Unitarity and the Holographic S-Matrix,” *JHEP*, vol. 10, p. 032, 2012.

[17] A. Fitzpatrick, J. Kaplan, D. Poland, and D. Simmons-Duffin, “The Analytic Bootstrap and AdS Superhorizon Locality,” *JHEP*, vol. 12, p. 004, 2013.

[18] Z. Komargodski and A. Zhiboedov, “Convexity and liberation at large spin,” *Journal of High Energy Physics*, vol. 2013, Nov 2013.

[19] S. Caron-Huot, “Analyticity in Spin in Conformal Theories,” *JHEP*, vol. 09, p. 078, 2017.

[20] M. S. Costa, V. Goncalves, and J. Penedones, “Conformal regge theory,” *Journal of High Energy Physics*, vol. 2012, Dec 2012.

[21] D. McAvity and H. Osborn, “Conformal field theories near a boundary in general dimensions,” *Nucl. Phys. B*, vol. 455, pp. 522–576, 1995.

[22] P. Liendo, L. Rastelli, and B. C. van Rees, “The Bootstrap Program for Boundary CFT_d,” *JHEP*, vol. 07, p. 113, 2013.

[23] M. Billò, V. Gonçalves, E. Lauria, and M. Meineri, “Defects in conformal field theory,” *JHEP*, vol. 04, p. 091, 2016.

[24] L. F. Alday, J. Henriksson, and M. van Loon, “Taming the ϵ-expansion with large spin perturbation theory,” *JHEP*, vol. 07, p. 131, 2018.

[25] K. G. Wilson and J. B. Kogut, “The Renormalization group and the epsilon expansion,” *Phys.*

Rept., vol. 12, pp. 75–199, 1974.

[26] K. G. Wilson, “Quantum field theory models in less than four-dimensions,” *Phys. Rev.*, vol. D7, pp. 2911–2926, 1973.

[27] D. Poland, D. Simmons-Duffin, and A. Vichi, “Carving Out the Space of 4D CFTs,” *JHEP*, vol. 05, p. 110, 2012.

[28] S. Guha and B. Nagaraj, “Correlators of mixed symmetry operators in defect cfts,” *Journal of High Energy Physics*, vol. 2018, Oct 2018.

[29] M. S. Costa and T. Hansen, “Conformal correlators of mixed-symmetry tensors,” *JHEP*, vol. 02, p. 151, 2015.

[30] V. Dobrev, V. Petkova, S. Petrova, and I. Todorov, “Dynamical Derivation of Vacuum Operator Product Expansion in Euclidean Conformal Quantum Field Theory,” *Phys. Rev. D*, vol. 13, p. 887, 1976.

[31] A. Gadde, “Conformal constraints on defects,” *JHEP*, vol. 01, p. 038, 2020.

[32] M. Fukuda, N. Kobayashi, and T. Nishioka, “Operator product expansion for conformal defects,” *JHEP*, vol. 01, p. 013, 2018.

[33] E. Lauria, M. Meineri, and E. Trevisani, “Spinning operators and defects in conformal field theory,” *JHEP*, vol. 08, p. 066, 2019.

[34] F. Gliozzi, P. Liendo, M. Meineri, and A. Rago, “Boundary and Interface CFTs from the Conformal Bootstrap,” *JHEP*, vol. 05, p. 036, 2015.

[35] E. Lauria, M. Meineri, and E. Trevisani, “Radial coordinates for defect CFTs,” *JHEP*, vol. 11, p. 148, 2018.

[36] J.-F. Fortin and W. Skiba, “Conformal Bootstrap in Embedding Space,” *Phys. Rev. D*, vol. 93, no. 10, p. 105047, 2016.

[37] J.-F. Fortin and W. Skiba, “Conformal Differential Operator in Embedding Space and its Applications,” *JHEP*, vol. 07, p. 093, 2019.

[38] M. S. Costa, T. Hansen, J. Penedones, and E. Trevisani, “Projectors and seed conformal blocks for traceless mixed-symmetry tensors,” *JHEP*, vol. 07, p. 018, 2016.

[39] D. Simmons-Duffin, D. Stanford, and E. Witten, “A spacetime derivation of the Lorentzian OPE inversion formula,” *JHEP*, vol. 07, p. 085, 2018.

[40] C. Cardona, “OPE inversion in Mellin space,” 2018 [PREPRINT].

[41] C. Cardona, S. Guha, S. K. Kanumilli, and K. Sen, “Resummation at finite conformal spin,” *Journal of High Energy Physics*, vol. 2019, Jan 2019.

[42] L. F. Alday, A. Bissi, and T. Lukowski, “Large spin systematics in CFT,” *JHEP*, vol. 11, p. 101, 2015.

[43] L. F. Alday and A. Zhiboedov, “Conformal Bootstrap With Slightly Broken Higher Spin Symmetry,” *JHEP*, vol. 06, p. 091, 2016.

[44] L. F. Alday and A. Zhiboedov, “An Algebraic Approach to the Analytic Bootstrap,” *JHEP*, vol. 04, p. 157, 2017.

[45] A. Kaviraj, K. Sen, and A. Sinha, “Analytic bootstrap at large spin,” *JHEP*, vol. 11, p. 083, 2015.

[46] A. Kaviraj, K. Sen, and A. Sinha, “Universal anomalous dimensions at large spin and large twist,” *JHEP*, vol. 07, p. 026, 2015.

[47] J. Liu, E. Perlmutter, V. Rosenhaus, and D. Simmons-Duffin, “d-dimensional SYK, AdS Loops, and $6j$ Symbols,” *JHEP*, vol. 03, p. 052, 2019.

[48] C. Sleight and M. Taronna, “Spinning Mellin Bootstrap: Conformal Partial Waves, Crossing Kernels and Applications,” *Fortsch. Phys.*, vol. 66, no. 8-9, p. 1800038, 2018.

[49] L. F. Alday, “Large Spin Perturbation Theory for Conformal Field Theories,” *Phys. Rev. Lett.*, vol. 119, no. 11, p. 111601, 2017.

[50] M. S. Costa, V. Goncalves, and J. Penedones, “Conformal Regge theory,” *JHEP*, vol. 12, p. 091, 2012.

[51] F. A. Dolan and H. Osborn, "Conformal Partial Waves: Further Mathematical Results," *DAMTP*, vol. 11-64, 2011.

[52] M. Hogervorst and B. C. van Rees, "Crossing symmetry in alpha space," *JHEP*, vol. 11, p. 193, 2017.

[53] I. Heemskerk, J. Penedones, J. Polchinski, and J. Sully, "Holography from Conformal Field Theory," *JHEP*, vol. 10, p. 079, 2009.

[54] Z. Komargodski and A. Zhiboedov, "Convexity and Liberation at Large Spin," *JHEP*, vol. 11, p. 140, 2013.

[55] A. L. Fitzpatrick, J. Kaplan, D. Poland, and D. Simmons-Duffin, "The Analytic Bootstrap and AdS Superhorizon Locality," *JHEP*, vol. 12, p. 004, 2013.

[56] F. A. Dolan and H. Osborn, "Conformal four point functions and the operator product expansion," *Nucl. Phys.*, vol. B599, pp. 459–496, 2001.

[57] W. Groenevelt, "The Wilson function transform," *ArXiv Mathematics e-prints*, June 2003.

[58] R. Gopakumar and A. Sinha, "On the Polyakov-Mellin bootstrap," *JHEP*, vol. 12, p. 040, 2018.

[59] S. Rychkov and Z. M. Tan, "The ϵ-expansion from conformal field theory," *J. Phys.*, vol. A48, no. 29, p. 29FT01, 2015.

[60] K. Sen and A. Sinha, "On critical exponents without Feynman diagrams," *J. Phys.*, vol. A49, no. 44, p. 445401, 2016.

[61] J. Henriksson and M. Van Loon, "Critical O(N) model to order ϵ^4 from analytic bootstrap," *J. Phys.*, vol. A52, no. 2, p. 025401, 2019.

[62] L. F. Alday, J. Henriksson, and M. van Loon, "An alternative to diagrams for the critical O(N) model: dimensions and structure constants to order $1/N^2$," *JHEP*, vol. 01, p. 063, 2020.

[63] L. F. Alday, "Solving CFTs with Weakly Broken Higher Spin Symmetry," *JHEP*, vol. 10, p. 161, 2017.

[64] C. Cardona and K. Sen, “Anomalous dimensions at finite conformal spin from OPE inversion,” *JHEP*, vol. 11, p. 052, 2018.

[65] C. Cardona, S. Guha, S. K. Kanumilli, and K. Sen, “Resummation at finite conformal spin,” *JHEP*, vol. 01, p. 077, 2019.

[66] F. A. Dolan and H. Osborn, “Conformal partial waves and the operator product expansion,” *Nucl. Phys.*, vol. B678, pp. 491–507, 2004.

[67] P. Dey, A. Kaviraj, and A. Sinha, “Mellin space bootstrap for global symmetry,” *JHEP*, vol. 07, p. 019, 2017.

[68] T. Huber and D. Maitre, “HypExp: A Mathematica package for expanding hypergeometric functions around integer-valued parameters,” *Comput. Phys. Commun.*, vol. 175, pp. 122–144, 2006.

[69] N. I. Usyukina and A. I. Davydychev, “Exact results for three and four point ladder diagrams with an arbitrary number of rungs,” *Phys. Lett.*, vol. B305, pp. 136–143, 1993.

[70] N. I. Usyukina and A. I. Davydychev, “An Approach to the evaluation of three and four point ladder diagrams,” *Phys. Lett.*, vol. B298, pp. 363–370, 1993.

[71] J. M. Drummond, J. Henn, V. A. Smirnov, and E. Sokatchev, “Magic identities for conformal four-point integrals,” *JHEP*, vol. 01, p. 064, 2007.

[72] M. Lemos, P. Liendo, M. Meineri, and S. Sarkar, “Universality at large transverse spin in defect CFT,” *JHEP*, vol. 09, p. 091, 2018.

[73] A. Karch and Y. Sato, “Conformal Manifolds with Boundaries or Defects,” *JHEP*, vol. 07, p. 156, 2018.

[74] A. Bissi, T. Hansen, and A. Söderberg, “Analytic Bootstrap for Boundary CFT,” *JHEP*, vol. 01, p. 010, 2019.

[75] S. Guha and B. Nagaraj, “Correlators of Mixed Symmetry Operators in Defect CFTs,” *JHEP*, vol. 10, p. 198, 2018.

[76] E. Lauria, M. Meineri, and E. Trevisani, “Spinning operators and defects in conformal field theory,” *JHEP*, vol. 08, p. 066, 2019.

[77] G. Mack, “D-dimensional Conformal Field Theories with anomalous dimensions as Dual Resonance Models,” *Bulg. J. Phys.*, vol. 36, pp. 214–226, 2009.

[78] L. U. Ancarani and G. Gasaneo, “Derivatives of any order of the hypergeometric function ${}_pf_q(a_1, \cdots, a_p; b_1, \cdots, b_q; z)$ with respect to the parameters a_i and b_i,” *Journal of Physics A: Mathematical and Theoretical*, vol. 42, no. 39, p. 395208, 2009.

[79] C. Duhr and F. Dulat, “PolyLogTools — polylogs for the masses,” *JHEP*, vol. 08, p. 135, 2019.

[80] H. Frellesvig, D. Tommasini, and C. Wever, “On the reduction of generalized polylogarithms to Li_n and $\mathrm{Li}_{2,2}$ and on the evaluation thereof,” *JHEP*, vol. 03, p. 189, 2016.

APPENDIX A

SECTION 2

A.1 Notations

We will summarize the notation used throughout the paper in this section. Notations for directions are,

$$\begin{aligned}
&M, N, \cdots \rightarrow \text{Directions of the embedding space.}\\
&A, B, \cdots \rightarrow \text{Directions parallel to the defect in the embedding space.}\\
&I, J, \cdots \rightarrow \text{Directions orthogonal to the defect in the embedding space.}\\
&m, n, \cdots \rightarrow \text{Directions in physical space.}\\
&a, b, \cdots \rightarrow \text{Direction parallel to defect in physical space.}\\
&i, j, \cdots \rightarrow \text{Directions othogonal to the defect in physical space.}
\end{aligned} \tag{A.1}$$

Notation for position and auxiliary vectors:

$$\begin{aligned}
&P_a \rightarrow \text{Position of bulk local operator a.}\\
&P_{\hat{a}} \rightarrow \text{Position of defect local operator } \hat{a}.\\
&\Theta_a^{(i)}/Z_a^{(i)} \rightarrow \text{Auxiliary vector associated with i-th column/row of bulk operator.}\\
&\Theta_{\hat{a}}^{(i)}/Z_{\hat{a}}^{(i)} \rightarrow \text{Auxiliary vector associated with i-th column/row of defect operator } (SO(p+1,1)).\\
&\bar{\Theta}_{\hat{a}}^{(i)}/\bar{Z}_{\hat{a}}^{(i)} \rightarrow \text{Auxiliary vector associated with i-th column/row of defect operator } (SO(q)).
\end{aligned} \tag{A.2}$$

Notation for representation:

$$
\begin{aligned}
&n_a^{C/R} \to \text{Number of columns/rows in bulk-operator a.}\\
&n_{\hat{a}}^{C/R} \to \text{Number of columns/rows in defect-operator } \hat{a}.\\
&n_{\hat{a}}^{C/R} \to \text{Number of columns/rows in defect-operator } \hat{a}.\\
&\lambda_a \to \text{Representation of a bulk operator under } SO(d+1,1).\\
&\lambda_{\hat{a}} \to \text{Representation of a defect operator under } SO(1+p,1).\\
&\bar{\lambda}_{\hat{a}} \to \text{Representation of a defect operator under } SO(q).\\
&l_a^{(i)}/h_a^{(i)} \to \text{Length/height of i-th row/column of bulk operator.}\\
&l_{\hat{a}}^{(i)}/h_{\hat{a}}^{(i)} \to \text{Length/height of i-th row/column of defect operator under } SO(p+1,1).\\
&\bar{l}_{\hat{a}}^{(i)}/\bar{h}_{\hat{a}}^{(i)} \to \text{Length/height of i-th row/column of defect operator under } SO(q).
\end{aligned}
\tag{A.3}
$$

Notation of operators and couplings:

$$
\begin{aligned}
&O \to \text{Bulk operator.}\\
&\hat{O} \to \text{Defect operator.}\\
&b_{O\hat{O}} \to \text{Bulk-to-defect coupling between bulk } O \text{ and defect } \hat{O}.\\
&f_{OOO} \to \text{Three-point coupling of Bulk sector.}\\
&\hat{f}_{\hat{O}\hat{O}\hat{O}} \text{Three-point coupling of defect sector.}\\
&\Delta \to \text{Scaling dimension of bulk operator.}\\
&\hat{\Delta} \to \text{Scaling dimension of defect operator.}
\end{aligned}
\tag{A.4}
$$

A.2 Invariants

We will list down all invariants schematically (and suppressing the i-indices) beginning with no C-tensor case. Hats on vectors means that they are associated with defect local operators. We consider both $SO(1+p,1)$ and $SO(q)$ contractions together:

$$\begin{aligned} &P\Phi \to G_{a\hat{a}}, \\ &\Phi\Phi \to \tilde{H}_{\hat{a}\hat{b}}. \end{aligned} \tag{A.5}$$

Moving on to single C-tensor case:

$$\begin{aligned} &CPP \to K_{ab}, \bar{K}_{ab}, \\ &CP\hat{P} \to K_{a\hat{a}}, \\ &C\hat{P}\hat{P} \to \text{can be reduced using } K_{a\hat{a}}, \\ &CP\Phi \to \tilde{G}_{a\hat{a}}, \qquad C\hat{P}\Phi \to \text{can be reduced using } \tilde{G}_{a\hat{a}} \text{ and } K_{a\hat{a}} \ , \\ &\hat{C}PP \to N_{\hat{k}ab}, \\ &\hat{C}P\hat{P} \to \tilde{N}_{\hat{a}a}, \\ &\hat{C}\hat{P}\hat{P} \to \tilde{K}_{\hat{a}\hat{b}}, \\ &\hat{C}P\Phi \to \text{not possible}, \qquad C\hat{P}\Phi \to \text{not possible}. \end{aligned} \tag{A.6}$$

Moving on to two bulk C-tensor contractions:

$$\begin{aligned} &CC \to H_a, \\ &CCPP \to S_{ab}, \bar{S}_{ab}, \\ &CCP\hat{P} \to \text{can be reduced using } S_{ab}, \bar{S}_{ab}, \\ &CC\hat{P}\hat{P} \to \text{can be reduced using } S_{ab}, \bar{S}_{ab}, \\ &CCP\Phi \to \text{can be reduced using } CP\Phi \text{ and } H_{ab}, \qquad CC\hat{P}\Phi \to \text{can be reduced}. \end{aligned} \tag{A.7}$$

Two defect C-tensor contractions:

$$\begin{aligned}
&\hat{C}\hat{C} \to H_{\hat{a}\hat{b}},\\
&\hat{C}\hat{C}PP \to \text{can be reduced using } H_{\hat{a}\hat{b}},\\
&\hat{C}\hat{C}P\hat{P} \to \text{can be reduced,}\\
&\hat{C}\hat{C}\hat{P}\hat{P} \to \text{can be reduced,}\\
&\hat{C}\hat{C}P\Phi \to \text{not possible,} \qquad \hat{C}\hat{C}\hat{P}\Phi \to \text{not possible.}
\end{aligned} \tag{A.8}$$

Lastly we consider one defect C-tensor and one bulk C-tensor contractions,

$$\begin{aligned}
&\hat{C}C \to H_{a\hat{a}},\\
&\hat{C}CPP \to \text{can be reduced using } H_{a\hat{a}},\\
&\hat{C}CP\hat{P} \to \text{can be reduced,}\\
&\hat{C}C\hat{P}\hat{P} \to \text{can be reduced,}\\
&\hat{C}CP\Phi \to \text{can be reduced,} \qquad \hat{C}C\hat{P}\Phi \to \text{can be reduced.}
\end{aligned} \tag{A.9}$$

A.3 Useful Identities

In this section we will list down some important identities involving C-tensors. We will first begin with single C-tensor case:

$$(P_1 \circ P_2)C_2^{AI}P_{1A}P_{2I} = (P_1 \bullet P_2)C_2^{AI}P_{2A}P_{1I} + (P_2 \circ P_2)C_2^{AI}P_{1A}P_{1I}, \tag{A.10}$$

$$\begin{aligned}
C_1^{AI}P_{2A}P_{3I} =& \frac{(P_1 \bullet P_2)}{(P_1 \bullet P_1)}C_1^{AI}P_{1A}P_{3I} + \frac{(P_1 \circ P_3)}{(P_1 \circ P_2)}C_1^{AI}P_{2A}P_{2I}\\
&- \frac{(P_1 \circ P_3)(P_1 \bullet P_2)}{(P_1 \circ P_2)(P_1 \bullet P_1)}C_1^{AI}P_{1A}P_{2I}.
\end{aligned} \tag{A.11}$$

Moving on to two C-tensor identities,

$$(P_1 \circ P_1)C_1^{AI}C_2^{AJ}P_{3I}\Phi_J = (P_1 \circ P_3)C_1^{AI}C_2^{AJ}P_{1I}\Phi_J - (C_2^{AI}P_{1A}\Phi_J)(C_1^{AI}P_{1A}P_{3I}), \tag{A.12}$$

$$
\begin{aligned}
C_1^{AI}C_2^{AJ}P_{2I}P_{1J} =& \frac{(P_1\circ P_2)^2}{(P_1\circ P_1)(P_2\circ P_2)}C_1^{AI}C_2^{AJ}P_{1I}P_{2J} - \frac{(P_1\bullet P_2)}{(P_1\circ P_1)(P_2\circ P_2)}C_1^{AI}P_{1A}P_{2I}C_2^{BJ}P_{2B}P_{1J} \\
&- \frac{1}{(P_1\circ P_1)}C_1^{AI}P_{1A}P_{2I}C_2^{BJ}P_{1B}P_{1J} - \frac{1}{(P_2\circ P_2)}C_1^{AI}P_{2A}P_{2I}C_2^{BJ}P_{2B}P_{1J},
\end{aligned}
\tag{A.13}
$$

$$
(P_2\bullet P_2)C_1^{AI}C_2^{BI}P_{1I}P_{3J} = (P_2\bullet P_3)C_1^{AI}C_2^{BI}P_{1A}P_{2B} + (C_1^{AI}P_{1A}P_{2I})(C_2^{AB}P_{3A}P_{2B}). \tag{A.14}
$$

A.4 Equation for Tensor Structures

In this section we will list down the non-negative integer equations for different correlators.

A.4.1 $\langle OO\rangle$

We list down the powers of different invariants in a tensor structure,

$$
\begin{aligned}
&H_1^{(i,j)} \to a_{ij}, \quad H_2^{(i,j)} \to b_{ij}, \quad S_{12}^{(i,j)} \to c_{ij}, \quad \bar{S}_{12}^{(i,j)} \to d_{ij}, \quad K_{12}^{(i)} \to e_i, \\
&K_{21}^{(i)} \to f_i, \quad \bar{K}_{12}^{(i)} \to g_i, \quad \bar{K}_{21}^{(i)} \to h_i.
\end{aligned}
\tag{A.15}
$$

Using a similar notation listed in (2.66) we have:

$$
\begin{aligned}
h_1^{(i)} &= \sum_j^{n_1^C} a_{ij} + \sum_j^{n_2^C} c_{ij} + \sum_j^{n_2^C} d_{ij} + e_i + g_i \\
h_2^{(i)} &= \sum_j^{n_1^C} b_{ij} + \sum_j^{n_1^C} c_{ji} + \sum_j^{n_1^C} d_{ji} + f_i + h_i
\end{aligned}
\tag{A.16}
$$

A.4.2 $\langle OOO\rangle$

Powers of each invarinat are denoted as,

$$
\begin{aligned}
&H_1^{(i,j)} \to a_{ij}, \quad H_2^{(i,j)} \to b_{ij}, \quad H_3^{(i,j)} \to c_{ij}, \\
&S_{12}^{(i,j)} \to d_{ij}, \quad S_{23}^{(i,j)} \to e_{ij}, \quad S_{31}^{(i,j)} \to f_{ij}, \\
&\bar{S}_{12}^{(i,j)} \to g_{ij}, \quad \bar{S}_{23}^{(i,j)} \to h_{ij}, \quad \bar{S}_{31}^{(i,j)} \to i_{ij}, \\
&K_{12}^{(i)} \to j_i, \quad K_{21}^{(i)} \to k_i, \quad K_{23}^{(i)} \to l_i, \quad K_{32}^{(i)} \to m_i, \quad K_{31}^{(i)} \to n_i, \quad K_{13}^{(i)} \to o_i, \\
&\bar{K}_{12}^{(i)} \to p_i, \quad \bar{K}_{21}^{(i)} \to q_i, \quad \bar{K}_{23}^{(i)} \to r_i, \quad \bar{K}_{32}^{(i)} \to s_i, \quad \bar{K}_{31}^{(i)} \to t_i, \quad \bar{K}_{13}^{(i)} \to u_i.
\end{aligned}
\tag{A.17}
$$

We get the following system of equation:

$$
\begin{aligned}
h_1^{(i)} &= \sum_j^{n_1^C} a_{ij} + \sum_j^{n_2^C} d_{ij} + \sum_j^{n_3^C} f_{ji} + \sum_j^{n_2^C} g_{ij} + \sum_j^{n_3^C} i_{ji} + j_i + o_i + p_i + u_i, \\
h_2^{(i)} &= \sum_j^{n_2^C} b_{ij} + \sum_j^{n_1^C} d_{ji} + \sum_j^{n_3^C} e_{ij} + \sum_j^{n_1^C} g_{ji} + \sum_j^{n_3^C} h_{ij} + k_i + l_i + q_i + r_i, \\
h_3^{(i)} &= \sum_j^{n_3^C} c_{ij} + \sum_j^{n_2^C} e_{ji} + \sum_j^{n_1^C} f_{ij} + \sum_j^{n_2^C} h_{ji} + \sum_j^{n_1^C} i_{ij} + m_i + n_i + s_i + t_i.
\end{aligned}
\tag{A.18}
$$

A.4.3 $\langle OO\hat{O}\rangle$

Let us denote the power of each invariant by the following symbols,

$$
\begin{aligned}
&G_{1\hat{3}}^{(i)} \to a_i, \quad G_{2\hat{3}}^{(i)} \to b_i, \quad H_1^{(i,j)} \to c_{ij}, \quad H_2^{(i,j)} \to d_{ij}, \quad \tilde{K}_{12}^{(i)} \to e_i, \quad K_{12}^{(i)} \to f_i \\
&\tilde{K}_{21}^{(i)} \to g_i, \quad K_{21}^{(i)} \to h_i, \quad \tilde{G}_{1\hat{3}}^{(i,j)} \to i_{ij}, \quad \tilde{G}_{2\hat{3}}^{(i,j)} \to j_{ij}, \quad H_{1\hat{3}}^{(i,j)} \to k_{ij}, \quad H_{2\hat{3}}^{(i,j)} \to l_{ij}, \\
&S_{12}^{(i,j)} \to m_{ij}, \quad \bar{S}_{12}^{(i,j)} \to n_{ij}, \quad K_{1\hat{3}}^{(i)} \to o_i, \quad K_{2\hat{3}}^{(i)} \to p_i, \quad N_{\hat{3},12}^{(i)} \to q_i.
\end{aligned}
\tag{A.19}
$$

Let the number of **Θ**-rows of the bulk operators be n_1^C and n_1^C. For the defect operator we have two quantum number whose Θ and Φ rows are $n_{\hat{3}}^C$ and $\bar{n}_{\hat{3}}^C$,

$$
\begin{aligned}
h_1^{(i)} &= \sum_j^{n_1^C} c_{ij} + e_i + f_i + \sum_j^{\bar{n}_{\hat{3}}^C} i_{ij} + \sum_j^{n_{\hat{3}}^C} k_{ij} + \sum_j^{n_2^C} m_{ij} + \sum_j^{n_2^C} n_{ij} + o_i, \\
h_2^{(i)} &= \sum_j^{n_2^C} d_{ij} + g_i + h_i + \sum_j^{\bar{n}_{\hat{3}}^C} j_{ij} + \sum_j^{n_{\hat{3}}^C} l_{ij} + \sum_j^{n_1^C} m_{ji} + \sum_j^{n_1^C} n_{ji} + p_i, \\
h_{\hat{3}}^{(i)} &= \sum_j^{n_1^C} k_{ji} + \sum_j^{n_2^C} l_{ji} + q_i, \\
\bar{h}_{\hat{3}}^{(i)} &= a_i + b_i + \sum_j^{n_1^C} i_{ji} + \sum_j^{n_2^C} j_{ji}.
\end{aligned}
\tag{A.20}
$$

APPENDIX B

SECTION 3

B.1 Integral Representation

We will start with the integral representation of the conformal blocks following [77, 56, 51]. The integral representation for the four point function $\langle \mathcal{O}_1 \mathcal{O}_2 \mathcal{O}_3 \mathcal{O}_4 \rangle$ in the OPE decomposition $\mathcal{O}_1 \times \mathcal{O}_2$ and $\mathcal{O}_3 \times \mathcal{O}_4$ due to the exchange of an operator $\mathcal{O}_{J,\Delta}$, is given by,

$$\begin{aligned} f_{\Delta,J}(u,v) = \frac{1}{\gamma_{\lambda_1,a}\gamma_{\bar{\lambda}_1,b}} \int_{\mathcal{C}} ds dt \, \Gamma(\lambda_2 - s)\Gamma(\bar{\lambda}_2 - s)\Gamma(-t)\Gamma(-t-a-b) \\ \times \Gamma(s+t+a)\Gamma(s+t+b)\mathcal{P}_{\Delta,J}(s,t,a,b)u^s v^t \, , \end{aligned} \tag{B.1}$$

where we have stripped off the overall kinematical factors. The contour $\mathcal{C}$ extends from $\gamma - i\infty$ to $\gamma + i\infty$ where following [56, 51],

$$\text{Re}(s) < \lambda_2, \bar{\lambda}_2 \, , \; \text{Re}(t) < 0, -a-b \, , \; \text{Re}(c) < a, b \, , \tag{B.2}$$

and for the t integral, $-a-s, -b-s < \gamma < 0, -a-b$. In general,

$$f_{\Delta,J}(u,v) = \frac{1}{k_{d-\Delta,J}} \frac{\gamma_{\lambda_1,a}}{\gamma_{\bar{\lambda}_1,b}} G_{\Delta,J}(u,v) + \frac{1}{k_{\Delta,J}} \frac{\gamma_{\bar{\lambda}_1,a}}{\gamma_{\lambda_1,a}} G_{d-\Delta,J}(u,v) \, , \tag{B.3}$$

is a linear combination of the physical block and the shadow respectively from the $s = \lambda_2 + n$ and $s = \bar{\lambda}_2 + n$ poles. We have also used the definitions,

$$\lambda_1 = \frac{\Delta + J}{2} \, , \; \bar{\lambda}_1 = \frac{d - \Delta + J}{2} \, , \tag{B.4}$$

$$\lambda_2 = \frac{\Delta - J}{2} \, , \; \bar{\lambda}_2 = \frac{d - \Delta - J}{2} \, . \tag{B.5}$$

$a = \frac{\Delta_{21}}{2}$ and $b = \frac{\Delta_{34}}{2}$ where $\Delta_{ij} = \Delta_i - \Delta_j$, and,

$$k_{\Delta,J} = \frac{1}{(\Delta-1)_J}\frac{\Gamma(d-\Delta+J)}{\Gamma(\Delta-h)}\,, \quad \gamma_{x,y} = \Gamma(x+y)\Gamma(x-y)\,, \text{ and } h = d/2\,. \tag{B.6}$$

d is the space-time dimension. $\mathcal{P}_{\Delta,J}(s,t,a,b)$ is the Mack polynomial given by,

$$\begin{aligned}\mathcal{P}_{\Delta,J}(s,t,a,b) =& \frac{1}{(d-2)_J}\sum_{m+n+p+q=J}\frac{J!}{m!n!p!q!}(-1)^{p+n}(2\bar{\lambda}_2+J-1)_{J-q}(2\lambda_2+J-1)_n(\bar{\lambda}_1+a-q)_q \\ &\times(\bar{\lambda}_1+b-q)_q(\lambda_1+a-m)_m(\lambda_1+b-m)_m(d-2+J+n-q)_q(h-1)_{J-q} \\ &\times(h-1+n+a+b)_p(\lambda_2-s)_{p+q}(-t)_n\,.\end{aligned} \tag{B.7}$$

The Mack polynomial and it's derivative for $a = b = 0$ are,

$$\begin{aligned}\mathcal{P}_{\Delta,J}(s,0) &= \frac{(d-\Delta-1)_J}{(d-2)_J}\sum_{m=0}^{J}A_m(J,\Delta)(\lambda_2-s)_{J-m}\,, \\ \mathcal{P}'_{\Delta,J}(s,0) &= \frac{(d-\Delta-1)_J}{(d-2)_J}\sum_{1\le m+n\le J}B_{m,n}(J,\Delta)(\lambda_2-s)_{J-m-n}\,,\end{aligned} \tag{B.8}$$

with

$$\begin{aligned}A_m(J,\Delta) =& \frac{(1+J-m)_m(h-1)_m(\lambda_1-m)_m^2(\bar{\lambda}_2+m)_{J-m}^2(2h-2+m)_{J-m}(2\bar{\lambda}_2-1+J)_m}{\Gamma(m+1)(d-\Delta-1)_J} \\ &\times{}_4F_3\left[\begin{matrix}h-1,h+m-1,m-J,2\bar{\lambda}_2+J-1+m \\ 2h-2+m,\bar{\lambda}_1-J+m,\bar{\lambda}_1-J+m\end{matrix};1\right], \\ B_{m,n}(J,\Delta) =& \frac{(-1)^{n+1}(1-\delta_{0,n})(\Delta-1)_n}{n}(\lambda_1-m)_m^2(1+J-m-n)_{m+n} \\ &\times\frac{(h-1)_{m+n}(h+m+n-\lambda_1)_{J-m-n}^2\Gamma(2h+m+2n-2)_{J-m-n}(2\bar{\lambda}_2-1+J)_{m+n}}{\Gamma(m+1)(d-\Delta-1)_J} \\ &\times{}_4F_3\left[\begin{matrix}-1+h+n,-1+h+m+n,-J+m+n,-1+2h+m+n-\Delta \\ -2+2h+m+2n,h+m+n-\lambda_1,h+m+n-\lambda_1\end{matrix};1\right].\end{aligned} \tag{B.9}$$

In what follows, we will select a scheme to write down the integral representation corresponding to the physical block itself in d dimensions. We consider the integral representation of the conformal blocks for a general spin exchange, given by,

$$G_{\Delta,J}(1-z,1-\bar{z}) = \frac{k_{d-\Delta,J}}{\gamma^2_{\lambda_1}} \int_{\mathcal{C}} dsdt\, \Gamma(\lambda_2-s)\Gamma(\bar{\lambda}_2-s)\Gamma(-t)^2\Gamma(s+t)^2 P_{\Delta,J}(s,t)(z\bar{z})^t[(1-z)(1-\bar{z})]^s \,. \tag{B.10}$$

By closing the contour on the *rhs* of the complex $s-$plane, one finds there are two sets of poles at $s = \lambda_2 + n$ and $s = \bar{\lambda}_2 + n$ characterizing the physical and the shadow blocks respectively. The idea is to remove the contribution of the shadow block completely. This is achieved by multiplying the integral representation by a phase,

$$p(s) = \frac{\sin\pi(\bar{\lambda}_2 - s)}{\sin\pi(\lambda_2 - \bar{\lambda}_2)} \frac{\sin\pi s}{\sin\pi\lambda_1}\,, \tag{B.11}$$

such that the shadow poles are now completely removed. The phase satisfies the shift symmetry property such that for $s \to s \pm k$, $p(s \pm k) = p(s)$. We then write the modified integral definition for the physical block as,

$$\begin{aligned} G_{\Delta,J}(1-z,1-\bar{z}) = \frac{k_{d-\Delta,J}}{\gamma^2_{\lambda_1}} \int_{\mathcal{C}} dsdt\, \Gamma(\lambda_2 - s)\Gamma(\bar{\lambda}_2 - s)\Gamma(-t)^2\Gamma(s+t)^2 p(s) \\ \times P_{\Delta,J}(s,t)(z\bar{z})^t[(1-z)(1-\bar{z})]^s \,. \end{aligned} \tag{B.12}$$

We will be mainly interested in the $z \to 0$ limit of the block for the leading corrections to the dimension and the OPE coefficients discussed in the paper. Notice that for this limit, only the contribution from the $t = 0$ pole suffices. Moreover, we can rewrite $\bar{z}^{s+t}$ as,

$$\bar{z}^{s+t} = \sum_{k=0}^{\infty} \frac{(-1)^k}{k!}(s+t)_k \left(\frac{1-\bar{z}}{\bar{z}}\right)^k, \tag{B.13}$$

Thus, after taking the $t=0$ pole,

$$\begin{aligned}\lim_{z\to 0} G_{\Delta,J}(1-z,1-\bar{z}) =& \frac{k_{d-\Delta,J}}{\gamma^2_{\lambda_1}}\int_{\mathcal{C}} ds\, \Gamma(\lambda_2-s)\Gamma(\bar{\lambda}_2-s)\Gamma(s)p(s)\\ &\times\sum_{k=0}^{\infty}\frac{(-1)^k}{k!}\Gamma(s+k)\left(\frac{1-\bar{z}}{\bar{z}}\right)^{s+k}\Big[P_{\Delta,J}(s,0)(\log z+H_{s-k-1}+H_{s-1})\\ &+\mathcal{P}'_{\Delta,J}(s,0)\Big]\,,\end{aligned} \tag{B.14}$$

where H_n is the Harmonic number $H(n)$. Before separating out the contributions to the anomalous dimensions and the OPE coefficients, we will perform a succession of shifts in the $s-$variable (mainly for the convenience of the computations to be followed). First we shift $s\to s-k$, such that,

$$\begin{aligned}\lim_{z\to 0} G_{\Delta,J}(1-z,1-\bar{z}) =& \frac{k_{d-\Delta,J}}{\gamma^2_{\lambda_1}}\int_{\mathcal{C}} ds\, \Gamma(s)p(s)\left(\frac{1-\bar{z}}{\bar{z}}\right)^{s}\\ &\times\sum_{k=0}^{\infty}\frac{(-1)^k}{k!}\Gamma(\lambda_2-s+k)\Gamma(\bar{\lambda}_2-s+k)\Gamma(s-k)\Big[P_{\Delta,J}(s-k,0)\\ &\times(\log z+H_{s-k-1}+H_{s-1})+\mathcal{P}'_{\Delta,J}(s-k,0)\Big]\,.\end{aligned} \tag{B.15}$$

The forms of the Mack polynomial and its derivative is given in (B.8) along with the coefficients in (B.9). Plugging in those simplifications, we find,

$$\begin{aligned}\lim_{z\to 0} G_{\Delta,J}(1-z,1-\bar{z}) =& \frac{\Gamma(\Delta+J)}{\Gamma(\frac{\Delta+J}{2})^4\Gamma(h-\Delta)(d-2)_J}\int_{\mathcal{C}} ds\, \Gamma(s)p(s)\left(\frac{1-\bar{z}}{\bar{z}}\right)^{s}\\ &\times\sum_{k=0}^{\infty}\frac{(-1)^k}{k!}\Gamma(\lambda_2-s+k)\Gamma(\bar{\lambda}_2-s+k)\Gamma(s-k)\Big[\sum_{m=0}^{J}A_m(J,\Delta)(\lambda_2-s+k)_{J-m}\\ &\times(\log z+H_{s-k-1}+H_{s-1})+\sum_{1\leq m+n\leq J}B_{m,n}(J,\Delta)(\lambda_2-s+k)_{J-m-n}\Big]\,.\end{aligned} \tag{B.16}$$

Based on the above separation, we can identify the coefficients of the log and regular terms as,

$$
\begin{aligned}
\lim_{z\to 0} G_{\Delta,J}(1-z,1-\bar{z})\Big|_{\log z} =& \frac{\Gamma(\Delta+J)}{\Gamma(\frac{\Delta+J}{2})^4\Gamma(h-\Delta)(d-2)_J}\sum_{m=0}^{J} A_m(J,\Delta)\int_{\mathcal{C}} ds\, \Gamma(s)p(s)\left(\frac{1-\bar{z}}{\bar{z}}\right)^s \\
&\times \sum_{k=0}^{\infty}\frac{(-1)^k}{k!}\Gamma(\lambda_2-s+k)\Gamma(\bar{\lambda}_2-s+k)\Gamma(s-k)(\lambda_2-s+k)_{J-m}\,, \\
\lim_{z\to 0} G_{\Delta,J}(1-z,1-\bar{z})\Big|_{\text{reg}} =& \frac{\Gamma(\Delta+J)}{\Gamma(\frac{\Delta+J}{2})^4\Gamma(h-\Delta)(d-2)_J}\int_{\mathcal{C}} ds\, \Gamma(s)p(s)\left(\frac{1-\bar{z}}{\bar{z}}\right)^s \\
&\times \sum_{k=0}^{\infty}\frac{(-1)^k}{k!}\Gamma(\lambda_2-s+k)\Gamma(\bar{\lambda}_2-s+k)\Gamma(s-k)\Bigg[\sum_{m=0}^{J} A_m(J,\Delta)(\lambda_2-s+k)_{J-m} \\
&\times (H_{s-k-1}+H_{s-1}) + \sum_{1\le m+n\le J} B_{m,n}(J,\Delta)(\lambda_2-s+k)_{J-m-n}\Bigg]\,.
\end{aligned}
\tag{B.17}
$$

This separation will form the starting point of discussion in the main text. However, as it stands (B.17) is still not ready in its final form to proceed with calculations. To put this in its final form, we will have to perform the $k-$sum now. As it stands,

$$
\begin{aligned}
&\sum_{k=0}^{\infty}\frac{(-1)^k}{k!}\Gamma(\lambda_2-s+k)\Gamma(\bar{\lambda}_2-s+k)\Gamma(s-k)(\lambda_2-s+k)_{J-m} \\
&= \frac{\pi}{\sin\pi s}\frac{\Gamma(\lambda_1-m-s)\Gamma(1-J+m+s-\lambda_2-\bar{\lambda}_2)\Gamma(\bar{\lambda}_2-s)}{\Gamma(1-\lambda_1+m)\Gamma(1-\bar{\lambda}_2)}\,,
\end{aligned}
\tag{B.18}
$$

within the chosen domain of the $s-$contour. Similarly,

$$
\begin{aligned}
&\sum_{k=0}^{\infty}\frac{(-1)^k}{k!}\Gamma(\lambda_2-s+k)\Gamma(\bar{\lambda}_2-s+k)\Gamma(s-k)(\lambda_2-s+k)_{J-m}(H_{s-k-1}+H_{s-1}) \\
=&\frac{\pi}{\sin\pi s}\frac{\Gamma(\lambda_1-m-s)\Gamma(1-J+m+s-\lambda_2-\bar{\lambda}_2)\Gamma(\bar{\lambda}_2-s)}{\Gamma(1-\lambda_1+m)\Gamma(1-\bar{\lambda}_2)}(H_{s-1}-\pi\cot\pi s+H_{m-\lambda_1} \\
&-H_{s-\lambda_1+m-\bar{\lambda}_2}+H_{-\bar{\lambda}_2})\,,
\end{aligned}
\tag{B.19}
$$

We will now proceed with each of these terms separately.

B.1.1 Log Term

Consider the integral representation of the $\log z$ term. After the $k-$summation, we get,

$$\lim_{z\to 0} G_{\Delta,J}(1-z,1-\bar{z})\Big|_{\log z} = \frac{\Gamma(\Delta+J)}{\Gamma(\frac{\Delta+J}{2})^4\Gamma(h-\Delta)(d-2)_J}\sum_{m=0}^{J} A_m(J,\Delta)\int_{\mathcal{C}} ds\, \Gamma(s)p(s)\left(\frac{1-\bar{z}}{\bar{z}}\right)^s \times \frac{\pi}{\sin\pi s}\frac{\Gamma(\lambda_1-m-s)\Gamma(1-J+m+s-\lambda_2-\bar{\lambda}_2)\Gamma(\bar{\lambda}_2-s)}{\Gamma(1-\lambda_1+m)\Gamma(1-\bar{\lambda}_2)}\,, \tag{B.20}$$

The choice of the phase factor now becomes more transparent. We can write,

$$p(s)\frac{\pi}{\sin\pi s}\frac{\Gamma(\bar{\lambda}_2-s)}{\Gamma(h-\Delta)} = \frac{-\pi}{\sin\pi\lambda_1}\frac{\Gamma(1+\Delta-h)}{\Gamma(1+s-\bar{\lambda}_2)}\,, \tag{B.21}$$

from which,

$$= \lim_{z\to 0} G_{\Delta,J}(1-z,1-\bar{z})\Big|_{\log z} = -\frac{\Gamma(2\lambda_1)\Gamma(1+\Delta-h)}{\Gamma(\lambda_1)^4(d-2)_J}\sum_{m=0}^{J} A_m(J,\Delta)\int_{\mathcal{C}} ds\, \Gamma(s)\left(\frac{1-\bar{z}}{\bar{z}}\right)^s \times \frac{\pi}{\sin\pi\lambda_1}\frac{\Gamma(\lambda_1-m-s)\Gamma(1+m+s-\lambda_1-\bar{\lambda}_2)}{\Gamma(1-\lambda_1+m)\Gamma(1+s-\bar{\lambda}_2)\Gamma(1-\bar{\lambda}_2)}\,, \tag{B.22}$$

Finally we shift $s\to s+\lambda_1-m$ so that,

$$G^t_{\Delta,J}|_{\log} = \lim_{z\to 0} G_{\Delta,J}(1-z,1-\bar{z})\Big|_{\log z} = -\frac{\Gamma(2\lambda_1)}{\Gamma(\lambda_1)^2(d-2)_J}\sum_{m=0}^{J}(-1)^m\frac{A_m(J,\Delta)}{(\lambda_1-m)_m^2}\int_{\mathcal{C}} ds\,\left(\frac{1-\bar{z}}{\bar{z}}\right)^{\lambda_1-m+s}\frac{\Gamma(-s)(\lambda_1-m)_s(1-\bar{\lambda}_2)_s}{(1+\Delta-h)_{s+J-m}}\,, \tag{B.23}$$

The $s=n$ poles (closing the contour along $\mathcal{C}$) reproduces the physical block.

B.1.2 Regular Terms

Similar to the log, term we can evaluate the regular term (the correction to the OPE coefficients) by following the exact same steps as above. Starting with the second term in (B.17), and performing the $k-$sum,

$$\begin{aligned}
&\lim_{z\to 0} G_{\Delta,J}(1-z,1-\bar{z})\Big|_{\text{reg}} \\
&= -\frac{\Gamma(2\lambda_1)\Gamma(1+\Delta-h)}{\Gamma(\lambda_1)^4(d-2)_J}\frac{\pi}{\sin\pi\lambda_1}\int_{\mathcal{C}} ds\, \frac{\Gamma(s)}{\Gamma(1+s-\bar{\lambda}_2)\Gamma(1-\bar{\lambda}_2)}\left(\frac{1-\bar{z}}{\bar{z}}\right)^s \\
&\times\Bigg[\sum_{m=0}^{J} A_m(J,\Delta)\frac{\Gamma(\lambda_1-m-s)\Gamma(1+m+s-\lambda_1-\bar{\lambda}_2)}{\Gamma(1-\lambda_1+m)}(H_{s-1}-\pi\cot\pi s+H_{m-\lambda_1} \\
&-H_{s-\lambda_1+m-\bar{\lambda}_2}+H_{-\bar{\lambda}_2})+\sum_{1\le m+n\le J} B_{m,n}(J,\Delta)\frac{\Gamma(\lambda_1-m-n-s)\Gamma(1+m+n+s-\lambda_1-\bar{\lambda}_2)}{\Gamma(1-\lambda_1+m+n)}\Bigg],
\end{aligned} \tag{B.24}$$

To get the final form we can shift the variables $s \to s+\lambda_1-m$. However, in order to keep coherence with the expressions used in the main text, we will treat the integrals separately, by writing,

$$\begin{aligned}
&\lim_{z\to 0} G_{\Delta,J}(1-z,1-\bar{z})\Big|_{\text{reg}} \\
&= -\frac{\Gamma(2\lambda_1)\Gamma(1+\Delta-h)}{\Gamma(\lambda_1)^4(d-2)_J}\frac{\pi}{\sin\pi\lambda_1}\Bigg[\sum_{m=0}^{J} A_m(J,\Delta) \\
&\times\int_{\mathcal{C}} ds\, \frac{\Gamma(s)\Gamma(\lambda_1-m-s)\Gamma(1+m+s-\lambda_1-\bar{\lambda}_2)}{\Gamma(1+s-\bar{\lambda}_2)\Gamma(1-\bar{\lambda}_2)\Gamma(1-\lambda_1+m)}\left(\frac{1-\bar{z}}{\bar{z}}\right)^s(H_{s-1}-\pi\cot\pi s+H_{m-\lambda_1}-H_{s-\lambda_1+m-\bar{\lambda}_2} \\
&+H_{-\bar{\lambda}_2})+\sum_{1\le m+n\le J} B_{m,n}(J,\Delta)\int_{\mathcal{C}} ds\, \frac{\Gamma(s)\Gamma(\lambda_1-m-n-s)\Gamma(1+m+n+s-\lambda_1-\bar{\lambda}_2)}{\Gamma(1+s-\bar{\lambda}_2)\Gamma(1-\bar{\lambda}_2)\Gamma(1-\lambda_1+m+n)}\left(\frac{1-\bar{z}}{\bar{z}}\right)^s\Bigg].
\end{aligned} \tag{B.25}$$

Note that the general contour $\mathcal{C}$ works for both the integrals since we are choosing the contour in a way such that apart from the poles $s=\lambda_1-m+k$ for the first integral and $s=\lambda_1-m-n+k$ for the second integral, there are no new poles. For any general m,n,k values the minimal pole in both the integrals is at $s=\lambda_2$ (for maximal m and $m+n$ values and $k=0$). The contour $\mathcal{C}$ is chosen such that $s=\lambda_2+n$ poles are always allowed. Now we shift $s\to s+\lambda_1-m$ in the first integral and $s \to s + \lambda_1 - m - n$ in the second integral, so that,

$$
\begin{aligned}
&G^t_{\Delta,J}|_{\text{reg}} = \lim_{z\to 0} G_{\Delta,J}(1-z,1-\bar{z})\Big|_{\text{reg}} \\
=& -\frac{\Gamma(2\lambda_1)}{\Gamma(\lambda_1)^2(d-2)_J}\Bigg[\sum_{m=0}^{J}(-1)^m\frac{A_m(J,\Delta)}{(\lambda_1-m)_m^2}\int_{\mathcal{C}}ds\,\frac{\Gamma(-s)(\lambda_1-m)_s(1-\bar{\lambda}_2)_s}{(1+\lambda_2-\bar{\lambda}_2)_{s+J-m}}\left(\frac{1-\bar{z}}{\bar{z}}\right)^{s+\lambda_1-m}(H_{s+\lambda_1-m-1} \\
&-\pi\cot\pi(s+\lambda_1)+H_{m-\lambda_1}-H_{s-\bar{\lambda}_2}+H_{-\bar{\lambda}_2}) \\
&+\sum_{1\le m+n\le J}(-1)^{m+n}\frac{B_{m,n}(J,\Delta)}{(\lambda_1-m-n)_{m+n}^2}\int_{\mathcal{C}}ds\,\frac{\Gamma(-s)(\lambda_1-m-n)_s(1-\bar{\lambda}_2)_s}{(1+\lambda_2-\bar{\lambda}_2)_{s+J-m-n}}\left(\frac{1-\bar{z}}{\bar{z}}\right)^{s+\lambda_1-m-n}\Bigg],
\end{aligned}
\tag{B.26}
$$

which is the starting point for (3.46) and (3.47) in section 3.4.

B.2 Integrals with Harmonic Number

In this appendix we will show in detail the steps required to evaluate the integral I_1 in (3.49). The difficulty in integrating it is that the expression contains a Harmonic number. Harmonic numbers are difficult to sum over once summing over residues. The equation (3.49) has the following functional form,

$$
\int_{\mathcal{C}} ds\, f(s,a,b,\cdots)\Gamma(s+k)H_{s+k-1}. \tag{B.27}
$$

We will solve this issue by generating this expression by differentiating one of the Gamma functions. We begin with the I_1 integral,

$$
\begin{aligned}
I_1 = \alpha_J\sum_{m=0}^{J}\frac{(-1)^{m+1}}{(\lambda_1-m)_m^2}\int_{\mathcal{C}}ds\Gamma(-s)\frac{(\lambda_1-m)_s(1-\bar{\lambda}_2)_s}{(1+\lambda_2-\bar{\lambda}_2)_{s+J-m}}\frac{\Gamma(\frac{\beta-\tau}{2}-\lambda_1+m-1-s)\Gamma(\frac{\tau}{2}-m+\lambda_1+1+s)^2}{\Gamma(\frac{\beta+\tau}{2}-m+1+s+\lambda_1)} \\
\times A_m(J,\Delta)(H_{s+\lambda_1-m-1}-H_{s-\bar{\lambda}_2})\,.
\end{aligned}
\tag{B.28}
$$

To perform the integral we first take the integrand without the Harmonic numbers. We then shift the Gamma functions whose argument corresponds to the Harmonic numbers and shift them by an arbitrary variable ϵ and then perform the integral. In a functional form (B.27) this looks like,

$$\int_{\mathcal{C}} ds\, f(n,a,\cdots)\Gamma(n+k+\epsilon) = g(k,a,\epsilon,\cdots)\,. \tag{B.29}$$

Performing the shift and the integral gives rise to the following result for I_1,

$$\begin{aligned}
&\alpha_J \sum_{m=0}^{J} \frac{(-1)^{m+1}}{(\lambda_1-m)_m^2} A_m(J,\Delta) \int_{\mathcal{C}} ds \Gamma(-s) \frac{\Gamma(s+\lambda_1-m+\epsilon)\Gamma(s+1-\bar{\lambda}_2-\epsilon)}{\Gamma(1+\lambda_2-\bar{\lambda}_2+s+J-m)} \\
&\frac{\Gamma(1+\lambda_2-\bar{\lambda}_2)}{\Gamma(\lambda_1-m)\Gamma(1-\bar{\lambda}_2)} \frac{\Gamma(\frac{\beta-\Delta-J-\tau}{2}+m-1-s)\Gamma(\frac{\Delta+J+\tau}{2}-m+1+s)^2}{\Gamma(\frac{\beta+\Delta+J+\tau}{2}-m+1+s)} \\
=&\alpha_J \sum_{m=0}^{J} \frac{(-1)^{m+1}}{(\lambda_1-m)_m^2} A_m(J,\Delta) \frac{\Gamma(1+\lambda_2-\bar{\lambda}_2)}{\Gamma(\lambda_1-m)\Gamma(1-\bar{\lambda}_2)} \\
&\times \left(\frac{\Gamma(\lambda_1-h+1-\epsilon)\Gamma(\lambda_1-m+\epsilon)\Gamma\left(\frac{\tau}{2}+\lambda_1-m+1\right)^2 \Gamma\left(m-1+\frac{\beta-\tau}{2}-\lambda_1\right)}{\Gamma(-h+2\lambda_1-m++1)\Gamma\left(\frac{\beta+\tau}{2}+\lambda_1-m+1\right)} \right. \\
&\times_4 F_3\left[\begin{matrix} 1-h+\lambda_1-\epsilon, \lambda_1-m+\epsilon, \frac{\tau}{2}+\lambda_1-m+1, \frac{\tau}{2}+\lambda_1-m+1 \\ -h+2\lambda_1-m+1, \frac{-\beta+\tau}{2}+\lambda_1-m+2, \frac{\beta+\tau}{2}+\lambda_1-m+1 \end{matrix};1\right] \\
&+ \frac{\Gamma\left(\frac{\beta}{2}\right)^2 \Gamma\left(\frac{\beta-\tau}{2}-1+\epsilon\right)\Gamma\left(-h+m+\frac{\beta-\tau}{2}-\epsilon)\right)\Gamma\left(\frac{-\beta+\tau}{2}+\lambda_1-m+1\right)}{\Gamma(\beta)\Gamma\left(\frac{\beta-\tau}{2}+\lambda_1-h\right)} \\
&\left. \times_4 F_3\left[\begin{matrix} \frac{\beta}{2}, \frac{\beta}{2}, \frac{\beta-\tau}{2}-1+\epsilon, \frac{\beta-\tau}{2}-h+m-\epsilon \\ \beta, \frac{\beta-\tau}{2}-\lambda_1+m, -h+\frac{\beta-\tau}{2}+\lambda_1 \end{matrix};1\right]\right).
\end{aligned} \tag{B.30}$$

Now we can take derivatives of both sides with respect to ϵ [1] and set ϵ to 0. The left side becomes exactly the integral we wanted (B.28) as derivative of Gamma functions generate Polygamma functions,

$$\frac{d}{d\epsilon}\Gamma(a+\epsilon) = \Gamma(a+\epsilon)\psi^{(0)}(a+\epsilon) = \Gamma(a+\epsilon)(H_{a+\epsilon-1}-\gamma)\,. \tag{B.31}$$

In the above equation γ is the Euler-Mascheroni constant. The right side (B.30) result would involve derivative of ${}_4F_3$ with respect to its parameters. We will first discuss the expressions for derivative of hypergeometric functions in terms of Kampé de Fériet-like functions. We begin with

[1] This procedure is well defined if the infinite sum is convergent.

the expression of a generalized hypergeometric function [2][3],

$$ {}_pF_q(a_1,\ldots,a_p;b_1,\ldots,b_q;z)=\sum_{n=0}^{\infty}\frac{(a_1)_n\cdots(a_p)_n}{(b_1)_n\cdots(b_q)_n}\frac{z^n}{n!}=\sum_{n=0}^{\infty}A_n\frac{z^n}{n!}\,. \tag{B.32} $$

The parameters of each row of a hypergeometric are symmetric so we can just consider derivative of hypergeometric with respect to the first parameter a_1,

$$ G_{a_1}=\frac{d\left({}_pF_q[(a_1,\cdots,a_p);(b_1,\cdots,b_q);1]\right)}{da_1}\,. \tag{B.33} $$

Before proceeding further let us introduce some notations for Kampé de Fériet-like double sum functions,

$$ {}_p\Theta_q\left[\begin{matrix}\alpha_1,\,\alpha_2\mid a_1,\,a_2,\,\cdots,\,a_p\\ \gamma\mid b_1,\,b_2,\,\cdots,\,b_q\end{matrix}\mid x,\,y\right] \tag{B.34} $$

$$ =\sum_{m=0}^{\infty}\sum_{n=0}^{\infty}\frac{(\alpha_1)_m(\alpha_2)_n(a_1)_m}{(\gamma)_m}\frac{(a_2)_{m+n}(\cdots)(a_p)_{m+n}}{(b_1)_{m+n}(b_2)_{m+n}(\cdots)(b_q)_{m+n}}\frac{x^my^n}{m!n!}\,. \tag{B.35} $$

In this paper we only encounter the derivatives of ${}_4F_3$ with argument 1. Specializing the above equation to our case we obtain,

$$ \frac{d({}_4F_3(1))}{da_1}=G_{a_1}(1)=\frac{1}{a_1}A_1\,{}_4\Theta_3\left[\begin{matrix}1,\,1\mid a_1,\,a_1+1,\,a_2+1,\,a_3+1,\,a_4+1\\ a_1+1\mid 2,\,b_1+1,\,b_2+1,\,b_3+1\end{matrix}\mid 1,\,1\right]. \tag{B.36} $$

The hypergeometric and its derivatives have argument 1 and A_1 is defined in (B.32). For convenience we provide the expanded expression for the double sum below,

$$ {}_4\Theta_3\left[\begin{matrix}1,\,1\mid a_1,\,a_1+1,\,a_2+1,\,a_3+1,\,a_4+1\\ a_1+1\mid 2,\,b_1,\,b_2,\,b_3\end{matrix}\mid 1,\,1\right] \tag{B.37} $$

$$ =\sum_{m=0}^{\infty}\sum_{n=0}^{\infty}\frac{(a_1)_m}{(a_1)_{m+1}}\frac{(a_1+1)_{m+n}(a_2+1)_{m+n}(a_3+1)_{m+n}(a_4+1)_{m+n}}{(2)_{m+n}(b_1)_{m+n}(b_2)_{m+n}(b_3)_{m+n}}\,. \tag{B.38} $$

[2]We follow the conventions and notations of [78].

[3]We will refer to z as the argument of the hypergeometric.

We will further define two notations which will be used in the maintext,

$$\begin{aligned}\mathcal{G}_1 =&\frac{A_1}{a_1}\,{}_4\Theta_3\left[\begin{matrix}1,\ 1\mid\ a_1,\ a_1+1,\ a_2+1,\ a_3+1,\ a_4+1\\ a_1+1\mid 2,\ b_1+1,\ b_2+1,\ b_3+1\end{matrix}\mid 1,\ 1\right]-(a_1\leftrightarrow a_2)\,,\\ \mathcal{G}_2 =&\frac{C_1}{c_1}\,{}_4\Theta_3\left[\begin{matrix}1,\ 1\mid\ c_1,\ c_1+1,\ c_2+1,\ c_3+1,\ c_4+1\\ c_1+1\mid 2,\ d_1+1,\ d_2+1,\ d_3+1\end{matrix}\mid 1,\ 1\right]-(c_1\leftrightarrow c_2)\,,\end{aligned}\tag{B.39}$$

with ,

$$\begin{aligned}&a_1=1-h+\lambda_1, && a_2=\lambda_1-m, && a_3=a_4=\frac{\tau}{2}+\lambda_1-m+1,\\ &b_2=\frac{\tau-\beta}{2}+\lambda_1-m+2, && b_1=1-h+J-m, && b_3=\frac{\tau-\beta}{2}+\lambda_1-m+1,\\ &c_1=\frac{\beta-\tau}{2}-1, && c_2=\frac{\beta-\tau}{2}-h+m, && c_3=c_4=\frac{\beta}{2},\\ &d_2=\frac{\beta-\tau}{2}-\lambda_1+m, && d_1=\beta, && d_3=\frac{\beta-\tau}{2}+\lambda_1-h,\\ &A_1=\frac{\prod_{i=1}^4 a_i}{\prod_{i=1}^3 b_i}, && C_1=\frac{\prod_{i=1}^4 c_i}{\prod_{i=1}^3 d_i}.\end{aligned}\tag{B.40}$$

Returning to (B.30), on taking the derivative of the right side with ϵ and using the expression for double sums we obtain,

$$\begin{aligned}&\alpha_J\sum_{m=0}^{J}\frac{(-1)^{m+1}}{(\lambda_1-m)_m^2}\int_{\mathcal{C}}ds\Gamma(-s)\frac{(\lambda_1-m)_s(1-\bar\lambda_2)_s}{(1+\lambda_2-\bar\lambda_2)_{s+J-m}}\frac{\Gamma(\frac{\beta-\tau}{2}-\lambda_1+m-1-s)\Gamma(\frac{\tau}{2}-m+\lambda_1+1+s)^2}{\Gamma(\frac{\beta+\tau}{2}-m+1+s+\lambda_1)}\\ &\times A_m(J,\Delta)\left(H_{s+\lambda_1-m-1}-H_{s-\bar\lambda_2}\right)\\ =&\alpha_J\sum_{m=0}^{J}\frac{(-1)^{m+1}}{(\lambda_1-m)_m^2}A_m(J,\Delta)\frac{\Gamma(1+\lambda_2-\bar\lambda_2)}{\Gamma(\lambda_1-m)\Gamma(1-\bar\lambda_2)}\\ &\Bigg[C_m(J,\Delta)\Bigg({}_4F_3\left[\begin{matrix}1-h+\lambda_1,\lambda_1-m,\frac{\tau}{2}+\lambda_1-m+1,\frac{\tau}{2}+\lambda_1-m+1\\ -h+2\lambda_1-m+1,\frac{-\beta+\tau}{2}+\lambda_1-m+2,\frac{\beta+\tau}{2}+\lambda_1-m+1\end{matrix};1\right]\\ &(H_{\lambda_1-m-1}-H_{-h+\lambda_1})-\mathcal{G}_1\Bigg)\\ &+D_m(J,\Delta)\Bigg({}_4F_3\left[\begin{matrix}\frac{\beta}{2},\frac{\beta}{2},\frac{\beta-\tau}{2}-1,\frac{\beta-\tau}{2}-h+m\\ \beta,\frac{\beta-\tau}{2}-\lambda_1+m,-h+\frac{\beta-\tau}{2}+\lambda_1\end{matrix};1\right](H_{\frac{\beta-\tau}{2}-2}-H_{\frac{\beta-\tau}{2}-h+m-1})+\mathcal{G}_2\Bigg)\Bigg].\end{aligned}\tag{B.41}$$

This completes our derivation of (3.53).

B.3 Wilson Function

We now describe the procedure to write the two ${}_4F_3$s as a single ${}_7F_6$. Following the conventions of [52], Wilson function can be written as a linear combination of two balanced ${}_4F_3(1)$ as,

$$\phi_\alpha(\beta;a,b,c,d) = \frac{\Gamma(d-a)}{\Gamma(a+b)\Gamma(a+c)\Gamma(d\pm\beta)\Gamma(\tilde{d}\pm\alpha)}\, {}_4F_3\left[\begin{matrix} a+\beta, a-\beta, \tilde{a}+\alpha, \tilde{a}-\alpha \\ a+b, a+c, 1+a-d \end{matrix}; 1\right] + (a\leftrightarrow d), \tag{B.42}$$

where,

$$\begin{aligned} \tilde{a} &= \frac{1}{2}(a+b+c-d), & \tilde{d} &= \frac{1}{2}(-a+b+c+d), \\ \tilde{b} &= \frac{1}{2}(a+b-c+d), & \tilde{c} &= \frac{1}{2}(a-b+c+d), \end{aligned}$$
$$\Gamma(a\pm b) = \Gamma(a+b)\Gamma(a-b). \tag{B.43}$$

Wilson function can also be written [57][4] as,

$$\begin{aligned} \phi_\alpha(\beta;a.b.c.d) =& \frac{\Gamma(\tilde{a}+\tilde{b}+\tilde{c}-\alpha)}{\Gamma(a+b)\Gamma(a+c)\Gamma(a+d)\Gamma(\tilde{d}-\alpha)\Gamma(\tilde{b}+c-\alpha-\beta)\Gamma(\tilde{b}+c-\alpha+\beta)} \\ & \times W(\tilde{a}+\tilde{b}+\tilde{c}-1-\alpha; a-\beta, a+\beta, \tilde{a}-\alpha, \tilde{b}-\alpha, \tilde{c}-\alpha), \end{aligned} \tag{B.44}$$

where the W-function above can be written as a ${}_7F_6$,

$$W(a;b,c,d,e,f) = {}_7F_6\left[\begin{matrix} a\,,\, \frac{a}{2}+1\,,\, b\,,\, c\,,\, d\,,\, e\,,\, f \\ \frac{a}{2}, 1+a-b, 1+a-c, 1+a-d, 1+a-e, 1+a-f \end{matrix}; 1\right]. \tag{B.45}$$

This procedure gives us same final result as the one given in [58].

[4] Our conventions are related to those of [57] as $\phi_\alpha(\beta;a,b,c,d) = \phi_{i\,\alpha}(i\,\beta;a,b,c,1-d)$.

APPENDIX C

SECTION 4

C.1 Important Identities

We list down some important integrals that we will use throughout our calculations. We first write down result of 3-external-point integral,

$$
\begin{aligned}
I_{a,b,c}(x_1,x_2,x_3) &= \int \frac{d^4x}{((x_1-x)^2)^a((x_2-x)^2)^b((x_3-x)^2)^c} \\
&= \frac{\Gamma(\frac{a+b-c}{2})\Gamma(\frac{a+c-b}{2})\Gamma(\frac{b+c-a}{2})}{\Gamma(a)\Gamma(b)\Gamma(c)}(x_{12}^2)^{-\frac{a+b-c}{2}}(x_{13}^2)^{-\frac{a+c-b}{2}}(x_{23}^2)^{-\frac{b+c-a}{2}}\,.
\end{aligned}
\tag{C.1}
$$

for $a+b+c=d$ and the result for 4-external points $(a_1+a_2+a_3+a_4=d)$ is,

$$
\begin{aligned}
&I_{\{a_i\}}(x_i) = \int d^4x \prod_{i=1}^{4} \frac{1}{((x_i-x)^2)^{a_i}} \\
=&\frac{1}{\prod_i \Gamma(a_i)} \frac{(x_{12}^2)^{\frac{a_3+a_4-a_1-a_2}{2}}(x_{14}^2)^{\frac{a_3+a_2-a_1-a_4}{2}}(x_{24}^2)^{\frac{a_1+a_4-a_3-a_2}{2}}}{(x_{13}^2)^{a_3}(x_{24}^2)^{a_4}} \\
&\times \int dsdt\, \Gamma(-s)\Gamma(-t)\Gamma(s+t+a_3)\Gamma(s+t+\frac{a_2+a_3+a_4-a_1}{2})\Gamma(\frac{a_1+a_2-a_3-a_4}{2}-s) \\
&\times \Gamma(\frac{a_1+a_4-a_2-a_3}{2}-t)u^s v^t\,.
\end{aligned}
\tag{C.2}
$$

We also list down the conversion of an integral from a Mellin-type to an Euler type,

$$
\begin{aligned}
&\oint ds \Gamma(a_1+s)\Gamma(a_2+s)\Gamma(b_1-s)\Gamma(b_2-s)z^{-s} \\
=&\Gamma(a_1+b_1)\Gamma(a_2+b_2)\int_0^1 \frac{dp}{p(1-p)} p^{b_2+a_1}(1-p)^{b_1+a_2}[1-p(1-z)]^{-b_1-a_1}
\end{aligned}
\tag{C.3}
$$

C.2 Conformal Blocks: Details

The details of the derivation of the conformal blocks (both scalar and spin exchanges) are given here.

C.2.1 Scalar Conformal Block

We will explicitly compute the expansion of the conformal blocks in $d = 4 - \epsilon$ dimensions as a specific expansion in both the coupling$-g$ and ϵ. To start with, we will consider the specific example of scalar conformal block in the $t-$channel, in the integral representation,

$$G_{\Delta,0}(1-z,1-\bar{z}) = \frac{k_{d-\Delta,0}}{\gamma^2_{\lambda_1,0}} \int dsdt\, \Gamma(\lambda_2 - s)\Gamma(\bar{\lambda}_2 - s)\Gamma(-t)^2\Gamma(s+t)^2(z\bar{z})^t((1-z)(1-\bar{z}))^s\,. \tag{C.4}$$

To explain the notation,

$$\lambda_2 = \Delta/2 = \lambda_1\,, \bar{\lambda}_2 = (d-\Delta)/2\,, k_{d-\Delta,\ell} = \frac{1}{(d-\Delta-1)_\ell}\frac{\Gamma(\Delta+\ell)}{\Gamma(h-\Delta)}\,, \gamma_{x,y} = \Gamma(x+y)\Gamma(x-y)\,. \tag{C.5}$$

We have $\Delta = 2\Delta_\phi + g$, $\Delta_\phi = (d-2)/2$ and $d = 4-\epsilon$, we can immediately see how the expansion should work. We start by projecting out the poles from the shadow part. For this, we multiply the integral representation by a phase,

$$p(s) = \frac{\sin\pi(\bar{\lambda}_2 - s)}{\sin\pi(\bar{\lambda}_2 - \lambda_2)}e^{i\pi s}\,, \tag{C.6}$$

and performing the $t-$integral by keeping only the leading term in the $z \to 0$ limit, we can write,

$$\begin{aligned}G_{\Delta,0}(1-z,1-\bar{z}) &= -\frac{\Gamma(\Delta)}{\Gamma(\frac{\Delta}{2})^4}\Gamma(1+\Delta-h)\int ds\,\frac{\Gamma(\Delta/2-s)\Gamma(s)^2}{\Gamma(1+s+\Delta/2-h)}(\bar{z}-1)^s(\log z\bar{z} + 2H_{s-1})\\ &= D_\alpha\Big[-(z\bar{z})^{\alpha/2}\frac{\Gamma(\Delta)}{\Gamma(\frac{\Delta}{2})^4}\Gamma(1+\Delta-h)\int ds\,\frac{\Gamma(\Delta/2-s)\Gamma(s)\Gamma(s+\alpha)}{\Gamma(1+s+\Delta/2-h)}(\bar{z}-1)^s\Big]\Big|_{\alpha=0}\,,\end{aligned} \tag{C.7}$$

where $D_\alpha \equiv 2(\gamma+\partial_\alpha)$. Now we shift, $s \to s+\Delta/2$ so that,

$$G_{\Delta,0}(1-z,1-\bar{z}) =(1-\bar{z})^{\Delta/2} D_\alpha \Big[-(z\bar{z})^{\alpha/2} \frac{\Gamma(\Delta)(\Delta/2)_\alpha}{\Gamma(\frac{\Delta}{2})^2} \int ds\, \frac{\Gamma(-s)(\Delta/2)_s(\Delta/2+\alpha)_s}{(1+\Delta-h)_s} (\bar{z}-1)^s \Big] \Big|_{\alpha=0} . \tag{C.8}$$

Notice that,

$$\int ds\, \frac{\Gamma(-s)(\Delta/2)_s(\Delta/2+\alpha)_s}{(1+\Delta-h)_s}(1-\bar{z})^s = -{}_2F_1[\Delta/2,\Delta/2+\alpha,1+\Delta-h,1-\bar{z}]\,. \tag{C.9}$$

However the integrand inside the Euler-representation of the above is not convergent itself. We use the following transformation,

$$\begin{aligned} {}_2F_1[A_1,A_2,B_1,z] =& \frac{(2B_1-A_1-A_2+1)z-B_1}{B_1(z-1)} {}_2F_1[A_1,A_2,B_1+1,z] \\ &- \frac{(B_1-A_1+1)(B_1-A_2+1)z}{B_1(B_1+1)(z-1)} {}_2F_1[A_1,A_2,B_1+2,z]\,. \end{aligned} \tag{C.10}$$

to write,

$$\begin{aligned} G_{\Delta,0}(1-z,1-\bar{z}) =& -\frac{(1-\bar{z})^{\Delta/2}}{\bar{z}} D_\alpha \Big[(z\bar{z})^{\alpha/2} \frac{\Gamma(1+\Delta-h)\Gamma(\Delta)(\Delta/2)_\alpha}{\Gamma(\frac{\Delta}{2})^3\Gamma(\frac{\Delta}{2}-h+2)} \\ &\times \int_0^1 dx \frac{x^{\Delta/2-1}(1-x)^{\Delta/2-h+1}}{(1-x(1-\bar{z}))^{\Delta/2+\alpha}} ((h-1-\Delta/2)\bar{z} + x(\bar{z}-1)(h+\alpha-2-\Delta/2)-\Delta/2) \Big]\,. \end{aligned} \tag{C.11}$$

We define,

$$\begin{aligned} \mathcal{I}_1^{\Delta,h}(x,\alpha,1-\bar{z}) &= \frac{x^{\Delta/2-1}(1-x)^{\Delta/2-h+1}}{(1-x(1-\bar{z}))^{\Delta/2+\alpha}}\,, \\ \mathcal{I}_2^{\Delta,h}(x,\alpha,1-\bar{z}) &= \frac{x^{\Delta/2}(1-x)^{\Delta/2-h+1}}{(1-x(1-\bar{z}))^{\Delta/2+\alpha}}\,. \end{aligned} \tag{C.12}$$

With all these results we get,

$$G_{\Delta,0}(1-z,1-\bar{z}) = \frac{(1-\bar{z})^{\Delta/2}}{\bar{z}} D_\alpha \Bigg[(z\bar{z})^{\alpha/2} \frac{\Gamma(1+\Delta-h)\Gamma(\Delta)(\Delta/2)_\alpha}{\Gamma(\frac{\Delta}{2})^3\Gamma(\frac{\Delta}{2}-h+2)} \times \Bigg((\Delta/2-(h-1-\Delta/2)\bar{z}) \int_0^1 dx\, \mathcal{I}_1^{\Delta,h}(x,\alpha,1-\bar{z}) + (1-\bar{z})(h+\alpha-2-\Delta/2) \int_0^1 dx\, \mathcal{I}_2^{\Delta,h}(x,\alpha,1-\bar{z})\Bigg)\Bigg]. \tag{C.13}$$

Finally taking the derivative *wrt* α, we can write,

$$G_{\Delta,0}(1-z,1-\bar{z}) = \frac{(1-\bar{z})^{\Delta/2}}{\bar{z}} \frac{\Gamma(1+\Delta-h)\Gamma(\Delta)}{\Gamma(\frac{\Delta}{2})^3\Gamma(\frac{\Delta}{2}-h+2)} \Bigg[(\Delta/2-(h-1-\Delta/2)\bar{z}) \times \int_0^1 dx\, \mathcal{I}_1^{\Delta,h}(x,0,1-\bar{z})\Bigg(2H_{\Delta/2-1} + \log\frac{z\bar{z}}{(1-x(1-\bar{z}))^2}\Bigg) + (1-\bar{z}) \int_0^1 dx\, \mathcal{I}_2^{\Delta,h}(x,0,1-\bar{z})\Bigg(2+(h-2-\Delta/2)(2H_{\Delta/2-1}+\log\frac{z\bar{z}}{(1-x(1-\bar{z}))^2})\Bigg)\Bigg]. \tag{C.14}$$

C.2.2 $\tau = 2$, $\ell \geq 2$ Conformal Blocks

We will mimic the calculation of the previous section directly from the integral representation of the conformal blocks. We start with,

$$G_{\Delta,\ell}(z,\bar{z}) = \frac{k_{d-\Delta,\ell}}{\gamma^2_{\lambda_1,0}} v^{\lambda_2} \int dsdt\, \frac{\Gamma(-s)}{\Gamma(1+s+\lambda_2-\bar{\lambda}_2)} \Gamma(-t)^2\Gamma(s+\lambda_2+t)^2\alpha_\ell(s,t)(-v)^s u^t\,, \tag{C.15}$$

where $u = z\bar{z}$, $v = (1-z)(1-\bar{z})$, we have first removed the effect of the shadow poles by introducing a suitable phase and further shifted $s \to s+\lambda_2$ so that now we can only consider the poles at $s=n$ to retrieve the phsyical conformal block. $\alpha_\ell(s,t)$ is the Mack polynomial, given by,

$$\begin{aligned}\alpha_\ell(s,t) =& \frac{1}{(d-2)_\ell}\sum_{m+n+p+q=\ell}\frac{(-1)^{p+n}\ell!}{m!n!p!q!}(2\bar{\lambda}_2+\ell-1)_{\ell-q}(2\lambda_2+\ell-1)_n(\bar{\lambda}_1-q)_q^2(\lambda_1-m)_m^2 \\ &\times (d-2+\ell+n-q)_q(d/2-1)_{\ell-q}(d/2-1+n)_p(-s)_{p+q}(-t)_n\,.\end{aligned} \tag{C.16}$$

For our purposes, $\Delta = 2\Delta_\phi+\ell+g^2\gamma_\ell$ and $d=4-\epsilon$ and $\Delta_\phi=(d-2)/2+g^2\gamma_\phi$. Hence,

$$\lambda_2 = \Delta_\phi + \frac{g^2}{2}\gamma_\ell\,,\;\; \bar{\lambda}_2 = \frac{d}{2}-\Delta_\phi-\ell-\frac{g^2}{2}\gamma_\ell\,, \tag{C.17}$$

$$\lambda_1 = \Delta_\phi +\ell+ \frac{g^2}{2}\gamma_\ell\,,\;\; \bar{\lambda}_1 = \frac{d}{2}-\Delta_\phi-\frac{g^2}{2}\gamma_\ell\,. \tag{C.18}$$

Since the double discontinuity will only come from the outside factor $(1-\bar{z})^{\lambda_2}$ and we are only interested in the leading and next to leading order in the computation, it suffices to ignore the $O(g^2)$ terms in (C.17). Thus to the desired order of computation, we can always write,

$$\lambda_2 = 1-\frac{\epsilon}{2}\,,\;\; \bar{\lambda}_2 = 1-\ell\,,\;\; \lambda_1 = 1-\frac{\epsilon}{2}+\ell\,,\;\; \bar{\lambda}_1 = 1\,, \tag{C.19}$$

where we have neglected $O(g^2)$ contributions both from Δ_ϕ and Δ_ℓ. The overall factors associated with the normalization of the conformal block is given by,

$$k_{d-\Delta,\ell} = \frac{\Gamma(\Delta+1-d/2)\Gamma(\Delta+\ell)}{(d-\Delta-1)_\ell}\,,\;\; \gamma_{x,0}=\Gamma(x)^2\,. \tag{C.20}$$

With the values of $\lambda_{1,2}$ given in (C.19), it is not difficult to see that (C.16) undergoes fair amount of simplifications. Firstly, the amount of sum reduces since the only term that survives is $q=0$.

Then,

$$
\begin{aligned}
\alpha_\ell(s,t) =&\frac{(d/2-1)_\ell}{(d-2)_\ell}\sum_{m+n+p=\ell}\frac{(-1)^{p+n}\ell!}{m!n!p!}(1-\ell)_\ell(2\lambda_2+\ell-1)_n(\lambda_1-m)_m^2(d/2-1+n)_p(-s)_p(-t)_n\\
=&\frac{(d/2-1)_\ell\Gamma(\lambda_1)^2}{(d-2)_\ell\Gamma(1-\ell)}\sum_{n+p\leq\ell}\frac{(-1)^{p+n}\ell!(2\lambda_2+\ell-1)_n(-s)_p(-t)_n}{(\ell-n-p)!n!p!\Gamma(d/2-1+n+p)\Gamma(d/2-1+n)}\\
=&\frac{(d/2-1)_\ell\Gamma(\lambda_1)^2}{(d-2)_\ell\Gamma(1-\ell)}\frac{\Gamma(d/2-1+\ell+s)}{\Gamma(d/2-1+\ell)}\sum_{n\leq\ell}\frac{(-1)^n\ell!(d+\ell-3)_n(-t)_n}{n!(\ell-n)!\Gamma(d/2-1+n)\Gamma(d/2-1+n+s)}\\
=&\frac{(d/2-1+s)_\ell\Gamma(\lambda_1)^2}{\Gamma(d/2-1)^2\Gamma(1-\ell)(d-2)_\ell}{}_3F_2\left[\begin{matrix}-\ell,\ell+d-3,-t\\ d/2-1,d/2-1+s\end{matrix};1\right].
\end{aligned}
\tag{C.21}
$$

Finally, performing the $n-$sum, we can write, upto the desired order, a closed form expression, given by,

$$
\frac{k_{d-\Delta,\ell}}{\gamma^2_{\lambda_1}}\alpha_\ell(s,t)=\frac{(d/2-1+s)_\ell\Gamma(d-2+2\ell)}{(d-2)_\ell\Gamma(d/2-1)^2\Gamma(d/2-1+\ell)}\,{}_3F_2\left[\begin{matrix}-\ell,\ell+d-3,-t\\ d/2-1,d/2-1+s\end{matrix};1\right]. \tag{C.22}
$$

Thus the conformal block for each spin can be written as (upto $O(\epsilon^5)$)[1],

$$
\begin{aligned}
G_{\Delta,\ell}(z,\bar z)=\frac{\Gamma(d-2+2\ell)v^{\lambda_2}}{\Gamma(d/2-1)\Gamma(d/2-1+\ell)^2}\int dsdt\,&\frac{\Gamma(-s)\Gamma(-t)^2\Gamma(d/2-1+s+t)^2}{\Gamma(d/2-1+s)}(-v)^s u^t\\
&\times{}_3F_2\left[\begin{matrix}-\ell,\ell+d-3,-t\\ d/2-1,d/2-1+s\end{matrix};1\right].
\end{aligned}
\tag{C.23}
$$

[1]We have included the overall factor $(d-2)_\ell/(d/2-1)_\ell$ in the definition so that it coincides with the usual conformal block.

To proceed, we decompose ${}_3F_2$ into its integral representation,

$$
\begin{aligned}
&{}_3F_2\left[\begin{matrix}-\ell,\ell+d-3,-t\\ d/2-1,d/2-1+s\end{matrix};1\right]\\
&=\frac{\Gamma(d/2-1+s)}{\Gamma(-t)\Gamma(d/2-1+s+t)}\int_0^1 dx x^{-t-1}(1-x)^{d/2-2+s+t}\frac{\Gamma(1+\ell)\Gamma(d-3)}{\Gamma(\ell+d-3)}C_\ell^{(d-3)/2}(1-2x)\,,
\end{aligned}
\tag{C.24}
$$

where $C_\ell^\lambda(x)$ is the Gegenbauer polynomial. Plugging this back in (C.24), we can write,

$$
\begin{aligned}
G_{\Delta,\ell}(z,\bar z)=&\frac{\Gamma(d-2+2\ell)v^{\lambda_2}}{\Gamma(d/2-1)\Gamma(d/2-1+\ell)^2}\int dsdt\,\Gamma(-s)\Gamma(-t)\Gamma(d/2-1+s+t)(-v)^s u^t\\
&\times\int_0^1 dx x^{-t-1}(1-x)^{d/2-2+s+t}\frac{\Gamma(1+\ell)\Gamma(d-3)}{\Gamma(\ell+d-3)}C_\ell^{(d-3)/2}(1-2x)\,.
\end{aligned}
\tag{C.25}
$$

Now, notice that for twist-2 higher spin conformal blocks, $\Delta=2\Delta_\phi+\ell+g^2\gamma_\ell$, where,

$$
\gamma_\ell=-\frac{12\gamma_\phi^{(2)}}{\ell(\ell+1)}\,,\quad a_\ell=\frac{\Gamma(d/2-1+\ell)^2\Gamma(\ell+d-3)}{\ell!\Gamma(d/2-1)^2\Gamma(d-3+2\ell)}\,,
\tag{C.26}
$$

upto the order of expansion we are interested in. Thus, we define the twist-2 (sum over) higher spin blocks as,

$$
\begin{aligned}
\mathcal{G}_2(z,\bar z)&=\left(\frac{u}{v}\right)^{\Delta_\phi}\sum_{\ell=2}^{\infty}\gamma_\ell^2 a_\ell G_{\tau+\ell,\ell}(z,\bar z)\\
&=u^{\Delta_\phi}v^{\lambda_2-\Delta_\phi}\int_0^1 dx x^{-t-1}(1-x)^{d/2-2+s+t}\int dsdt\,\Gamma(-s)\Gamma(-t)\Gamma(d/2-1+s+t)\\
&\times(-v)^s u^t\frac{\Gamma(d-3)}{\Gamma(d/2-1)^3}\sum_{\ell=2}^{\infty}\frac{(d-3+2\ell)}{\ell^2(\ell+1)^2}C_\ell^{(d-3)/2}(1-2x)\,.
\end{aligned}
\tag{C.27}
$$

The s, t integral can be done exactly, and with the substitution $u = z\bar{z}\,, v = (1-z)(1-\bar{z})$,

$$\begin{aligned}
&\int dsdt\, \Gamma(-s)\Gamma(-t)\Gamma(d/2-1+s+t)u^t \left(\frac{1-x}{x}\right)^t (1-x)^s(-v)^s \\
&= \Gamma(d/2-1)\frac{x^{d/2-1}}{(z+x(1-z))^{d/2-1}(\bar{z}+x(1-\bar{z}))^{d/2-1}}\,.
\end{aligned} \tag{C.28}$$

Substituting this in (C.27), we can write,

$$\begin{aligned}
\mathcal{G}_2(z,\bar{z}) =&(z\bar{z})^{\Delta_\phi}[(1-\bar{z})(1-z)]^{\lambda_2-\Delta_\phi}\int_0^1 dx\frac{(x(1-x))^{d/2-2}}{(z+x(1-z))^{d/2-1}(\bar{z}+x(1-\bar{z}))^{d/2-1}} \\
&\times \frac{\Gamma(d-3)}{\Gamma(d/2-1)^2}\sum_{\ell=2}^{\infty}\frac{(d-3+2\ell)}{\ell^2(\ell+1)^2}C_\ell^{(d-3)/2}(1-2x)\,.
\end{aligned} \tag{C.29}$$

Starting from this we will extend the analysis of the scalar conformal blocks to the twist-2 higher spin blocks in the main text.

C.2.3 Functions in (4.14)

We will write down the basis functions at each order in α starting from the leading term for $\alpha = 0$. For $\alpha = 0$, *i.e.* the leading order, we have,

$$f_{0,0} = \frac{\log\bar{z} - \log z}{\bar{z}}\,, \tag{C.30}$$

while for $\alpha = 1$,

$$f_{1,0} = \frac{\log\bar{z} - \log z + \mathrm{Li}_2(1-\bar{z}) - \zeta_2}{\bar{z}}\,,\quad f_{0,1} = \frac{(\log z - \log\bar{z})(\log z + 2) + 2\zeta_2}{2\bar{z}}\,, \tag{C.31}$$

For the higher $i + j = \alpha \geq 2$, we get more basis elements which can be obtained systematically from the HypExp package. For $\alpha = 2$,

$$
\begin{aligned}
f_{2,0} &= \frac{1}{12\bar{z}}\Bigg[6\mathrm{Li}_3\left(\frac{\bar{z}-1}{\bar{z}}\right) - 6\mathrm{Li}_3(1-\bar{z}) - \log^3\bar{z} + 6\zeta_3 + 14(\mathrm{Li}_2(1-\bar{z}) - \zeta_2) - 3\log z\bar{z}\mathrm{Li}_2(1-\bar{z}) \\
&\quad + 3(\log\bar{z} - \log z)\zeta_2 - (\log z - \log\bar{z})(2 + \log z\bar{z})\Bigg], \\
f_{1,1} &= -\frac{1}{12\bar{z}}\Bigg[\log^3\bar{z} - 12\mathrm{Li}_3(1-\bar{z}) - 6\mathrm{Li}_3\left(\frac{\bar{z}-1}{\bar{z}}\right) + 12\zeta_3 + 12(\mathrm{Li}_2(1-\bar{z}) - 2\zeta_2) + 6\log z\bar{z}\mathrm{Li}_2(1-\bar{z}) \\
&\quad + 6\log z(\log\bar{z} - \log z) - 6\zeta_2(2\log z - \log\bar{z})\Bigg], \\
f_{0,2} &= \frac{1}{8\bar{z}}\Big[4\zeta_3 + 2\zeta_2(\log\bar{z} - 3\log z - 4) + \log z(4 + \log z)(\log\bar{z} - \log z)\Big].
\end{aligned}
\tag{C.32}
$$

For the next order $\alpha = 3$,

$$
\begin{aligned}
f_{3,0} &= \frac{1}{72\bar{z}}\Bigg[3(\log z - \log\bar{z})(6 + \log z\bar{z}) - 8\log^3\bar{z} + 6(1 - 3\log z\bar{z})\mathrm{Li}_2(1-\bar{z}) + 18(\log z - \log\bar{z})(\mathrm{Li}_3(1-\bar{z}) + \zeta_3) \\
&\quad - 48\mathrm{Li}_3(1-\bar{z}) + 48\mathrm{Li}_3\left(\frac{\bar{z}-1}{\bar{z}}\right) + 48\zeta_3 + 72\mathrm{Li}_4(1-\bar{z}) - 6(1 + 5\log z - 3\log\bar{z})\zeta_2 - 63\zeta_4 - 36S_{2,2}(1-\bar{z})\Bigg], \\
f_{2,1} &= \frac{1}{144\bar{z}}\Bigg[2(11 - 6\log z)(\log\bar{z} - \log z) - (1 + 6\log z)(\log\bar{z} - \log z)(\log\bar{z} + \log z) + \log^3\bar{z}(-2 + 9\log z + 6\log\bar{z}) \\
&\quad - 2(1 + 24\log z\bar{z} - 9\log^2 z\bar{z})\mathrm{Li}_2(1-\bar{z}) - 18\mathrm{Li}_2(1-\bar{z})^2 + 12(20 + 3\log z)\mathrm{Li}_3(1-\bar{z}) \\
&\quad + 6(2 - 9\log z\bar{z})\mathrm{Li}_3\left(\frac{\bar{z}-1}{\bar{z}}\right) - 216\mathrm{Li}_4(1-\bar{z}) - 72\mathrm{Li}_4\left(\frac{\bar{z}-1}{\bar{z}}\right) + 2\zeta_2(13 + 108\log z + 9\log z(\log z - \log\bar{z}) \\
&\quad - 54\log\bar{z} - 18\mathrm{Li}_2(1-\bar{z})) + 378\zeta_4 - 240\zeta_3 + 36\zeta_3(3\log\bar{z} - 4\log z) + 108S_{2,2}(1-\bar{z})\Bigg], \\
f_{1,2} &= \frac{1}{96\bar{z}}\Bigg[12\log^2 z(\log\bar{z} - \log z) + 8\log^3\bar{z} + 4\log z\log^3\bar{z} + 3\log^4\bar{z} + 12\mathrm{Li}_2(1-\bar{z})^2 - 48(2 + \log z)\mathrm{Li}_3(1-\bar{z}) \\
&\quad - 24(2 + \log z\bar{z})\mathrm{Li}_3\left(\frac{\bar{z}-1}{\bar{z}}\right) - 24\mathrm{Li}_4\left(\frac{\bar{z}-1}{\bar{z}}\right) - 12\zeta_2\log z(14 + 3\log z) + 24\zeta_2(3 + \log z)\log\bar{z} \\
&\quad + 12\mathrm{Li}_2(1-\bar{z})(\log z\bar{z}(4 + \log z\bar{z}) + 2\zeta_2) + 24\zeta_3(6 + 5\log z - 3\log\bar{z}) - 252\zeta_4\Bigg], \\
f_{0,3} &= \frac{1}{48\bar{z}}\Bigg[42\zeta_4 - 12\zeta_3(2 + 2\log z - \log\bar{z}) + 6\zeta_2(2\log z(3 + \log z) - (2 + \log z)\log\bar{z}) \\
&\quad + \log^2 z(6 + \log z)(\log z - \log\bar{z})\Bigg].
\end{aligned}
\tag{C.33}
$$

C.2.4 List of Integrals

The basic list of integrals contain the following kinds,

$$I_{m,n,p}(u) = u \int_0^1 dx \frac{\log^m x \log^n(1-x) \log^p(1-ux)}{(1-ux)}\,, \tag{C.34}$$

The above form entail most of the integrals to be performed for the twist-2 integrals. The general form of the integral introduced in section 4.3,

$$\mathcal{I}_{m,n,p}(z,\bar{z}) = \int_0^1 dx \frac{f(x)}{(z+x(1-z))(\bar{z}+x(1-\bar{z}))} = \frac{1}{\bar{z}-z}\Big[u_{\bar{z}} I_{m,n,p}(u_{\bar{z}}) - u_z I_{m,n,p}(u_z)\Big]\,, \tag{C.35}$$

for $u_x = (x-1)/x$ and $f(x)$ has the general form,

$$f(x) = \log^m x \log^n(1-x) \log^p(1-ux)\,, \tag{C.36}$$

Using this, some of the integrals used in the main text are,

$$\mathcal{I}_{0,0,0}(z,\bar{z}) = \frac{\log(\bar{z}/z)}{z-\bar{z}}\,,\ \mathcal{I}_{0,1,0}(z,\bar{z}) = \frac{\mathrm{Li}_2(1-\bar{z}) - \mathrm{Li}_2(1-z)}{z-\bar{z}}\,, \tag{C.37}$$

$$\mathcal{I}_{1,0,0}(z,\bar{z}) = \frac{2\mathrm{Li}_2(1-\bar{z}) + \log^2\bar{z} - 2\mathrm{Li}_2(1-z) - \log^2 z}{2(z-\bar{z})}\,, \tag{C.38}$$

$$\mathcal{I}_{1,1,0}(z,\bar{z}) = \frac{\log(1-z)\log^2 z - \log(1-\bar{z})\log^2\bar{z} + 4\mathrm{Li}_3(1-z) + 2\mathrm{Li}_3(z) - 4\mathrm{Li}_3(1-\bar{z}) - 2\mathrm{Li}_3(\bar{z})}{2(z-\bar{z})}\,, \tag{C.39}$$

$$\mathcal{I}_{0,3,0}(z,\bar{z}) = \frac{6(\mathrm{Li}_4(1-\bar{z}) - \mathrm{Li}_4(1-z))}{z-\bar{z}}\,. \tag{C.40}$$

The other two integrals are (we only give their expressions for $z \to 0$),

$$\begin{aligned}
\lim_{z\to 0} \mathcal{I}_{2,1,0}(z,\bar{z}) =& \frac{1}{12\bar{z}}\Bigg[\log^4\bar{z} + 24\log\bar{z}(\mathrm{Li}_3(1-\bar{z}) - \zeta_3) + 12\zeta_2(2\mathrm{Li}_2(1-\bar{z}) + \log^2\bar{z}) \\
&+ 24\left(\zeta_4 + S_{2,2}(1-\bar{z}) + \mathrm{Li}_4\left(\frac{\bar{z}-1}{\bar{z}}\right) - 2\mathrm{Li}_4(1-\bar{z})\right)\Bigg], \\
\lim_{z\to 0} \mathcal{I}_{1,2,0}(z,\bar{z}) =& \frac{1}{2\bar{z}}\Big[4\zeta_2\mathrm{Li}_2(1-\bar{z}) + 4\log\bar{z}(\mathrm{Li}_3(1-\bar{z}) - \zeta_3) + 4(S_{2,2}(1-\bar{z}) \\
&- 3\mathrm{Li}_4(1-\bar{z})) + \zeta_4\Big].
\end{aligned} \tag{C.41}$$

The additional integrals are,

$$\begin{aligned}
\lim_{z\to 0}\mathcal{J}_1 &= \lim_{z\to 0}\int_0^1 dx \frac{\log((z + x(1-z))(\bar{z} + x(1-\bar{z})))}{(z + x(1-z))(\bar{z} + x(1-\bar{z}))} \\
&= \frac{4\mathrm{Li}_2(1-\bar{z}) + (\log\bar{z} - \log z)(\log z + 3\log\bar{z})}{2\bar{z}}.
\end{aligned} \tag{C.42}$$

Two additional integrals we require, are

$$\begin{aligned}
\mathcal{J}_2 &= \int_0^1 dx \frac{\log x \log(1-x)\log((z + x(1-z))(\bar{z} + x(1-\bar{z})))}{(z + x(1-z))(\bar{z} + x(1-\bar{z}))}, \\
\mathcal{J}_3 &= \int_0^1 dx \frac{\log\frac{1-x}{x}\mathrm{Li}_2(\frac{x}{x-1}) + 2\mathrm{Li}_3(\frac{x}{x-1})}{(z + x(1-z))(\bar{z} + x(1-\bar{z}))}
\end{aligned} \tag{C.43}$$

where $u_x = (x-1)/x$. In a similar fashin we will evaluate the final forms of the integrals $\mathcal{J}_2$ and $\mathcal{J}_3$ after the $z \to 0$ limit. To evaluate $\mathcal{J}_2$ and $\mathcal{J}_3$, we use the PolyLogTools Mathematica package ([79])[2]. The result of $\mathcal{J}_3$ integral is,

$$\begin{aligned}
\lim_{z\to 0}\mathcal{J}_3 =& \frac{1}{24\bar{z}}\Bigg[-72\mathrm{Li}_4(1-\bar{z}) - 72\mathrm{Li}_4\left(\frac{\bar{z}-1}{\bar{z}}\right) + 12\mathrm{Li}_2(1-\bar{z})\log^2\bar{z} + 24\mathrm{Li}_3(1-\bar{z})\log\bar{z} \\
&- 48\mathrm{Li}_3\left(\frac{\bar{z}-1}{\bar{z}}\right)\log\bar{z} + 72S_{2,2}(1-\bar{z}) - 24\zeta_3\log\bar{z} + 5\log^4\bar{z} - 72\zeta_4\Bigg].
\end{aligned} \tag{C.44}$$

[2]We thank Claude Duhr for helping us out with the integrals.

This result has no discontinuities. The final result for the $\mathcal{J}_2$ integral is,

$$\lim_{z\to 0}\mathcal{J}_2 = -\frac{1}{6\bar{z}}\Big(3\text{Li}_2(1-\bar{z})^2 + 18\zeta_2\text{Li}_2(1-\bar{z}) - 24\text{Li}_4(1-\bar{z}) + 24\text{Li}_4\left(\frac{\bar{z}-1}{\bar{z}}\right)$$
$$+ 18\text{Li}_3(1-\bar{z})\log\bar{z} + 6S_{2,2}(1-\bar{z}) - 18\zeta_3\log\bar{z} + \log^4\bar{z} + 12\zeta_2\log^2\bar{z} + 12\zeta_4\Big)\,. \tag{C.45}$$

This integral was performed using PolyLogTools and simplification was made using the rules listed in[80]. Again we find that there are no discontinuities in the final result.

C.3 Perturbative Diagrams

We will calculate perturbative diagrams up-to 3-loops in this section. Our focus is only the ring diagrams, which correspond to pure g terms in the conformal block expansion.

C.3.1 Master Integral

Before we begin computing loop integrals we will calculate a *master* integral. This is important because this will appear in each loop calculation. The integral is given as (in t-channel form),

$$\int \frac{d^4x_6}{x_{16}^{2+2g_1\delta}\, x_{26}^{2+2g_2\delta}\, x_{36}^{2+2g_3\delta}\, x_{46}^{2-2(g_1+g_2+g_3)\delta}}\,. \tag{C.46}$$

We evaluate this integral using (C.2) to obtain,

$$\int \frac{d^4x_6}{x_{16}^{2+2g_1\delta}\, x_{26}^{2+2g_2\delta}\, x_{36}^{2+2g_3\delta}\, x_{46}^{2-2(g_1+g_2+g_3)\delta}} =$$
$$\int_0^1 dp\,\frac{p^{\delta g_3}\Gamma((-g_1-g_2)\delta)((1-p)p)^{\delta(g_1+g_2)}(1-p\bar{z})^{\delta(-g_2)-1}(1-p)^{\delta(-g_1-g_2-g_3)}(z\bar{z})^{\delta(g_1+g_2)}}{\Gamma(g_3\delta+1)\Gamma(1-(g_1+g_2+g_3)\delta)}$$
$$+\int_0^1 dp\,\frac{\Gamma(1-g_1\delta)\Gamma(1-g_2\delta)p^{\delta g_3}\Gamma((g_1+g_2)\delta)(1-p)^{\delta(-g_1-g_2-g_3)}(1-p\bar{z})^{\delta(g_1+g_2)+\delta(-g_2)-1}}{\Gamma(g_1\delta+1)\Gamma(g_2\delta+1)\Gamma(g_3\delta+1)\Gamma(1-(g_1+g_2+g_3)\delta)}\,. \tag{C.47}$$

It is quite cumbersome to carry around all these factors and hence we will just stick to a particular regularization scheme, $g_1 = g_3$ and $g_1 = -g_2$. This is the same scheme used in the main text to obtain pure g terms. With this choice of regularization the *master* integral becomes,

$$\int \frac{d^4x_6}{x_{16}^{2-\delta}\, x_{46}^{2-\delta}\, x_{26}^{2+\delta}\, x_{36}^{2+\delta}}\,, \tag{C.48}$$

and (C.47) becomes,

$$\begin{aligned} &\frac{1}{\Gamma^2(1+\delta/2)\Gamma^2(1-\delta/2)}\left(\frac{x_{14}^2}{x_{24}^2}\right)^{\delta}\frac{1}{(x_{13}^2)^{1+\delta/2}(x_{24}^2)^{1-\delta/2}} \\ &\quad\times\int dsdt\Gamma^2(-s)\Gamma(-t)\Gamma(-t-\delta)\Gamma^2(s+t+1+\delta/2)(z\bar{z})^s(1-\bar{z})^t\,. \end{aligned} \tag{C.49}$$

We need to evaluate the integral in $z \to 0$ limit. The $s = 0$ residue will give us the leading z piece. Just like the conformal block case, we will write the $s = 0$ residue in this form,

$$\frac{(x_{14}^2)^{\delta}}{x_{13}^{2+\delta}x_{24}^{2+\delta}}\mathcal{D}_\alpha\int dt\,\frac{(1-\bar{z})^t\Gamma(-t)\Gamma(-t-\delta)\Gamma\left(t+\frac{\delta}{2}+1\right)(z\bar{z})^{\alpha/2}\Gamma\left(t+\alpha+\frac{\delta}{2}+1\right)}{\Gamma\left(1-\frac{\delta}{2}\right)^2\Gamma\left(\frac{\delta}{2}+1\right)^2}\,, \tag{C.50}$$

where,

$$\mathcal{D}_\alpha = (2\gamma + 2\partial_\alpha)|_{\alpha=0}\,. \tag{C.51}$$

The remaining t-integral can be performed using (C.3), which is then acted on by the $\mathcal{D}_\alpha$ operator yields the final result,

$$\begin{aligned} &\int \frac{d^4x_6}{x_{16}^{2-\delta}\, x_{46}^{2-\delta}\, x_{26}^{2+\delta}\, x_{36}^{2+\delta}} = \\ &\frac{(x_{14}^2)^{\delta}}{x_{13}^{2+\delta}x_{24}^{2+\delta}}\int_0^1 dp\,\frac{(1-p)^{\delta/2}p^{-\delta/2}(1-p\bar{z})^{\frac{\delta}{2}-1}\left(2\psi^{(0)}\left(\frac{\delta}{2}+1\right)+2\log(p)+\log(z\bar{z})+2\gamma\right)}{\Gamma\left(1-\frac{\delta}{2}\right)\Gamma\left(\frac{\delta}{2}+1\right)}\,. \end{aligned} \tag{C.52}$$

C.3.2 Regularization Prescription

The perturbative diagrams come with multiple divergences. The maximum divergence corresponds to the number of loops eg a 2-loop diagram would have a quadratic divergence. We notice a similarity between the finite contribution of these diagrams and the conformal correlator expansion.

With this in mind we will ignore the divergent contribution. Since finite pieces are regularization dependent we need to fix a scheme for regularization in position space. The similarity of finite piece with conformal correlator expansion prompted us to consider them as basis elements. As an example we will take the one-loop diagram whose integral form is,

$$I_{1L} = \int \frac{d^4x_5\, d^4x_6}{x_{15}^2\, x_{45}^2\, x_{56}^4\, x_{26}^2\, x_{36}^2}\,. \tag{C.53}$$

The integral is divergent so we first regularize the terms with the following rules,

1. Dress the propagator terms of each integrand variable with δ such that the sum of δs is zero. The sum of δs should vanish for each integrand to keep the integral conformal.

2. Multiply the integral with a pre-factor to cancel the δ-dependence of the external points. The whole dressed-integral is now scale-invariant.

With the above rules we obtain the following normalization,

$$I_{1L} = (x_{14}x_{23})^{\delta} \int \frac{d^4x_5\, d^4x_6}{x_{15}^{2+\delta}\, x_{45}^{2+\delta}\, x_{56}^{4-2\delta}\, x_{26}^{2+\delta}\, x_{36}^{2+\delta}}\,. \tag{C.54}$$

In the above expression we will first perform the x_5 integral . The sum of δ vanishes for x_5 and x_6-integrals. Once we perform the x_5-integral it is still required that the $x_6 - \delta$ sum vanishes. With this regularization one can perform the integral using (C.1) and (C.2) and then expand in δ. We will neglect the divergent piece in $\frac{1}{\delta}$ and keep only the finite piece. As expected we will find that divergent pieces at higher order contain finite piece result of lower orders. Schematically we can write the three-loop results as,

$$= \frac{1}{\delta^3}(tree) + \frac{1}{\delta^2}(\text{1-loop}) + \frac{1}{\delta}(\text{2-loop}) + \text{finite} \tag{C.55}$$

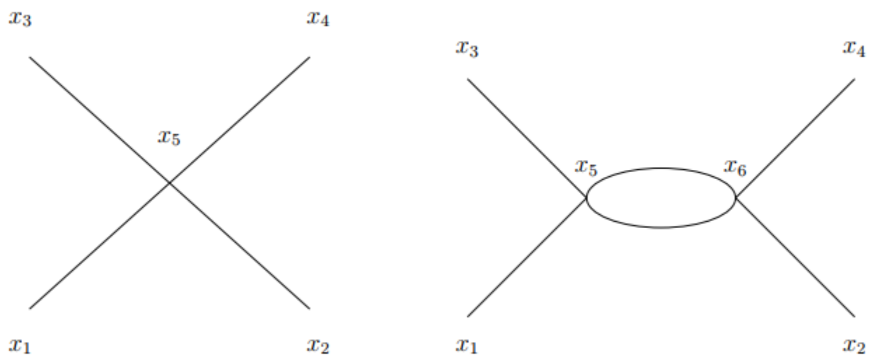

Figure C.1: Tree diagram and one-loop diagram.

C.3.2.1 *Generic Regularization*

Let us briefly mention what happens when we take generic regularizations. Let us again consider the 1-loop integral,

$$I_{1L} = \int \frac{d^4x_5\, d^4x_6}{x_{15}^{2+a\delta}\, x_{45}^{2+b\delta}\, x_{56}^{4+c\delta}\, x_{26}^{2+d\delta}\, x_{36}^{2+e\delta}}\,. \tag{C.56}$$

Now with the first condition on our regularization procedure we obtain two equations,

$$a + b + c = 0 \qquad c + d + e = 0\,. \tag{C.57}$$

Starting with 5 unknowns we have reduced our search space to 3 unknown. For rings diagrams we always have 3 unknown parameters for any loop. The was the motivation for us to construct a generating function (4.43) with three parameters. Starting from 3-loop we encounter additional generating function which has more parameters. With the regularization procedure under control we can start computing the loops.

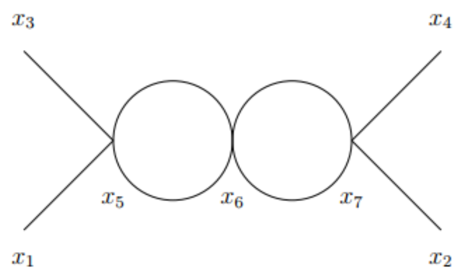

Figure C.2: Two loop ring.

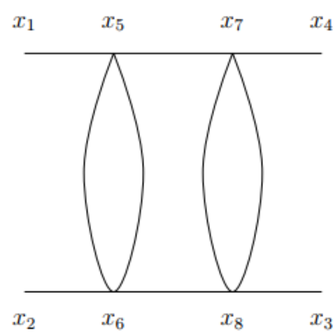

Figure C.3: Three loop ladder.

C.3.3 Tree Level Integral

As we can see from the figure (Figure C.1), the tree level integral is just (C.48) with $\delta = 0$.

$$I_{0L} = \int \frac{d^4 x_6}{x_{16}^2\, x_{46}^2\, x_{36}^2\, x_{26}^2}\,. \tag{C.58}$$

So now we plug in (C.52) $\delta = 0$ and obtain,

$$\int_0^1 dp\, \frac{2\log(p) + \log(z\bar{z})}{1 - p\bar{z}}\,. \tag{C.59}$$

This integrates to ,

$$\frac{6\mathrm{Li}_2(1-\bar{z}) - 3\log(z)\log(1-\bar{z}) + 3\log(\bar{z})\log(1-\bar{z}) - \pi^2}{3\bar{z}}\,. \tag{C.60}$$

Writing only the discontinuity we obtain,

$$\log(1-\bar{z})\frac{\log(z)-\log(\bar{z})}{\bar{z}}\,. \tag{C.61}$$

C.3.4 One Loop Ring Diagram

The one loop diagram integral is,

$$I_{1L}=\int\frac{d^4x_5\,d^4x_6}{x_{15}^2\,x_{45}^2\,x_{56}^4\,x_{26}^2\,x_{36}^2}\,. \tag{C.62}$$

We will use the follow normalization prescription,

$$I_{1L}=(x_{14}x_{23})^{\delta}\int\frac{d^4x_5\,d^4x_6}{x_{15}^{2+\delta}\,x_{45}^{2+\delta}\,x_{56}^{4-2\delta}\,x_{26}^{2+\delta}\,x_{36}^{2+\delta}}\,. \tag{C.63}$$

The justification to the prescription has already been given in (C.3.2).

We first perform the x_5-integral (ignoring the prefactors for a moment) using (C.1) to obtain,

$$I_{1L}=\frac{\Gamma\left(1-\frac{\delta}{2}\right)^2\Gamma(\delta)}{\Gamma(2-\delta)\Gamma\left(\frac{\delta}{2}+1\right)^2}\frac{1}{x_{14}^{2\delta}}\int\frac{d^4x_6}{x_{16}^{2-\delta}\,x_{46}^{2-\delta}\,x_{26}^{2+\delta}\,x_{46}^{2+\delta}}\,. \tag{C.64}$$

The final integral is of the form of master integral and we find,

$$\begin{aligned}I_{1L}=&\frac{1}{x_{13}^2x_{24}^2}\frac{\Gamma\left(1-\frac{\delta}{2}\right)^2\Gamma(\delta)}{\Gamma(2-\delta)\Gamma\left(\frac{\delta}{2}+1\right)^2}\frac{1}{x_{13}^{\delta}x_{24}^{\delta}}\\&\times\int_0^1 dp\,\frac{(1-p)^{\delta/2}p^{-\delta/2}(1-p\bar{z})^{\frac{\delta}{2}-1}\left(2\psi^{(0)}\left(\frac{\delta}{2}+1\right)+2\log(p)+\log(z\bar{z})+2\gamma\right)}{\Gamma\left(1-\frac{\delta}{2}\right)\Gamma\left(\frac{\delta}{2}+1\right)}\end{aligned} \tag{C.65}$$

Now we expand each term in δ and perform the integral. The divergent contribution is,

$$\frac{1}{\delta}\int_0^1 dp\frac{2\log(p)+\log(z\bar{z})}{(p\bar{z}-1)}=\frac{1}{\delta}\left(\frac{\log(\bar{z})-\log(z)}{\bar{z}}\right)\,. \tag{C.66}$$

The finite contribution is,

$$\begin{aligned}&\int_0^1 dp\frac{(-2\log(1-p\bar{z})-2\log(1-p)+2\log(p)+\log(1-\bar{z})-4)(2\log(p)+\log(z\bar{z}))-4\zeta_2}{4p\bar{z}-4}\\&=\log(1-\bar{z})\big(\frac{\log(z)-\log(\bar{z})}{4\bar{z}}\big)+\log^2(1-\bar{z})\big(\frac{\zeta_2-\mathrm{Li}_2(1-\bar{z})+2\log(z)-2\log(\bar{z})}{2\bar{z}}\big)\,.\end{aligned} \tag{C.67}$$

C.3.5 Two and Three Loop Ring

We will write down the final results of both 2-loop and 3-loop ring diagrams (Figure C.2) here. The 2-loop integral is given by,

$$I^r_{2L}=\int\frac{d^4x_5d^4x_6d^4x_7}{(x^2_{15})(x^2_{45})(x^2_{56})^2(x^2_{67})^2(x^2_{27})(x^2_{37})}. \tag{C.68}$$

While the three loop integral is,

$$I^r_{3L}=\int\frac{d^4x_5d^4x_6d^4x_7d^4x_8}{(x^2_{15})(x^2_{45})(x^2_{56})^2(x^2_{67})^2(x^2_{78})^2(x^2_{28})(x^2_{38})}. \tag{C.69}$$

On evaluating the integral we obtain the following finite piece for 2-loop ring diagram,

$$\begin{aligned}&\log(1-\bar{z})^3\left(\frac{\log(\bar{z})-\log(z)}{24\bar{z}}\right)+\log(1-\bar{z})^2\left(\frac{\mathrm{Li}_2(1-\bar{z})-\zeta_2}{4\bar{z}}\right)\\&-\log(1-\bar{z})\Bigg(\frac{-6\zeta_3+3\mathrm{Li}_2(1-\bar{z})\log(z)+6\mathrm{Li}_3(1-\bar{z})-6\mathrm{Li}_3\left(\frac{\bar{z}-1}{\bar{z}}\right)+3\mathrm{Li}_2(1-\bar{z})\log(\bar{z})}{12\bar{z}}\\&\frac{+3\zeta_2(\log(z)-\log(\bar{z}))+12\log(z)+\log^3(\bar{z})-12\log(\bar{z})}{12\bar{z}}\Bigg)\,,\end{aligned} \tag{C.70}$$

and for 3- loop diagram,

$$
\begin{aligned}
&\log^4(1-\bar{z})\big(\frac{\log(z)-\log(\bar{z})}{24\bar{z}}\big)\\
&+\log^3(1-\bar{z})\big(\frac{\zeta_2-\mathrm{Li}_2(1-\bar{z})-\log(z)+\log(\bar{z})}{6\bar{z}}\big)\\
&+\log^2(1-\bar{z})\big(\frac{-6\zeta_3+12\mathrm{Li}(1-\bar{z})+3\mathrm{Li}_2(1-\bar{z})\log(z)+6\mathrm{Li}_3(1-\bar{z})-6\mathrm{Li}_3\left(\frac{\bar{z}-1}{\bar{z}}\right)+3\mathrm{Li}_2(1-\bar{z})\log(\bar{z})}{12\bar{z}}\\
&\qquad+\frac{3\zeta_2(\log(z)-\log(\bar{z}))+24\log(z)+\log^3(\bar{z})-24\log(\bar{z})-12\zeta_2}{24\bar{z}}\big)\\
&-\frac{\log(1-\bar{z})}{24\bar{z}}\Big(-21\zeta_4+24\mathrm{Li}_4(1-\bar{z})-6\mathrm{Li}_3(1-\bar{z})\log(\bar{z})-12S_{2,2}(1-\bar{z})+18\zeta_3\log(\bar{z})\\
&-12\zeta_3+12\mathrm{Li}_3(1-\bar{z})-12\mathrm{Li}_3\left(\frac{\bar{z}-1}{\bar{z}}\right)+6\mathrm{Li}_2(1-\bar{z})\log(\bar{z})-6\zeta_2\log(\bar{z})+2\log^3(\bar{z})\\
&+48\mathrm{Li}_2(1-\bar{z})-48\zeta_2\\
&+\log(z)\big(6\zeta_2-18\zeta_3+6\mathrm{Li}_2(1-\bar{z})+6\mathrm{Li}_3(1-\bar{z})\big)\\
&+48\log(z)-48\log(\bar{z})\Big)\,.
\end{aligned}
\tag{C.71}
$$

Let us close this appendix with a few observations. The highest order discontinuity is always the tree level result. The lower order discontinuities at a given loop can be written in terms of discontinuities appearing in a lower loop diagram. The terms which appear in the discontinuities are similar to one that occur in conformal correlator expansion.

C.4 $Li_2(1-\bar{z})^2$ Origin

In this section we will demonstrate the origin of $\mathrm{Li}_2^2(1-\bar{z})$ from a new generating function. We encountered these terms in the conformal block expansion at 5th order. This corresponds to three loop in the diagrammatic expansion. At three loops we encounter diagrams which contribute to an additional generating function. Ladder diagram shown in the figure above (Figure C.3) is the one that generates such a term. We will report its integral,

$$
I=\int\frac{d^4x_5d^4x_6d^4x_7d^4x_8}{(x_{15}^2)(x_{47}^2)(x_{26}^2)(x_{38}^2)(x_{56}^2)^2(x_{78}^2)^2(x_{57}^2)(x_{68}^2)}\,. \tag{C.72}
$$

Proceeding along the lines of (C.3.2.1) we see that the most general regularization of the above integral has 8 parameters and we have 4 equations. This tells us that there would be 4 independent parameters and this would be our new generating function. We will regularize the integral as,

$$I \sim \int \frac{d^4x_5 d^4x_6 d^4x_7 d^4x_8}{(x_{15}^2)^{1-\delta/2}(x_{47}^2)^{1+3\delta/2}(x_{26}^2)^{1-3\delta/2}(x_{38}^2)^{1+\delta/2}(x_{56}^2)^{2+\delta}(x_{78}^2)^{2-\delta}(x_{57}^2)^{1-\delta/2}(x_{68}^2)^{1+\delta/2}} . \quad \text{(C.73)}$$

Performing the x_5 and x_6 integral one obtains,

$$I \sim \Gamma(\delta)\Gamma(-\delta) \int \frac{d^4x_6 d^4x_7}{(x_{17})^{-\delta}(x_{36})^{\delta}(x_{76})^2(x_{47})^{1+3\delta/2}(x_{26})^{1-3\delta/2}(x_{37})^{1-\frac{\delta}{2}}(x_{16})^{1+\frac{\delta}{2}}} \quad \text{(C.74)}$$

Our goal here is to schematically show the piece we want and so we will use a small trick to obtain the term of interest. For the lower loop calculations we first performed the integral and then took the $\delta \to 0$ limit. However this process should commute. In that spirit we will take $\delta \to 0$ limit right now and focus on a particular term. The term that we want to focus on is the above equation with $(x_{17})^{-\delta}$ set to 1. This is a genuine term which will appear when one takes the $\delta \to 0$ limit. Focusing on this terms is sufficient to generate the discontinuity we want.

$$I \sim \Gamma(\delta)\Gamma(-\delta) \int \frac{d^4x_6 d^4x_7}{(x_{36})^{\delta}(x_{76})^2(x_{47})^{1+3\delta/2}(x_{26})^{1-3\delta/2}(x_{37})^{1-\frac{\delta}{2}}(x_{16})^{1+\frac{\delta}{2}}} . \quad \text{(C.75)}$$

We can now perform the x_7 integral which gives rise to,

$$I \sim \Gamma(\delta)^2\Gamma(-\delta)^2 \int_0^1 dp \, \frac{(1-p)^{-\delta/2} p^{3\delta/2} (1-p\bar{z})^{-\frac{\delta}{2}}}{1-p\bar{z}} . \quad \text{(C.76)}$$

The integrand needs to be expanded to a maximum of fourth order in δ to perform the integral. It turns out that the fourth order term gives rise to $Li_2(1-\bar{z})^2$